Development of a Mouse Model of Sepsis Associated Encephalopathy and Delirium using Electroencephalography and Neurobehavior

By

David Christopher Consoli

Dissertation

Submitted to the Faculty of the

Graduate School of Vanderbilt University

in partial fulfillment of the requirements

for the degree of

DOCTOR OF PHILOSOPHY

in

Neuroscience

September 30, 2021

Nashville, Tennessee

Approved:

Fiona E. Harrison, Ph.D. (mentor)

Angela L. Jefferson, Ph.D. (chair)

Julie A. Bastarache, M.D.

Laura L. Dugan, M.D.

To my mother

who led me to science and shaped my worldview

ACKNOWLEDGMENTS

The work presented in this thesis was supported by funding from the National Institute of Health (NIH) and National Institute of Environmental Health Sciences (NIEHS) through R01 ES031401 to Fiona E. Harrison and Aaron B. Bowman and the U.S. Department of Veterans Affairs through a VA Merit I01 CX001610 to James M. May. We received additional support from the National Heart, Lung, and Blood Institute (NHLBI) through R01 HL135849-03 and HL135849-02S1 to Lorraine B. Ware and Julie A. Bastarache. Work presented in Chapter 4 was supported by grants to William P. Nobis from the American Epilepsy Society (Junior Investigator Award), a pilot grant from the National Institute for Neurologic Disease and Stroke Center for unexpected death in epilepsy (SUDEP) center for SUDEP research (CSR), and the Vanderbilt Faculty Research Scholars (VFRS) award. David C. Consoli received other training support from the National Institutes of General Medical Sciences (NIGMS) through the Vanderbilt Interdisciplinary Graduate Program T32 GM008554 to James G. Patton and from the NIH through the Training in Fundamentals of Neuroscience T32 MH064913 to Danny G. Winder.

First and foremost, I would like to thank Dr. Fiona Harrison for her never-ending guidance and support throughout my graduate studies. Thank you for helping me recognize and hone my strengths, develop a unique project, and explore my creative inclinations. Thank you for providing a rigorous training environment that encourages collaboration, innovation, and competition. I am grateful to work alongside the brilliant minds you attract to the lab, and I am especially grateful to each of my fellow lab members. Thanks to Dr. Brittany Spitznagel for always helping with experiments, hearing my petty grievances, and making space for me to accomplish everything I needed to graduate. Thanks to Dr. Jordyn Wilcox for always sharing her insight from having gone before me and allowing me to follow. Thanks to Amanda Marino and Rebecca Buchannan for helping me make sense of rambling thoughts and for bringing new levels of brilliance to the lab. Thanks to Adriana Tienda for keeping the lab running, maintaining the mouse colony, and assisting willingly with anything. Thanks to Kelly Klimo for running unprecedented levels of HPLC and never complaining. Thanks to Dr. John Allison for helping design behavioral studies and Krista Paffenroth for helping execute them. A special thanks to

former lab member Dr. Shilpy Dixit for providing comprehensive training in lab techniques, writing feedback, and infinite grace and wisdom.

I have many people to thank from outside the Harrison lab. I would like to acknowledge Dr. Julie Bastarache for lending her exceptional expertise, lab resources, and kindhearted encouragement. I am particularly grateful for your mentorship and sponsorship in my research endeavors and career development. Thanks to Bastarache lab members Nathan Putz and Jordan Jesse for sharing experimental reagents and supervising my execution of their laboratory protocols. I would like to thank the remaining two members of my committee, Drs. Angela Jefferson and Laura Dugan, for contributing to the definition of my thesis project, professional skills, and career path with immeasurable guidance and support. I would like to thank Drs. William Nobis and Benjamin Owen for offering their lab space and teaching me the ways of hippocampal electrophysiology. I would also like to thank Drs. Lillian Brady and Erin Calipari for teaching me voltammetry techniques and overseeing an exciting side project. Thanks to Jason Russell for aiding in the use of Neuroscore software for sleep scoring and periodogram analysis. Thanks to Dr. Hakmook Kang in the Vanderbilt Kennedy Center Biostatistics Core for aiding in statistical regressions of EEG power bands. And finally, I would like to thank the Critical Illness, Brain Dysfunction, and Survivorship Center (CIBS), which receives funding from the National Institute on Aging (NIA), specifically Drs. Wesley Ely, Pratik Pandharipande, and Shawniqua Williams Roberson for their friendly guidance on and enthusiasm for the delirium and EEG project.

Outside of Vanderbilt, I would first like to thank my beautiful and brilliant wife Suzie, without whom none of these achievements would have been possible. Suzie, you remain the smartest person I know, and I am extremely grateful to you for your unending love and support. Thank you for being my best friend and favorite person. Thank you for countlessly sacrificing your time and energy to listen to me, process with me, and encourage me. I would also like to thank my family. To my brother Jon and my sister Lauren, to my dad and my stepmother Amy, to my in-laws Ted and Laura, to my brothers Doug, Sam, and Cole, to Brian and Julia and Reghan and Shelby, and to my grandparents, thank you for caring about my work, asking meaningful questions, and listening intently. I am grateful to each of you for your influence on my perception of the world. And lastly, of course, thank you to our doggo Sally for bringing us new life in a difficult time and for keeping me company while writing a dissertation.

TABLE OF CONTENTS

LIST OF TABLES

LIST OF FIGURES

LIST OF ABBREVIATIONS

ASC	ascorbate (vitamin C)
CA1	Cornu ammonis 1
CAM	confusion assessment method
CLP	cecal ligation and puncture
CRP	C-reactive protein
CS	cecal slurry
DHA	dehydroascorbate
EEG	electroencephalography
EMG	electromyography
EPSP	excitatory post-synaptic potential
gulo$^{-/-}$	gulonolactone oxidase knockout
IFN	interferon
IL	interleukin
JAK-STAT	Janus kinases signal transducer and activators of transcription
LPS	lipopolysaccharide
LTP	long-term potentiation
NF	nuclear factor
NO, NOS	nitric oxide, nitric oxide synthase
PPI	pre-pulse inhibition
RBANS	repeatable battery for the assessment of neuropsychological status
REM, NREM	rapid eye movement, non-rapid eye movement
RNS	reactive nitrogen species
ROS	reactive oxygen species
SVCT1/2	sodium dependent vitamin C transporter 1/2
TBS	theta-burst stimulation
TNF	tumor necrosis factor

CHAPTER 1

Introduction – Sepsis and Brain Dysfunction

Overview

The overall goal is to greater understand how sepsis pathophysiology impacts the brain and contributes to development of long-term cognitive deficits. In this introduction, I first discuss how oxidative stress and endothelial dysfunction during sepsis affect the brain, and I review mouse models of sepsis and their contributions to our understanding of inflammatory driven cognitive decline. Next, I introduce vitamin C as a therapeutic strategy to mitigate neurological oxidative stress during sepsis through the specific tripartite role of vitamin C in the brain. Lastly, I describe delirium as the clinical presentation of sepsis associated encephalopathy and the strongest predictor of long-term cognitive deficits following illness, and I outline electroencephalography as a powerful biomarker for characterizing the complex pathophysiology of delirium.

1.1 Dysregulated Host Response During Sepsis Drives Long-Term Damage

1.1.1. Sepsis is a significant public health crisis exacerbated by long-term impairments following survival.

In 2017, sepsis was the most expensive condition for which to receive in-hospital treatment in the United States, and sepsis inpatient healthcare costs totaled over $38.2 billion (Liang *et al.* 2020). In the same year, the global estimated incidence of sepsis totaled 48 million, with estimated sepsis related deaths surpassing 11 million and accounting for approximately 20% of all global deaths (Rudd *et al.* 2020).

The economic and lethal burdens of sepsis are likely much greater when considering survivors experience lasting long-term complications and increased risk for re-hospitalization due to persistent cardiac, respiratory, and cerebral conditions. One study in older adults who had previously been living independently found that 44% of survivors of severe sepsis experienced quality of life deficits including mobility, hindrances in daily activities, and self-care domains one-year later (Yende *et al.* 2016). These progressive cognitive impairments in memory,

attention, and processing speed and functional disabilities in physical weakness, decreased endurance, and dependence on others for daily tasks suggest accelerated or de novo brain dysfunction following septic insult (Iwashyna *et al.* 2010; Rengel *et al.* 2019). While continued improvements in the treatment and management of sepsis increase survivorship (Kaukonen *et al.* 2014; Gaieski *et al.* 2013), long-term complications persist as a significant public health crisis that burdens patient populations and healthcare infrastructure.

1.1.2. Sepsis pathophysiology is driven by elevated inflammatory cytokines.

Long-term complications are largely driven by the acute injury during sepsis. Sepsis is defined as life-threatening organ dysfunction caused by a dysregulated host response to infection (Angus and van der Poll 2013; Singer *et al.* 2016b). The infection alone does not drive organ dysfunction. Instead, organ dysfunction is driven by the resulting dysregulated host inflammatory response to pathogens. Originally the term septicemia, or "blood poisoning" was used to describe sepsis, but the terminology was updated due to the complex host interactions that characterize the illness (Bone *et al.* 1992). While sepsis can originate from viruses or fungi, most infections are bacterial in origin. The most common infection is pnemoniae, followed by intraabdominal and urinary tract infections. Typical bacterial isolates include gram-positive bacteria such as *Staphylococcus aureus* and *Streptococcus pnemoniae* and gram-negative bacteria such as *Escherichia coli*, *Klebsiella* species, and *Pseudomonas aeruginosa* (Angus and van der Poll 2013). To coordinate the body's immune response to the infection, immune cells including monocytes, lymphocytes, and neutrophils release massive levels of cytokines during what is often referred to as the "cytokine storm." Most deaths due to sepsis occur during this acute phase of overwhelming inflammation, as the inflammation can trigger severe collateral damage and tissue injury (Cao *et al.* 2019).

Cytokines include several signaling proteins such as the interleukins (IL), interferons (IFN), chemokines, tumor necrosis factors (TNF). When bound to their receptors, cytokines trigger cascades of cellular pathways to recruit immune cells and activate the inflammatory response to pathogens and injury. Elevations in proinflammatory cytokines during sepsis including IL-1β, IL-6, TNF-α, IFN-γ, and another broad inflammatory protein complex, C-reactive protein (CRP), are well-documented in septic patients (Matsumoto *et al.* 2018; Pierrakos and Vincent 2010; Bozza *et al.* 2007). The degree of inflammatory status during sepsis

determines risk of organ failure and subsequent long-term patient outcomes (Lobo *et al.* 2003; Pierrakos and Vincent 2010). Elevated inflammatory markers at discharge predict long-term mortality (Yende *et al.* 2008). In a healthy inflammatory response, anti-inflammatory cytokines help to restore normal immune cell function following resolution of the infection or injury. However, in disease states such as sepsis, the immune response is persistently dysregulated due to the severity of the acute insult, and following sepsis patients show increased biomarkers of immunosuppression and persistent immune dysregulation (Yende *et al.* 2019). During the acute illness, the excessive inflammatory response induces persistent changes in critical tissues and vasculature that contributes to lasting damage.

1.1.3. During sepsis, oxidative stress and mitochondrial dysfunction damage the endothelium.

Due to the excessive inflammatory response, sepsis is consistently associated with high levels of oxidative stress. When activated, neutrophils and macrophages produce large amounts of radical species including reactive oxygen species (ROS) and reactive nitrogen species (RNS) to neutralize invading pathogens (Mantzarlis *et al.* 2017). These free radical species have an extra electron that readily oxidizes lipids, proteins, and other cellular structures compromising their function. ROS include superoxide (O_2^-) and hydroxyl (OH^-) radicals and hydrogen peroxide (H_2O_2) and are generally produced in mitochondria through the electron transport chain. RNS include nitric oxide (NO) radical and peroxynitrite ($ONOO^-$). NO is produced by nitric oxide synthases (NOS) which have several different isoforms specific to cellular compartmentalization including neuronal nNOS, inducible iNOS, endothelial eNOS, and mitochondrial mNOS (Knowles and Moncada 1994). Vasodilation in the periphery occurs primarily through electron radical signaling through increased NO production by iNOS (Russell *et al.* 2018). ROS and RNS are critical for neutralizing pathogens and initiating the inflammatory response but not without consequence.

Oxidative stress during sepsis through generation of ROS and RNS leads to shedding of the endothelial glycocalyx. The glycocalyx is a series of negatively charged extracellular matrix sugars including glycosaminoglycans and heparan sulfate that line endothelial cells and create an anticoagulant layer, since negative charges repel circulating platelets (Ait-Oufella *et al.* 2010). ROS during the severe inflammatory response are produced primarily in neutrophils to kill circulating invasive pathogens but consequently ROS oxidize these negatively charged

extracellular proteins (Ince *et al.* 2016). During severe sepsis, NADPH oxidase within endothelial cells also produces ROS that lead to intracellular damage to the endothelial lining (Marechal *et al.* 2008) and damage mitochondrial DNA driving mitochondrial dysfunction that further contributes to dysregulated ROS production (Cui *et al.* 2012). Damaged endothelium and mitochondria subsequently drive catecholamine-refractive vasodilation, endothelial barrier dysfunction, and disseminated intravascular coagulation (Kuhn *et al.* 2018; Rubio-Gayosso *et al.* 2006). The resulting microvasculature dysfunction is catastrophic to many organs and a primary driver of organ failure.

1.1.4. Cardiac, respiratory, renal, and hepatic dysfunction contribute to encephalopathy.

Endothelial dysfunction significantly contributes to cerebral pathology observed in sepsis (Hughes *et al.* 2013). Loss of barrier function leads to significant tissue hypoperfusion and an increase in coagulation. Insufficient tissue oxygenation and subsequent mitochondrial dysfunction elevate oxidative damage to critical tissues and drive organ failure (Angus and van der Poll 2013). Cardiovascular and respiratory dysfunctions impair nutrient and oxygen delivery. Hepatic stress and renal failure prevent proper detoxification. The resulting metabolic and inflammatory dysfunctions raise oxidative stress and further push organs including the brain towards persistent dysregulation and damage (Bauer *et al.* 2018; Mazeraud *et al.* 2016; Ince *et al.* 2016). This complex pathophysiology dramatically affects the brain leading to sepsis associated encephalopathy (**Fig. 1**).

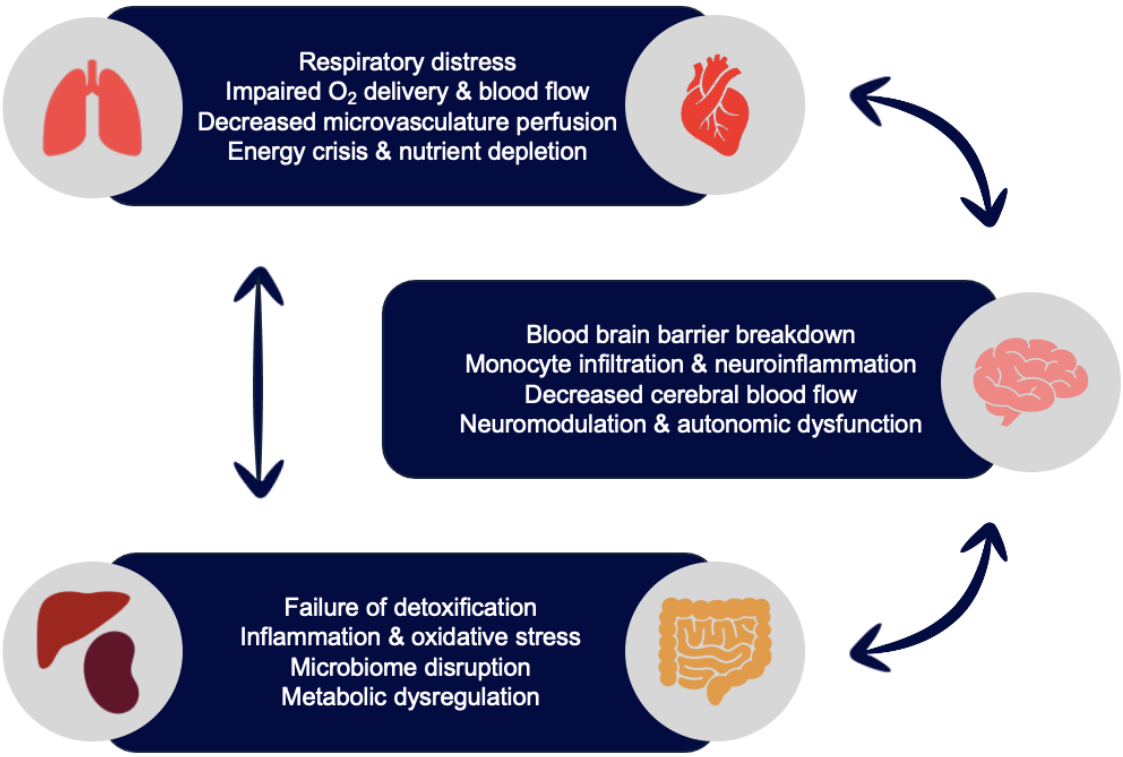

Figure 1 – Organ dysfunction during sepsis contributes to acute encephalopathy.

The brain is particularly susceptible to inflammation and oxidative stress due to its high rate of metabolic demand and enriched lipid composition (Harrison *et al.* 2014). Neurons are extremely sensitive to oxidative damage, toxin accumulation, nutrient deprivation, and elevated inflammation as these conditions can rapidly alter synapse structure, neuronal death, and functional connectivity. The brain is intimately involved in peripheral organ regulation through neuromodulatory and autonomic connections such that neurological dysfunction complicates efforts to preserve peripheral organ function. The acute sepsis-related neurologic dysfunction is the organ dysfunction most associated with short and long-term mortality and is a key mediator of long-term adverse outcomes following sepsis (Schuler *et al.* 2018).

1.1.5. Blood brain barrier breakdown and the neuroinflammatory response

The blood brain barrier is a critical barrier between the brain and periphery and is comprised mainly of the choroid plexus and tight junctions along the cerebral vasculature. The proximity of critical neuron rich structures including the hippocampus to the blood brain barrier is ideal for prioritizing adequate nutrient and oxygen delivery. However, during peripheral

dysfunction such as sepsis, the hippocampus is readily susceptible to inflammatory changes and oxidative damage in the presence of a compromised blood brain barrier. During an activated inflammatory response, sites of insult detect stimuli on cell surface receptors, activating inflammatory pathways that release cytokines and recruit monocytes and macrophages (Chen et al. 2018). In the brain, microglia are the resident immune cells recruited by these signals. In the absence of a stressor, microglia rest in a surveillance state, closely monitoring the surrounding brain environment for external stressors upon which they activate inflammatory pathways to initiate immune response (Jäkel and Dimou 2017).

Microglia activity is critical for maintaining neuronal homeostasis and maintaining neuronal synaptic networks through synaptic pruning, where microglia remove damaged or unnecessary synaptic connections to maximize efficiency (Yin et al. 2017; Wu et al. 2015). Peripheral insults trigger both neural and humoral signal transduction pathways and prompt the expression of proinflammatory cytokines in perivascular macrophages and cerebral microglia (Konsman *et al.* 2002). While cytokines released in the periphery can pass through the blood brain barrier (Banks *et al.* 1995; Banks *et al.* 2002), peripheral macrophages typically cannot. The brain was once regarded as "immune-privileged" and considered to have its own immune system that acts independently of the periphery. This claim is generally no longer accepted, because in many diseases including sepsis where blood brain barrier integrity has been drastically compromised, invasion of peripheral macrophages directly results in significant neuron loss (Aktas *et al.* 2007). Interestingly, a recent study showed that microglia play a crucial role in preventing peripheral immune cell invasion (Unger *et al.* 2018), and another study showed that microglia can actively recruit monocytes to the brain under conditions of extreme stress (McKim *et al.* 2018). These studies emphasize the important role of microglia in determining the appropriate immune response to handle stressors and highlight the capability of microglia to initiate robust response pathways.

1.1.6. Mouse models of sepsis and long-term cognitive decline.

Several rodent models have been utilized to study acute organ dysfunction during sepsis (**Table 1**) including lipopolysaccharide injection, cecal ligation and puncture surgery, and cecal slurry injection (Lewis *et al.* 2016). Studies have used these models of sepsis to determine long-term cognitive deficits and molecular changes following septic insult. The most common model

is use of lipopolysaccharide (LPS), an extracellular matrix sugar found on gram negative bacteria that readily induces an endotoxemia driven inflammatory response. LPS binds to toll-like receptors that ultimately activate nuclear factor (NF) kB transcription factors and elevate inflammatory cytokine expression levels. LPS administration is known for its reliability and simplicity as a model of endotoxemia. However, it has received some criticism as a model of sepsis, because it lacks the polymicrobial diversity associated with clinical sepsis cases (Remick and Ward 2005). LPS indeed activates a neuroinflammatory response and leads to persistent activation of microglia (Raetz and Whitfield 2002; Anderson *et al.* 2015; Qin *et al.* 2007). Chronic doses of LPS (500-750μg daily for 1 week) showed substantial neuronal loss amidst persistent microglial activation in the hippocampus (Zhao *et al.* 2019). These changes were followed by significantly poorer cognitive performance in Morris Water Maze that could be ameliorated by administration of a microglial receptor antagonist. In another study, LPS administration caused long term cognitive impairments measured by radial maze and open field tasks that were attributed to loss of neurons and decreased cholinergic innervation through lower levels of the vesicular acetylcholine transporter (Semmler *et al.* 2007). While perhaps only a model of endotoxemia, evidence suggests LPS initiates robust chronic neuroinflammation that can drive both neurodegeneration and long-term cognitive deficits.

Table 1 – Long-term cognitive impairments in rodent models of sepsis.

Reference	Method of Septic Insult	Behavioral Findings	Time Between Illness and Testing	Markers of Neurological Damage
(Zhao *et al.* 2019).	LPS	Deficits in memory through Morris water maze* and passive avoidance task	1-7 days	↓IL-4 & IL-10, ↓No. of neurons ↑TNF-α, IL-1β, NO
(Semmler *et al.* 2007)	LPS	Deficits in memory through radial arm maze task, open field assessment No deficits observed in inhibitory avoidance learning	12 weeks	↓No. of neurons ↓VAChT
(Hippensteel *et al.* 2019)	LPS, CLP	Deficits in memory by fear conditioning assessment†	7 days	↓LTP
(Chavan *et al.* 2013)	CLP	Deficits in clock maze spatial memory task	1 month	↓CA1 spine density

(Michels *et al.* 2019)	CLP	Deficits in step down inhibitory avoidance task* and open-field assessment*	10 days	↑CD11b, ↑iNOS
(Singer *et al.* 2016a)	CLP	Deficits in memory by fear conditioning assessment	2 months	↑TNF-α, CCR2 Persistent peripheral myeloid presence
(Zhang *et al.* 2021)	CLP	Deficits in learning and memory in Morris water maze task[#]	7 days	↑TNF-α, IL-6, MP-9 ↓IL-10
(Fujinami *et al.* 2021)	CS	Deficits in treadmill & grip strength, no deficits in novel-object recognition Anxiety implicated in open field & marble burying tasks	1-2 weeks	n/a

*Deficits reversed by anti-inflammatory targeting
[†] Deficits reversed by TrkB targeting
[#] Deficits reversed by ASC treatment (intraperitoneal, 200 mg/kg)
Abbreviations: LPS – lipopolysaccharide (5 mg/kg), CLP – cecal ligation and puncture, CS – cecal slurry. LTP – long-term potentiation.

Another commonly utilized model of sepsis involves a surgical procedure called cecal ligation and puncture (CLP), in which the mouse is anesthetized, and part of the cecum is cut and its contents squeezed into the peritoneal cavity (Medina 2010; Dejager *et al.* 2011; Rittirsch *et al.* 2009). This method adds significant microbial diversity that LPS lacks in relevance. Studies utilizing CLP have indeed demonstrated long-term cognitive changes. One study showed that CLP leads to long-term central nervous system dysfunction through prolonged proinflammatory profiles and persistent peripheral myeloid presence up to two months following recovery (Singer *et al.* 2016a). Another study showed reductions in spine density of CA1 hippocampal neurons lasted for up to 4 months and were accompanied by poorer performance in a clock maze spatial memory task for up to 1 month (Chavan *et al.* 2013).

One study connected sepsis associated endothelial shedding with cognitive dysfunction specific to the hippocampus simultaneously in LPS and CLP models (Hippensteel *et al.* 2019). Shedding of endothelial glycocalyx during each of the septic insults led to circulating heparin sulfate fragments that specifically damaged the hippocampus due to its proximity to the blood brain barrier. These fragments interacted specifically with growth factors, including BDNF, to

induce lasting cognitive changes. Using ex vivo electrophysiology and local field potential recordings to measure long-term potentiation (LTP), deficits in learning and memory on a molecular level were demonstrated 7 days after LPS and CLP independently. LTP is the molecular foundation of learning and memory through the capacity of a neuronal circuit to strengthen its signaling by NMDA receptor recruitment and activation (Lynch 2004). Lasting cognitive deficits were also observed in a fear conditioning behavioral assessment of learning and memory and were preventable by targeting the TrkB receptor to promote neuronal survival.

It is appropriate to consider that the burden of anesthesia and surgery significantly contribute to cognitive impairment independently of septic insult. Surgery and anesthesia are compounding factors that complicate the CLP model, because they could drastically affect experimental outputs through drug interactions, persistent pain, or sleep disruptions. One study investigated only the effects of surgery and intensive care unit conditions (Illendula *et al.* 2020) to assess delirium and post-op cognitive dysfunction. Using surgery, anesthesia, and disruptive environment resembling intensive care unit conditions (shaking cage, lights, sounds), mice showed behavioral and cognitive deficits following surgery through novel arm preference Y-maze, buried food task, attentional set shifting task 24 hrs following intensive care unit conditions without the development of sepsis. Synaptic biomarkers in the hippocampus including neurotrophic receptor TK1, syntaxin1a, alpha synuclein, p-syn alpha, synaptophysin, PSD-95, MAP-2 were also decreased 24 hours later due to the non-septic insult. The potential impact of these factors on long-term deficits in the CLP model should not be underestimated.

To separate the burdens of surgery and anesthesia as contributing factors to organ dysfunction, the cecal slurry (CS) injection method can be used which utilizes the cecal contents of donor mice to prepare a polymicrobial bacterial slurry for intraperitoneal injection (Starr *et al.* 2014; Steele *et al.* 2017). The CS method provides microbial diversity, allows precise dose control, and allows temporal control of group illness onset without the additional complications of anesthesia and surgery. CS method of sepsis induction is relatively recent development, and few studies have evaluated long-term deficits following CS treatment. One study showed at a CS dose with 70% survival, mice exhibited deficits in grip strength, activity, and anxiety (Fujinami *et al.* 2021), suggesting the use of cecal slurry as a model of long-term decline will lead to similar cognitive deficits as those observed in other models like LPS and CLP. The choice of

model for preclinical studies is an important consideration when reporting findings and their implications towards clinical studies.

1.2 Therapeutic Rationale for Vitamin C for Protection from Septic Insult

1.2.1. ASC demand is significantly increased during sepsis.

Decreased levels of the antioxidant vitamin C (ascorbate, ASC) in the plasma of patients with severe sepsis is well-documented (Wilson 2013; Carr *et al.* 2017; Schleicher *et al.* 2009). As the immune system activates an inflammatory response to infection, oxidative stress elevates substantially due to broad production of radical species and increased metabolic demand. Presumably, this elevation in oxidative stress consumes readily available ASC reserves and accounts for the depletion of ASC in septic patients.

In a study of 44 critically ill patients, 68% had hypovitaminosis with plasma ASC levels less than 23 uM and 32% were deficient with plasma ASC levels less than 11 uM (**Supp. Fig. 1**). Normal concentrations in healthy patients range 23-50 uM, with concentrations above 50 uM considered optimal for ASC distribution throughout tissues. Patients with septic shock showing significant signs of organ failure had overall lower plasma ASC concentrations than non-septic patients implicating greater disease severity correlates with less ASC availability or likewise greater ASC demand. Patients with lower ASC levels also had approximately two-fold higher CRP levels implicating ASC availability inversely correlates with heightened inflammatory status. Lastly, patients receiving ASC supplementation during their stay had 66% lower plasma ASC levels than were predicted based on normal ASC uptake modeling suggesting increased ASC consumption or need (Carr *et al.* 2017). Decreased ASC plasma levels, higher CRP levels, and increased ASC requirement all strongly suggest a significantly increased ASC demand and impaired ASC transport during severe sepsis.

Increased ASC demand is a common finding across studies of septic patients. ASC levels in critically ill patients were less than 25% of matched healthy controls and were not explained by age or intake. Lower ASC levels were also associated with greater illness severity and greater oxidative damage to DNA, lipid membranes, and proteins (Schorah *et al.* 1996). With the intention to improve immune function and prevent oxidative stress, patients in the intensive care unit regularly receive nutritional supplementation that includes ASC (Chan *et al.* 1999;

Wintergerst *et al.* 2007). However, normal supplementation is often insufficient to replenish healthy plasma levels (Baines and Shenkin 2002). Normal intensive care unit supplementation consists of about 100 mg/day, but in critically ill patients it takes approximately 30-fold higher intake to restore normal plasma ASC levels (Long *et al.* 2003). These observations are likely due to increased metabolic demands for ASC amidst inflammation or infectious processes (Carr *et al.* 2017), but may also be due to organ or circulation dysfunction preventing proper distribution of ASC through the multi-step and endothelial dependent sodium transport systems (Harrison and May 2009). Bypassing intestinal transport through intravenous administration allows significantly higher ASC concentrations in the blood. There is significant interest in high-dose intravenous ASC trials (Marik *et al.* 2017; Holford *et al.* 2020; Lindsell *et al.* 2019) though these trials have been largely inconclusive thus far. These studies have shown minimal benefits to acute mortality rates but have not investigated potential benefits of ASC maintenance during sepsis on long-term patient outcomes including physical impairments or cognitive decline.

1.2.2. ASC accumulates in critical tissues including the brain.

Vitamin C (ascorbate, ASC) is a powerful antioxidant with critical roles for managing oxidative stress throughout the body and particularly in the brain (Harrison *et al.* 2014; Harrison and May 2009; Wilson 2005). ASC is classified as a vitamin, because humans cannot synthesize ASC and consequently depend on dietary intake to prevent deficiency. Uptake of ASC into vital tissues occurs predominantly in a two-step transport process. First, sodium dependent vitamin C transporter 1 (SCVT1) is responsible for ASC uptake from the intestine and into the circulating blood plasma. Second, sodium dependent vitamin C transporter 2 (SVCT2), which is more ubiquitously expressed and has a higher affinity for ASC, transports ASC into vital tissues. To reach the high levels of ASC required for healthy brain activity and homeostasis, ASC first accumulates in the cerebral spinal fluid by SVCT2 transport across the choroid plexus followed by SVCT2 transport directly into neurons.

ASC pharmacokinetics have been well established based on normal dietary uptake. Recommended Daily Allowance for healthy individuals is 200 mg/day, and anything over 500 mg/day is excreted in urine showing no additional benefit on tissue levels (Levine *et al.* 1996). However, the optimal daily allowance may be higher for individuals at greater risk for oxidative damage due to age, lifestyle or disease factors (Carr and Frei 1999). Because the brain is highly

susceptible to oxidative damage due to its enriched lipid composition and high metabolic activity, maintaining ASC availability in the brain is especially important to preserve long-term cognition amidst insult or injury including pathological conditions such as sepsis.

1.2.3. ASC regulates the endothelium and protects microvasculature function during sepsis.

ASC serves critical antioxidant roles during sepsis by regulating the endothelium and attenuating microvasculature dysfunction. ASC repairs lipids and proteins and recycles vitamin E (α-tocopherol), but also directly affects NO production and signaling. During severe sepsis, NADPH oxidase and NOS are activated producing large amounts of superoxide and NO radicals respectively. These two radicals react to produce peroxynitrite which activates the phosphatase PP2A. PP2A dephosphorylates the tight junction protein occludin leading to leaky endothelial barriers. ASC protects against this process scavenging superoxide, NO, and peroxynitrite (May and Harrison 2013). Increased nitric oxide production also increases vasodilation but is mitigated by ASC which disrupts NO mediated breakdown of endothelial barriers (Russell *et al.* 2018). By also specifically inhibiting iNOS expression, ASC preserves vasoconstrictor responsiveness and prevents impaired arteriolar constriction during sepsis (Wu *et al.* 2004). ASC is a required cofactor for the synthesis of collagen (May and Harrison 2013) and a cofactor for the endogenous vasopressors norepinephrine and vasopressin (Carr *et al.* 2015). Through these roles, ASC modulates redox signaling in the endothelium by targeting microvasculature dysfunction (Wilson 2009). ASC neutralization of ROS and RNS and its function as a cofactor for critical proteins and vasopressors help maintain endothelial integrity. During sepsis, ASC depletion likely contributes to the complex endothelial pathophysiology that drives organ dysfunction.

1.2.4. ASC serves a tripartite role in the brain.

In addition to protecting peripheral vasculature and tissues to support healthy brain function, ASC has specific roles within the brain. These roles can be categorized into three overlapping areas (**Fig. 2**). First, ASC is critical for neuroprotection. Through its ability to readily donate electrons to radical species, ASC protects critical DNA, proteins, and lipids from oxidation (Rice 2000; Ballaz and Rebec 2019). DNA oxidation, especially mitochondrial DNA, can alter gene expression profiles or induce cellular apoptosis (Sram *et al.* 2012). Oxidized amino acid residues compromise the function of signaling proteins, receptors, and transporters

leading to a variety of cellular dysfunctions (Harrison *et al.* 2014). Similarly, oxidation of lipid membranes leads to lipid peroxidation end products that can alter gene regulation, expression, signaling, and disrupt membrane potential (Niki *et al.* 2005; Yoshida *et al.* 2013). ASC also recycles other antioxidants such as vitamin E (α-tocopherol), preserving lipid soluble antioxidant mechanisms, and preserves the electron state of essential metals such as iron and copper (Monacelli *et al.* 2017). The role of ASC in maintaining tight endothelial barriers and preserving capillary blood flow are also generally applicable to the neuroprotection category (Kuck *et al.* 2018; Zhou *et al.* 2012; Wilson and Wu 2012). Inadequate ASC availability or distribution during severe ASC demand could drive damage in DNA, proteins, and lipids leading to neuronal apoptosis or changes in gene expression that could drastically damage cognition.

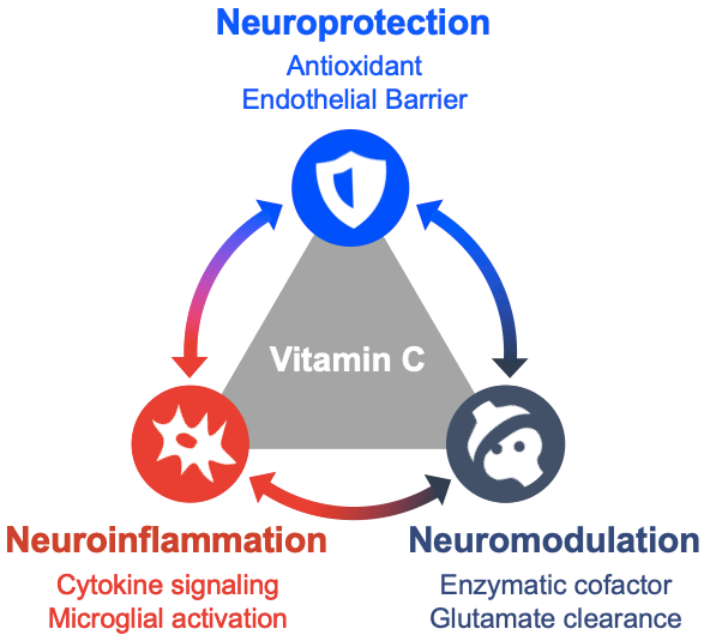

Figure 2 – Tripartite role for vitamin C in the brain.

Second, ASC serves as a neuromodulator. During excitatory neurotransmission, ASC is released by astrocytes into the synapse in exchange for glutamate uptake, preserving synapse receptor integrity and glutamate transporter function (Wilson *et al.* 2000; Rebec and Christopher Pierce 1994; Mi *et al.* 2018). ASC is required as cofactor for many enzymes including several involved in neurotransmitter synthesis. ASC is intimately involved in dopaminergic signaling through its role as a cofactor for tyrosine hydroxylase, the enzyme that catalyzes the rate limiting

step in dopamine synthesis (Opmeer *et al.* 2010; Daubner *et al.* 2011; Consoli *et al.* 2021; May 2012). Within dopaminergic synapses, ASC also protects dopamine from oxidation to which it is particularly susceptible (Rebec and Christopher Pierce 1994; Ballaz and Rebec 2019). ASC is involved in epigenetic regulation through its requirement for DNA methylation TET enzymes (Blaschke *et al.* 2013; Young *et al.* 2015; Spector and Johanson 2014). ASC also interacts with serotonin and acetylcholine, exerting neuromodulatory roles in their metabolism and binding (Ballaz and Rebec 2019; Ward *et al.* 2013). Given the direct roles of ASC in neuromodulation, the increased demand for ASC during sepsis likely contributes to neuromodulatory changes observed in sepsis including sepsis associated encephalopathy and cognitive dysfunctions.

Lastly, ASC has several roles in neuroinflammation. ASC is directly involved in the neuroinflammatory response through its neutralization of ROS and RNS which are actively produced during neuroinflammation. Activation of microglia and astrocytes during sepsis affects ASC dynamics in the brain. In the activated neuroinflammatory response, microglia produce excessive ROS and activate astrocytes. Astrocytes support neurons and synapse integrity with trophic and metabolic support (Liddelow *et al.* 2017), including uptake and recycling of the oxidized form of ASC, dehydroxyascorbate or DHA (Harrison and May 2009). ASC has suggested roles in astrocytes due to the observed upregulation of SVCT2 in reactive astrocytes (Salazar *et al.* 2018). Specific ASC regulation of microglial and astrocytic responses likely occurs through inflammatory signaling pathways. ASC inhibits transcription factor NF-kB, which regulates expression of several key cytokines (Engelmann *et al.* 2014). DHA has been shown to interact with intracellular kinase complexes that prevent NF-kB translocation to the nucleus to upregulate cytokine expression (Cárcamo *et al.* 2004), such that in conditions of high intracellular oxidative stress, sufficient ASC availability drives DHA accumulation which prevents NF-kB upregulation of proinflammatory genes (Ferrada *et al.* 2021). One group showed that LPS administration directly inhibited ASC uptake by decreasing SVCT1 and SVCT2 expression on a transcriptional level (Subramanian *et al.* 2021). These findings were observed in both a neuroblastoma cell line SH-SY5Y cells and *in vivo* in mice treated with LPS. Interestingly, they showed these changes were NF-kB pathway dependent, and found that administration of the pro-inflammatory cytokine TNF-α alone was sufficient to induce decreased ASC transporter expression and functional uptake (VS *et al.* 2021; Subramanian *et al.* 2018b; Subramanian *et al.* 2018a).

ASC also interacts with other kinase pathways, namely the Janus kinases signal transducer and activators of transcription (JAK-STAT) pathway which is intimately involved in the regulation of the inflammatory response (Seif *et al.* 2017). SVCT2 has recently been shown to interact with JAK2 when coupled with ASC transport, inducing the activation of STAT2 to induces proinflammatory cytokine gene transcription (Han *et al.* 2021). ASC regulation of the JAK-STAT pathway through a receptor-like role for SVCT2 would support ASC driven attenuation of neuroinflammation by decreasing proinflammatory gene profiles. The anti-inflammatory cytokine IL-10 plays a critical role in the brain to counteract damage following sepsis (Lobo-Silva *et al.* 2016). IL-10 also interacts with the JAK-STAT signaling pathway that leads to decreased pro-inflammatory cytokine expression, including downregulation of the major histone complex II and increases in Bcl-2 expression which inhibits apoptosis and promotes cell survival. Microglial modulation between inflammatory phenotypes also occurs partly through JAK-STAT signaling (Michels *et al.* 2019), and so ASC may promote both anti-inflammatory profiles in microglia and anti-apoptotic profiles in neurons.

1.2.5. ASC therapy shows variable efficacy in rodent models of sepsis.

Acute ASC administration in rodent models of sepsis have repeatedly shown beneficial effects on organ dysfunction outcomes. In wild-type mice, a lethal LPS dose induced lung injury evidenced by intense neutrophil sequestration, pulmonary inflammation, and microvascular thrombosis (Fisher *et al.* 2011). In two separate groups in this study, ASC or DHA (each intraperitoneal, 200mg/kg) were administered 30 min after LPS injection. Both ASC and DHA administration were sufficient to preserve lung architecture and endothelial barrier function. Similarly, the protective effects and mechanisms of ASC treatment have been shown in sepsis-associated cognitive impairment in rats (Zhang *et al.* 2021). ASC injection (intraperitoneal, 200 mg/kg) prior to CLP improved cognitive impairments 7 days following CLP in water maze task, indicated by improved escape latency and increased time spent in the target quadrant during the probe trial compared to CLP mice who received saline. 24 hours following CLP, mice treated with high dose ASC had greater number of pyramidal neurons intact in the hippocampus, decreased levels of the pro-inflammatory cytokines TNF-alpha and IL-6, and increased levels of the anti-inflammatory cytokine IL-10 in serum and hippocampal tissue extract. ASC treatment also appeared to limit blood brain barrier permeability as measured by decreased matrix

metalloproteinase 9, a collagenase that catalyzes breakdown of the endothelial extracellular matrix, and decreased levels of the lipid peroxidation product malondialdehyde. The neuroprotective effects of ASC on cognitive impairment are associated with global decreases in neuroinflammation, oxidative stress, and blood brain barrier permeability.

Most rodents except for guinea pigs can synthesize their own ASC in the presence of increased ASC demand (Harrison *et al.* 2010b) reducing the translational relevancy of such studies of sepsis in wild-type rodents. One method to overcome this obstacle is to utilize transgenic gulo$^{-/-}$ mice (Maeda *et al.* 2000). Like humans, gulo$^{-/-}$ mice lack the gene encoding gulonolactone oxidase which catalyzes the final step of ASC synthesis. Therefore, gulo$^{-/-}$ mice also depend on dietary ASC supplementation to prevent development of scurvy. Tissue levels of ASC in gulo$^{-/-}$ mice can be manipulated by modifying the supplementation provided in drinking water. Depleted tissue ASC levels can be achieved using a low supplementation dose of 0.033 g/L and anything over 0.33g/L saturates tissue levels analogous to wild-type levels (Harrison *et al.* 2008).

One sepsis study in gulo$^{-/-}$ mice compared survival following bacterial injection between mice maintained on adequate ASC supplementation (0.33 g/L) with mice provided no ASC supplementation for 25 days prior. ASC deficient mice showed increased mortality following bacterial injection by 60%, with undetectable levels of ASC in plasma at 16 hours following injection (Gaut *et al.* 2006). Interestingly, both groups showed comparable neutrophil activation, and there was no impact of ASC deficiency on oxidative products in the peritoneum lavage following the acute illness, suggesting that differences in inflammation in this model may not have contributed to the increased mortality. ASC reserves deplete readily in the absence of sufficient supplementation, so it is possible that the increased mortality was driven primarily by a lack of ASC supplementation rather than differences in inflammatory response driven by variable ASC availability.

In another study, gulo$^{-/-}$ mice were maintained on either sufficient 0.33 g/L ASC or deficient 0.033 g/L ASC prior to induction of sepsis intraperitoneal injection of a fecal stem solution (Fisher *et al.* 2014). Some of the deficient mice were given a parental infusion of ASC (200 mg/kg) 30 minutes after fecal injection. Significant tissue injury was observed in the lungs, kidney, and liver and coincided with severe coagulation abnormalities only in the ASC deficient mice. These injuries were attenuated in the group that received the ASC infusion during the onset

of illness, suggesting that ASC insufficiency directly contributes to severity of organ dysfunction. Interestingly, none of these studies in gulo$^{-/-}$ mice have investigated the neuroprotective effects of ASC sufficiency or deficiency on long-term cognitive impairment.

1.3 EEG as a Biomarker of Sepsis Associated Encephalopathy and Delirium

1.3.1. Delirium is the clinical presentation of sepsis associated encephalopathy.

Delirium during critical illness such as sepsis is one of the strongest risk factors for developing cognitive impairment following recovery (Pandharipande *et al.* 2013; Calsavara *et al.* 2018; Rengel *et al.* 2019; Iwashyna *et al.* 2010). The DSM-5 defines delirium as "primarily a disturbance of consciousness, attention, cognition, and perception that can also affect sleep, psychomotor activity, and emotions" (Nemeroff *et al.* 2013). There are four clinical criteria for delirium: acute onset or fluctuation of mental status, inattention, altered level of consciousness, and disorganized thinking with inattention being the paramount factor for delirium diagnosis (Ely *et al.* 2001). Delirium defines the clinical presentation of symptoms, but the acute cerebral pathophysiology is defined as sepsis associated encephalopathy (Zampieri *et al.* 2011). While the diagnosis criteria are well defined for delirium, little is known about what drives the acute cerebral pathophysiology. It is generally accepted that the endothelial dysfunction, cerebral hypoperfusion, and microglial-driven neuroinflammatory response associated with sepsis contribute to changes in neurotransmission (Atterton *et al.* 2020). The presence of delirium likely indicates acute underlying cognitive dysfunction driven by the acute inflammatory illness. However, other evidence suggests that delirium can be an early indicator of the onset of infection prior to clinical presentation of symptoms of sepsis (Gofton and Bryan Young 2012). Such data suggest that sepsis associated encephalopathy may instead be a driver of early organ dysfunction rather than a consequence.

Diagnosing delirium in patients is primarily performed using confusion assessment methods such as CAM-ICU (Ely *et al.* 2001). CAM-ICU evaluates the four criteria of delirium in a test that is easy to perform and takes less than three-minutes. First, it assesses the acute onset or fluctuation in mental status by noting changes from baseline or agitation severity. Then inattention is assessed using the attention screening exam (Hart *et al.* 1996) which consists of a

visual task where the patient is asked to remember 5 simple pictures over a short time interval and audio task where the patient is asked to respond to a series of letters read aloud. Disorganized thinking is assessed by asking simple reasoning questions such as "Will a stone float on water? Are there fish in the sea? Does one pound weigh more than two pounds? Can you use a hammer to pound a nail?" For patients with limited speech capability due to mechanical ventilation, the test can still be performed by asking the patient to respond by nodding of the head or squeezing of the hand. Lastly, the test defines each condition of consciousness: alert, vigilant, lethargic, stupor, coma. Incorrect answers to questions, missed responses, and any level of consciousness other than alert count towards delirium diagnosis.

Delirium is reported in up to 82% of patients in intensive care units and predicts mortality (Ely *et al.* 2004). Use of benzodiazepine, opioid, vasopressor infusions, antipsychotics, and mechanical ventilation all have higher risk of delirium the next day (Pun *et al.* 2021). While some of these are required for managing severe sepsis, minimizing use of benzodiazepines, and increasing socialization are modifiable strategies to reduce the risk of acute brain dysfunction.

1.3.2. Delirium severity and duration is associated with cognitive decline.

Risk factors for cognitive impairments following sepsis suggest that delirium is a strong clinical indicator of neurological damage. Prolonged mechanical ventilation, delirium, illness severity, acute respiratory distress syndrome, pre-existing comorbidities, heavy sedation exposure, and baseline cognitive dysfunction are all associated with functional and cognitive impairment following sepsis (Rengel *et al.* 2019; Calsavara *et al.* 2018; Sasannejad *et al.* 2019). The mechanisms by which delirium drives long-term cognitive changes are not well understood. Data suggest that the risk factors for delirium, including mechanical ventilation and acute respiratory distress syndrome, likely contribute to accumulation of cytokine-mediated hippocampal damage through weakening of the blood brain barrier which accelerates existing or predisposed cognitive dysfunction (Sasannejad *et al.* 2019).

In a study of 821 patients admitted to the intensive care unit, 74% of patients had delirium (Pandharipande *et al.* 2013). Global cognition scores determined by the Repeatable Battery for the Assessment of Neuropsychological Status (RBANS) found that 40% were equivalent to scores observed in patients with traumatic brain injury and 26% were comparable to mild Alzheimer's disease at three months follow-up (**Supp. Fig. 2**). At one year follow-up,

34% resembled traumatic brain injury and 24% still showed scores comparable to mild Alzheimer's disease. These findings were consistent across two different age demographics in both young and old patients. When RBANS score at 12 months follow-up was compared to duration of delirium during stay, delirium duration strongly correlated with worsened cognitive decline. This study and many similar studies provide evidence that delirium and its pathophysiology of acute sepsis associated encephalopathy are strong risk factors for long-term cognitive decline.

1.3.3. EEG abnormalities are prevalent in delirious patients and correlate with delirium severity.

Serum biomarkers of delirium have limited clinical utility in diagnosing delirium or predicting delirium duration and severity (Toft *et al.* 2019; Atterton *et al.* 2020). Electroencephalography, or EEG, is a relatively inexpensive and simple way to collect data that reflects global changes in brain activity. EEG metrics have been used for decades to study the acute pathophysiology associated with delirium (Engel and Romano 1959; Jacobson *et al.* 1993). However, research is just beginning to unravel the complex etiologies of EEG patterns during various brain dysfunctions (Palanca *et al.* 2017; Zarea *et al.* 2016). EEG activity is commonly separated into distinct power bands (**Table 2**) that separate patterns based on specific frequency ranges (Louis and Frey 2016). Delta (0-4 Hz) and Theta (4-8 Hz) frequencies are considered slow-wave brain activity and are associated with deep sleep and paradoxical sleep. Alpha (8-12 Hz) frequencies are associated with attention. During wakeful rest with eyes closed, healthy brain activity exhibits a posterior dominant alpha rhythm that is ablated when eyes are opened. Sigma (12-16 Hz) are not commonly reported and generally are unaffected by higher or lower frequency changes. Faster frequencies in the beta (16-20 Hz) and gamma (20-50 Hz) are associated with active, higher order thinking and problem solving.

Table 2 – EEG power bands associations with brain activity.

Power Band	Normal	During Critical Illness
Delta (0-4 Hz)	Deep Sleep	Generalized Increased Background
Theta (4-8 Hz)	Sleep and Paradoxical Sleep	Increased, Focal or General, Intermittent or Persistent

Alpha (8-12 Hz)	Wakeful Rest, General Attention, Posterior Dominant Rhythm	Decreased and Unresponsive
Sigma (12-16 Hz)	Not Frequently Observed or Reported	Not Frequently Observed or Reported
Beta (16-25 Hz)	Active Wake with Mental Activity	Decreased or Absent
Gamma (25-50 Hz)	Complex Tasks and Problem Solving	Decreased or Absent

(Louis and Frey 2016; Koponen *et al.* 1989; Palanca *et al.* 2017; Roberson *et al.* 2020; Atterton *et al.* 2020)

During critical illness, focal and generalized EEG slowing are regularly observed. Slowing may be intermittent or persistent and focal or generalized, with more consistent EEG slowing generally indicating more severe underlying cerebral dysfunction. Specific causes of EEG slowing remain elusive, however, EEG slowing occurs in a variety of inflammatory driven pathological conditions including ischemia, hemorrhage, tumors, traumatic injury, and sepsis associated encephalopathy (Louis and Frey 2016), suggesting injury and inflammation play key roles in decreasing healthy cerebral responsiveness. Anterior or bifrontal areas produce distinct patterns including frontal intermittent rhythmic delta activity and lateral periodic discharges (Palanca *et al.* 2017). In one study, sporadic EEG discharges without status epilepticus occurred in 15% of patients, and preserved beta activity showed lower incidence of delirium, presumably due to increased active thinking during illness (Nielsen *et al.* 2019). Slow-wave dominance, disrupted alpha rhythms, and increasingly well-defined EEG abnormalities are becoming strong biomarkers for delirium severity (Jacobson *et al.* 1993; Atterton *et al.* 2020; Palanca *et al.* 2017; Hirsch *et al.* 2021).

Classic studies defined delirium as a syndrome of cerebral insufficiency characterized by clinically observed inattention and generalized slowing of EEG activity. Without robust clinical testing such as the CAM-ICU, 70% of delirium goes undetected due to patients' ability to hide delirium with pleasantness or humor (Engel and Romano 1959; Ely *et al.* 2001), which effects sepsis treatment and management and contributes significantly to the risk for cognitive decline. Spectral analysis of EEG in delirium shows increased theta and delta activities, obvious changes in individual recordings, and decreased alpha power responsiveness all associated with poorer mini mental state score (Koponen *et al.* 1989). Clinical EEG slowing correlates with delirium severity and predicts poor clinical outcomes including mortality (**Supp. Fig. 3**) and long-term

cognitive impairments (Kimchi *et al.* 2019; Roberson *et al.* 2020). EEG as a biomarker for delirium has powerful clinical implications for managing delirium severity and preventing long-term cognitive damage.

1.3.4. Mouse models of sepsis using EEG and behavioral tasks are limited.

Some studies have performed EEG recordings in septic animals, but most of these studies utilize EEG only as a biomarker to confirm delirium incidence rather than to characterize the cerebral pathology of sepsis associated encephalopathy. Additionally, the use of tethered EEG systems limits synchronized behavioral assessments in these models. One group developed rodent models of delirium using the medicinal muscle relaxant atropine and tethered EEG systems (Trzepacz *et al.* 1992; Leavitt *et al.* 1994). These studies were not extensive in their EEG analysis but did note EEG changes including increased amplitude and decreased frequencies that were indicative of generalized EEG slowing. A more recent study investigated the contrasting effects of scopolamine and LPS on acute behavioral outcomes in rats (Kimchi *et al.* 2017). Both treatment groups showed delirium related phenotypes in EEG metrics including increased delta power and decreased gamma power. The rats simultaneously showed decreased auditory discrimination in a behavioral assessment of attention. No behavioral tasks were completed following recovery to evaluate the effects of delirium on long-term cognition. Another used EEG only to confirm the onset of sepsis associated encephalopathy, but did not further analyze EEG metrics or compare them to clinical data (He *et al.* 2018). In this study, increases in Delta power were associated with decreases in neurobehavioral score, suggesting that observed EEG slowing can predict delirium intensity during illness. However, the association between such delirium severity measured by EEG and long-term cognitive outcomes in rodent models of sepsis remains to be investigated.

Approach

To understand how sepsis pathophysiology impacts the brain and contributes to development of long-term cognitive deficits, we performed three overarching experiments. First, we established timelines for oxidative and ASC related changes following CS treatment in wild-type mice. Then we assessed behavioral and cognitive outcomes following long-term recovery from CS treatment in gulo$^{-/-}$ mice which like humans are incapable of synthesizing ASC. Finally,

we utilized surgically implanted telemetry devices to record and characterize EEG metrics during illness supplemented with synchronized cognitive behavioral testing and *ex vivo* hippocampal electrophysiology.

CHAPTER 2

A Cecal Slurry Mouse Model of Sepsis Leads to Acute Consumption of Vitamin C in the Brain

Publication Acknowledgement

This chapter is published in *Nutrients* and has been reproduced with the permission of the publisher and my co-authors (F.E. Harrison & J.A. Bastarache).

Consoli, D. C., Jesse, J. J., Klimo, K. R., Tienda, A. A., Putz, N. D., Bastarache, J. A., & Harrison, F. E. (2020). A Cecal Slurry Mouse Model of Sepsis Leads to Acute Consumption of Vitamin C in the Brain. *Nutrients*, *12*(4), 911. https://doi.org/10.3390/nu12040911

Abstract

Vitamin C (ascorbate, ASC) is a critical antioxidant in the body with specific roles in the brain. Despite a recent interest in vitamin C therapies for critical care medicine, little is known about vitamin C regulation during acute inflammation and critical illness such as sepsis. Using a cecal slurry (CS) model of sepsis in mice, we determined ASC and inflammatory changes in the brain following the initial treatment. ASC levels in brain were acutely decreased by approximately 10% at 4 and 24 hours post CS treatment. Changes were accompanied by robust increase in liver ASC levels of up to 50% indicating upregulation of synthesis beginning at 4 hours and persisting up to 7 days post CS treatment. Several key cytokines IL-6, IL-1β, TNFα, and CXCL1, KC/Gro were also significantly elevated in the cortex at 4 hours post CS treatment, although these levels returned to normal by 48 hours. These data strongly suggest that ASC reserves are directly challenged throughout illness and recovery from sepsis. Given the timescale of this response, decreases in cortical ASC are likely driven by hyper-acute neuroinflammatory processes. However, future studies are required to confirm this relationship and to investigate how this deficiency may subsequently impact neuroinflammation.

2.1 Introduction

Sepsis is estimated to affect more than 30 million people and account for more than 5 million deaths annually (Fleischmann *et al.* 2016). During this critical illness, the robust inflammatory response of the immune system includes release of multiple cytokines and other signaling molecules that can ultimately lead to severe tissue injury and multiple organ failure (Kuhn *et al.* 2018; Ince *et al.* 2016; Biesalski and McGregor 2007). This damage extends to the brain as evidenced by delirium in the majority of patients (Zampieri *et al.* 2011). Despite the advances in clinical understanding of delirium during sepsis, little is known about the cellular and molecular underpinnings of acute brain dysfunction in critically ill patients. Sepsis patients often exhibit low plasma levels of vitamin C (ascorbate, ASC) (Borrelli *et al.* 1996; Galley *et al.* 1996; Fujii *et al.* 2019; Hudson *et al.* 2019). In one study, as many as 88% of sepsis patients had subnormal plasma levels of ASC (<23 μM) and up to 38% had severe ASC deficiency (<11 μM) (Carr *et al.* 2017), suggesting high demand for ASC during septic insult. Lower plasma levels of ASC are also associated with increased incidence of multiple organ failure and decreased survival (Fowler *et al.* 2014). The brain is particularly susceptible to this dysregulated inflammatory response and suboptimal ASC levels, because higher oxidative stress levels in the brain are especially damaging to its enriched lipid composition and nutrient demanding metabolic rate (Magistretti and Allaman 2015; Cobley *et al.* 2018). Up to 30% of patients are reported to experience cognitive deficits following recovery from sepsis (Calsavara *et al.* 2018; Iwashyna *et al.* 2010; Annane and Sharshar 2015), and several studies using rodent sepsis models have shown that acute illness damages cognition in surviving animals (Anderson *et al.* 2015; Zaghloul *et al.* 2017; Hippensteel *et al.* 2019).

ASC is a critical antioxidant for cellular function and has an emerging role in immune function (Carr and Maggini 2017). Preclinical studies have shown a variety of beneficial effects on the pathophysiological changes in sepsis including protection against microvascular dysfunction and deficits in vasoconstriction (Armour *et al.* 2001; Wu *et al.* 2004; Mckinnon *et al.* 2007) by preserving tight endothelial barrier function and capillary blood flow (Han *et al.* 2010; Tyml *et al.* 2008; Zhou *et al.* 2012). ASC administration during sepsis also attenuates acute lung injury (Fisher *et al.* 2011) and improves multiple organ dysfunction syndrome in animal models of sepsis (Fisher *et al.* 2014; Gao *et al.* 2017). The role of intravenous ASC in

clinical practice to improve short term patient recovery is still under clinical investigation (Fujii *et al.* 2020; Fowler *et al.* 2019). ASC accumulates in the brain via the sodium dependent vitamin C transporter 2 (SVCT2) in a two-step process from blood into the choroid plexus cerebral spinal fluid and then into neurons (Harrison and May 2009). In the brain, ASC serves two primary roles as a neuroprotector and neuromodulator (Harrison and May 2009; Harrison *et al.* 2014; Ballaz and Rebec 2019). ASC maintains blood brain barrier integrity by preserving tight endothelial barriers (Kuck *et al.* 2018; Lin *et al.* 2010) and maintaining capillary blood flow (Wilson and Wu 2012). ASC is a critical enzymatic co-factor in neurotransmitter synthesis and DNA methylation (Harrison and May 2009; Young *et al.* 2015) and is intimately involved in preserving glutamatergic neurotransmission through the glutamate-uptake ASC-release exchange (Wilson *et al.* 2000; May 2012; Mi *et al.* 2018). Despite the interest in ASC as a treatment for preventing organ failure in sepsis, the roles of ASC in the brain, and the number of patients experiencing cognitive deficits following recovery from the acute trauma, the effects of sepsis on the brain are understudied. Furthermore, the specific role of ascorbate in sepsis induced brain dysfunction has not been studied. Here, we utilized a cecal slurry (CS) model of sepsis in mice to observe changes in ASC and inflammatory response in the brain during and following sepsis. We hypothesized that ASC is depleted in sepsis and sought to define a timeline for changes in ASC level and cytokine release, particularly in the brain.

2.2 Materials and Methods

2.2.1. Mouse CS or LPS Treatment

All experiments conducted with live mice were reviewed and approved by the Vanderbilt Institutional Animal Care and Use Committee. Cecal slurry (CS) was used to induce acute peritonitis in mice as a model of sepsis as previously described (Shaver *et al.* 2019; Meegan *et al.* 2020; Kerchberger *et al.* 2019). C57/Bl6J donor mice at six weeks of age were obtained from Jackson Laboratory (#000664) and euthanized within 7 days of arrival. Cecal contents were collected and resuspended in 5% dextrose at 80 mg/ml, then filtered through a 100 μm filter. Aliquots were stored at -80°C until ready for use.

All mice for treatment groups were bred in house from C57/Bl6J mice originally obtained from Jackson Laboratory. Mice at 10-12 weeks of age were treated with CS (1.5 mg/g; i.p.) or

the vehicle 5% dextrose for control groups. Another widely used model of peripheral inflammatory response utilizes lipopolysaccharide (LPS) administration. For LPS studies, mice at 6-8 weeks of age received LPS (3.75 µg/g; i.p.) or saline. Control and treated mice were distributed across cages and provided with supplemental nutrition on the floor of the cage (DietGel 76A, Clear H_2O) to promote survival.

2.2.2. Evaluation of Sickness Score

An observer blinded to treatment groups scored the mice on the severity of sepsis using a 12 point scale of sickness severity where 12 is healthy with normal activity and 0 is moribund (Su *et al.* 2013; Manley *et al.* 2005). In brief, the score is determined by response to finger poke (4 for normal, 3 for decreased, 2 for severely decreased, or 1 for minimal response), signs of encephalopathy (4 for normal, 3 for tremors or staggering, 2 for twisting movements, or 1 for turning), and general appearance (score is decreased by 1 for each display of piloerection, periorbital exudates, respiratory distress, or diarrhea). All mice were monitored closely for 48 hours or until mice recovered to a normal score of 12. CS treated mice that never received a score below 10 or died prior to assigned timepoint were excluded from analysis.

2.2.3. Tissue Collection

Mice were anesthetized with isoflurane then euthanized by decapitation at 4, 24, 48 hrs or 7 days post-injection. Control mice were euthanized at each timepoint, and data collapsed in to one group. Tissue samples were collected, flash frozen on dry ice, and stored at -80°C for further analysis.

2.2.4. Ascorbic Acid HPLC

Sample extracts were prepared by adding 10 µl extraction buffer (7:2 25% w/v metaphosphoric acid: 100 mM sodium phosphate, 0.05 mM EDTA pH 8.0) per mg of wet tissue to normalize by weight. Samples were homogenized with 0.5 mm ceria stabilized zirconium oxide beads (Next Advance, Inc.) in a bullet homogenizer, centrifuged at 10,000 rpm, and the clear supernatant transferred into a fresh tube. Concentrations of ASC were measured at 1:100 dilution in triplicate with ion pair HPLC using tetrapentyl ammonium bromide as the ion pair

reagent and electrochemical detection as previously described (Harrison *et al.* 2008; May *et al.* 1998).

2.2.5. Determination of gene expression

RNA was extracted using RNeasy Mini kit (Qiagen). qPCR was performed using PrimePCR Probe Assay consisting of iScript cDNA synthesis, PrimePCR Probes (PrimePCR™ Probe Assay: Slc23a1, Mouse), and Sso Advanced Universal Supermix (Bio Rad).

2.2.6. Measurement of Oxidative Stress Markers

Malondialdehyde, a lipid peroxidation end product, was measured by fluorescent spectrophotometric assay of thiobarbituric acid reactive substances (TBARS) as previously described (Harrison *et al.* 2009). Sulfhydryls were measured by reduction of DTNB to TNB by thiol groups and spectrophotometric analysis (Sgaravatti *et al.* 2009; Aksenov and Markesbery 2001).

2.2.7. Measurement of Cytokine Expression

Frozen mouse tissues were homogenized in volumes of RIPA buffer (Thermo Fisher Scientific) normalized by tissue weight. Tissue levels of IFN-y, IL-1b, IL-6, KC/GRO, IL-10, and TNF-alpha were assayed in duplicate using a V-PLEX Custom Mouse Cytokine Kit, (Meso Scale Diagnostics, LLC) according to manufacturer's instructions (Bastarache *et al.* 2014).

2.2.8. Statistical analyses

Statistical analyses were performed using Graphpad Prism software (version 8.3.0). Data were first checked for equality of group variances using the Brown-Forsyth test and analyzed using parametric statistics. We did not expect any differences in response to CS according to sex, and all data were first analyzed using a multivariate ANOVA analysis including sex as an additional variable. There were no main effects of sex on any of the key outcomes (sickness score, weight loss, ASC levels) so data were combined for all subsequent analysis. For outcomes following CS treatment data were analyzed with univariate ANOVA with group (encompassing treatments and time post treatment) as the main independent variable. Significant omnibus ANOVA were followed with Dunnett's post hoc analyses to test difference from control group.

Independent t-tests were used to test effects of LPS versus treatment with the vehicle. Numerical outliers that likely reflected experimental error were identified and removed using ROUT (Q = 5%). Error bars are shown as SEM or SD as indicated in figure legends.

2.3 Results

2.3.1. CS treatment induces acute peritonitis and weight loss.

Mice that received CS treatment became severely lethargic and exhibit decreased response, signs of encephalopathy, and worsened appearance by 12 hours (**Fig. 3A**). Sickness scores decreased as early as 4 hours, began to recover by 24 hours, and returned to normal appearance and activity by 48 hours (**Fig. 3B**; CS Treatment $F_{(1, 63)} = 113.8$, $P < 0.001$; Time $F_{(5, 59)} = 15.61$, $P < 0.001$). CS treatment also caused significant weight loss that persisted to 48 hours, although mice regained weight by 7 days post CS treatment (**Fig. 3C**; CS Treatment $F_{(1, 63)} = 121.3$, $P < 0.001$; Time $F_{(5, 59)} = 24.06$, $P < 0.001$). Out of 55 CS treated mice, only 2 mice died before their scheduled timepoint. This mild 1.5 mg/g dose was chosen to optimize survival to 7 days post CS treatment. The 4% mortality rate at this dose is low compared to other studies utilizing this CS model (2.0 mg/g, up to 67% by 48 hours) (Kerchberger *et al.* 2019; Shaver *et al.* 2019).

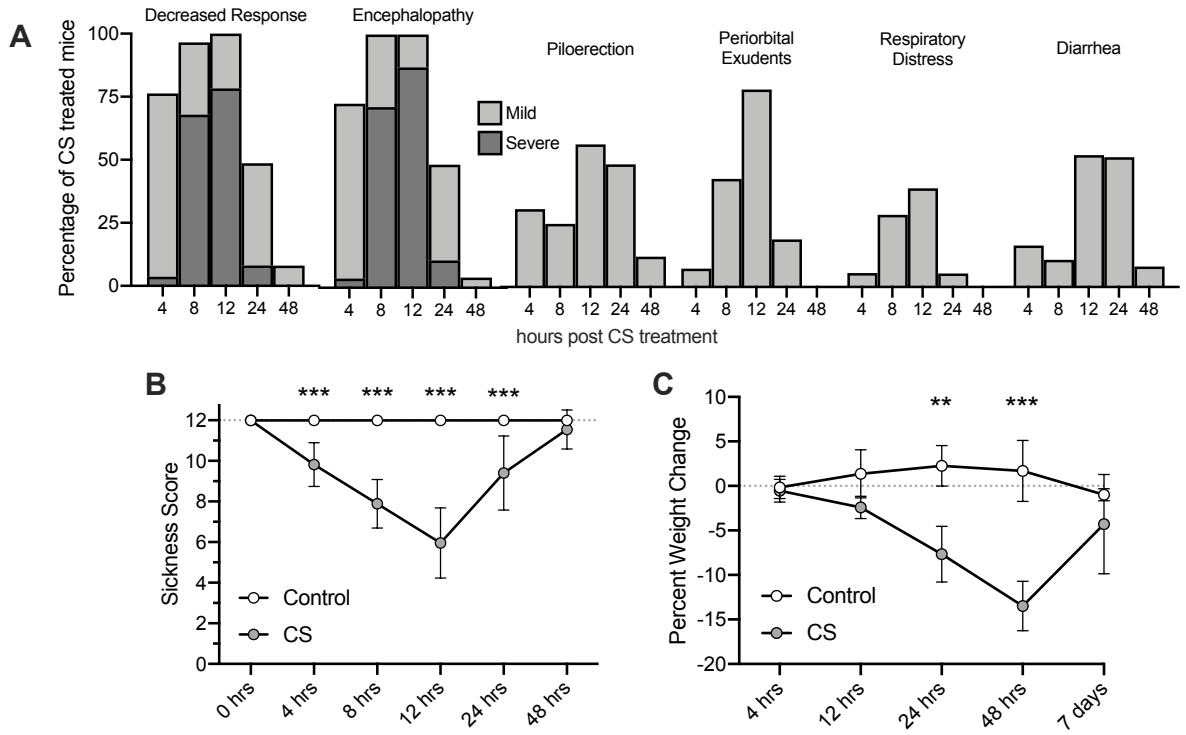

Figure 3 – Sickness scores and percent weight change following CS treatment. (**A**) Percentage of mice showing sickness behaviors and appearances. (**B**) Clinical Sickness Scores. (**C**) Weight loss. **P* < 0.05, ***P* < 0.01****P* < 0.001. Error bars plotted as mean ± SD.

2.3.2. Tissue ASC concentrations following CS treatment.

There was a small (~10% at 4 hrs) but significant decrease in cortical ASC at 4 and 24 hours following CS treatment compared to controls (**Fig. 4A**, $F_{(4, 54)} = 3.216$, $P = 0.0193$,), indicating consumption of brain ASC reserves. Liver ASC levels were significantly increased following CS treatment (~50% at 24 hrs) indicating robust upregulation of ASC synthesis (**Fig. 4B**, $F_{(4, 54)} = 5.090$, $P = 0.0015$) that persisted to 7 days post CS treatment. No significant differences in ASC levels were observed in peripheral organs of CS-treated mice compared to controls, although levels varied post CS treatment (Kidney: **Fig. 4C**, $F_{(4, 54)} = 2.153$, P = 0.0867; Lung: Fig. 2D, $F_{(4, 55)} = 3.188$, $P = 0.020$,). We hypothesized that a decrease in ASC levels in the brain would result in upregulation of SVCT2 expression, though no significant changes were observed in hippocampal SVCT2 expression in response to CS treatment (**Fig. 4E**, $F_{(4, 38)} = 2.235$, $P = 0.0833$).

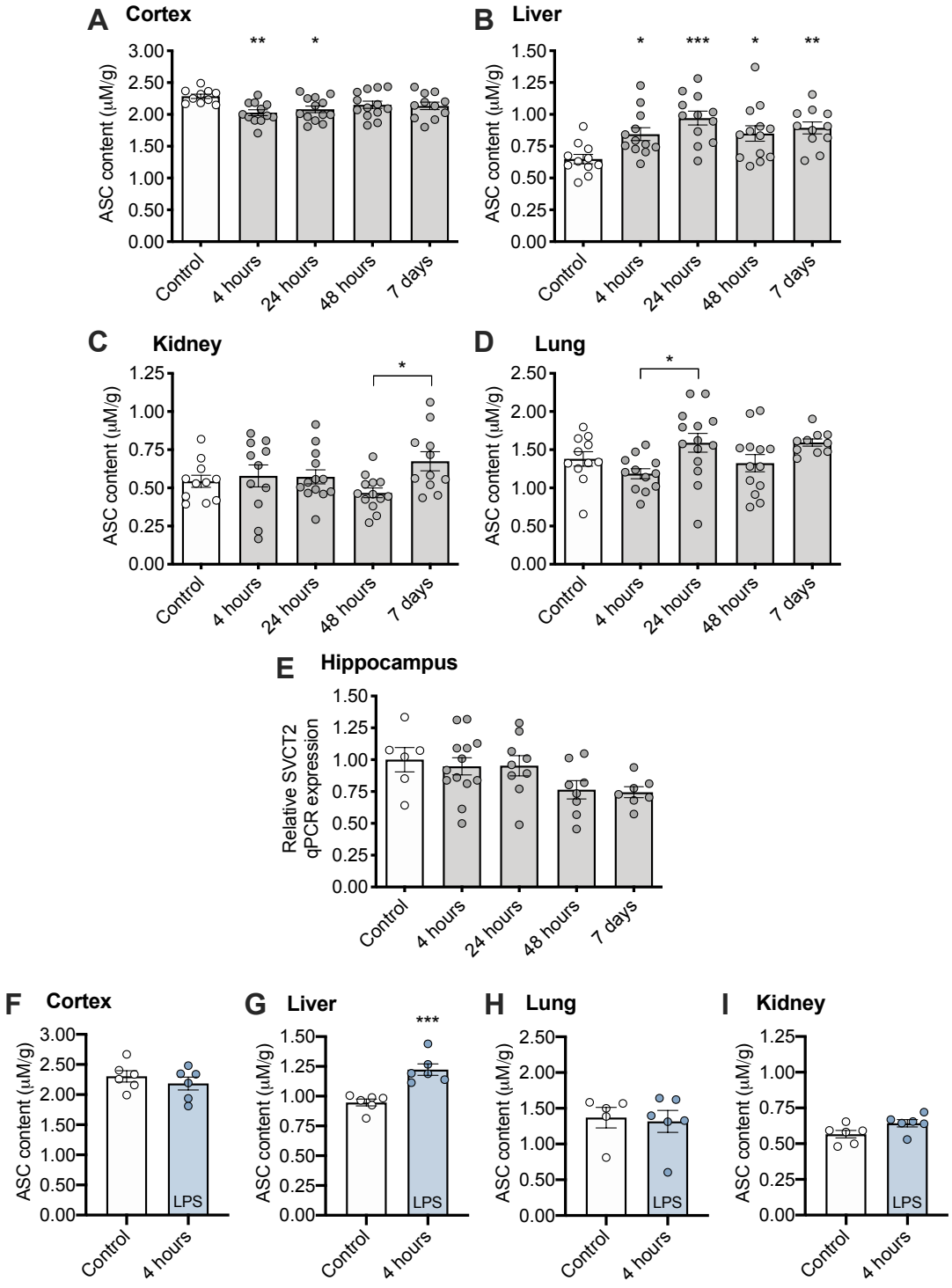

Figure 4 – Tissue ASC concentrations following CS treatment.
(**A**) Cortex, (**B**) liver, (**C**) kidney, (**D**) lung. (**E**) Sodium dependent vitamin C transporter 2, SVCT2 gene expression in brain following CS treatment. Tissue ASC concentrations following LPS treatment (**F**) brain, (**G**) liver, (**H**) lung, and (**I**) kidney. $*P < 0.05$ $**P < 0.01$ $***P < 0.001$ from control following significant ANOVA results unless otherwise indicated. Error bars plotted as mean ± SEM.

No decrease in brain ASC level was observed at 4 hours following LPS treatment (**Fig. 4F**, t(10) = 0.842, $P = 0.4197$). However, LPS treatment also induced upregulation of ASC synthesis in liver (**Fig. 4G**, t(10) = 4.913, $P < 0.001$). No changes were observed in lung (**Fig. 4H**, t(9) = 0.246, $P = 0.8111$,) or kidney (**Fig. 4I**, t(10) = 2.066, $P = 0.0658$).

2.3.3. CS treatment does not induce changes in oxidative stress measurements.

CS treatment did not increase either of the oxidative stress markers malondialdehyde (Cortex: **Fig. 5A**, $F_{(4, 33)} = 2.092$, P = 0.1042; Liver: **Fig. 5B**, $F_{(4, 33)} = 1.833$, P = 0.1459) or sulfhydryls (Cortex: **Fig. 5C**, $F_{(4, 30)} = 0.6471$, P = 0.6333; Liver: **Fig. 5D**, $F_{(4, 35)} = 2.210$, P = 0.0880) in the brain.

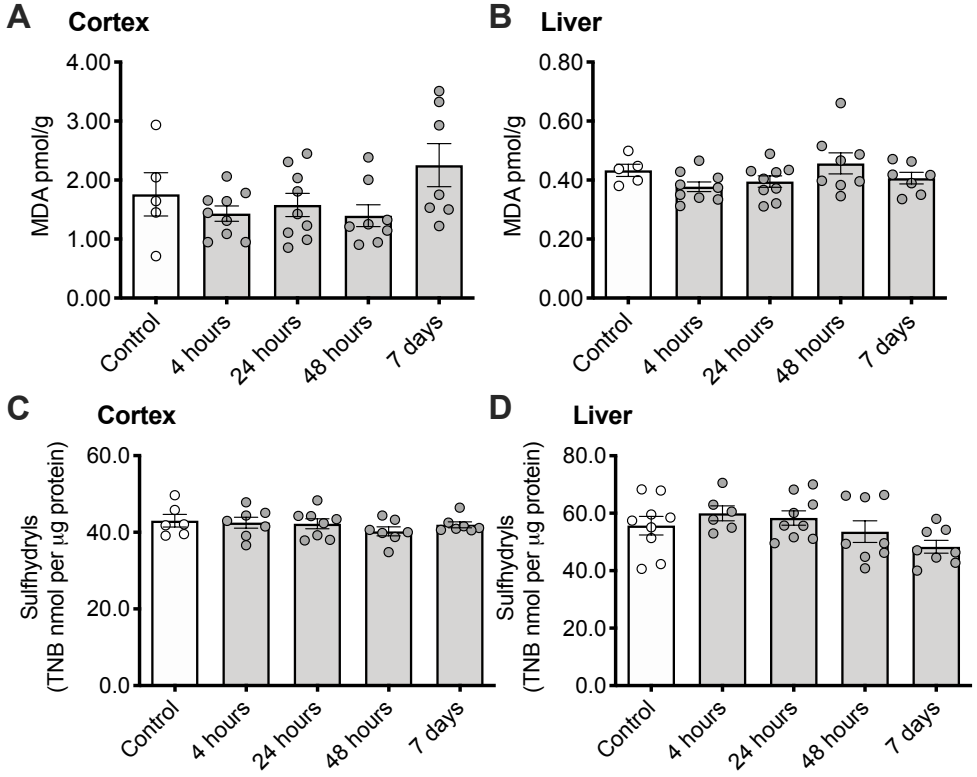

Figure 5 – Indicators of oxidative stress following CS treatment.
Malondialdehyde (MDA) in cortex (**A**) and liver (**B**) or sulfhydryls in cortex (**C**) and liver (**D**).
Error bars plotted as mean ± SEM.

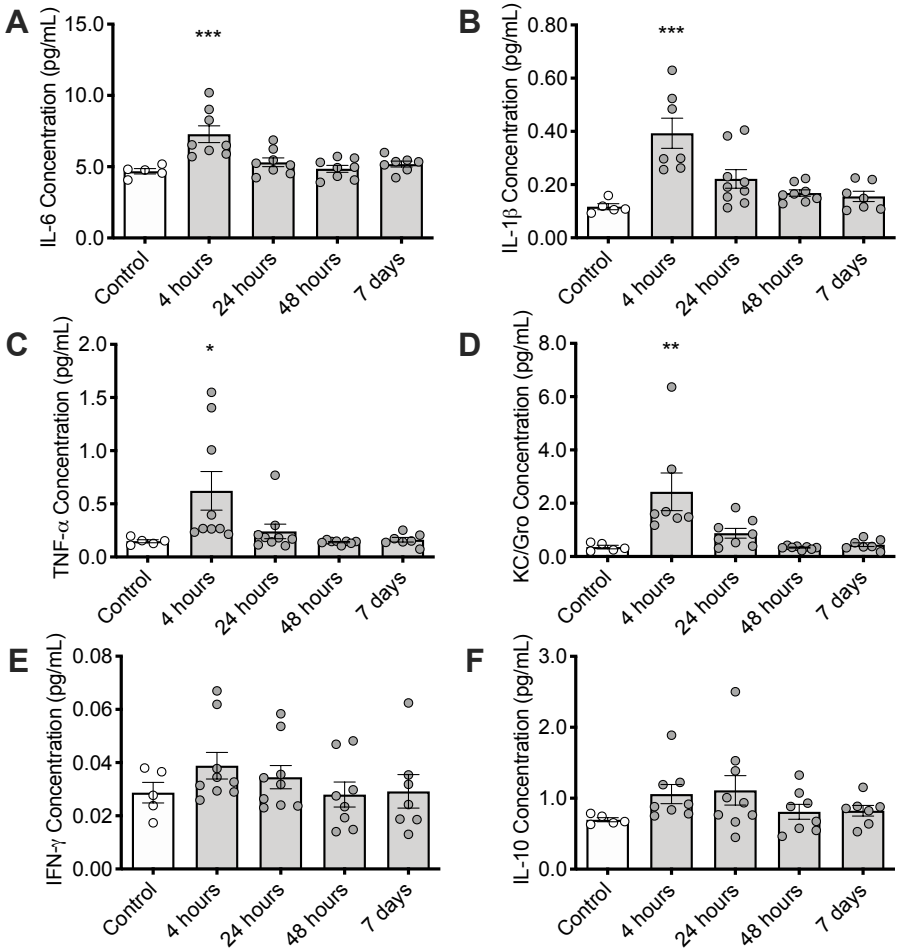

Figure 6 – Timeline of inflammatory changes in the brain following CS treatment. Cortical cytokine levels of (**A**) interleukin 6 (IL-6), (**B**) interleukin 1β (IL-1β), (**C**) tumor necrosis factor alpha (TNFα), and (**D**) chemokine (C-X-C motif) ligand 1 (CXCL1, KC/Gro), (**E**) Interferon gamma (INFγ) and (**F**) interleukin 10 (IL-10) $*P < 0.05$, $**P < 0.01$, $***P < 0.001$. Error bars plotted as mean ± SEM.

2.3.4. CS treatment initiates an inflammatory response in the brain.

In cortex, expression of several proinflammatory cytokines was elevated at 4 hours post CS treatment including Interleukin 6 (IL-6: $F_{(4, 31)} = 8.356$, $P < 0.001$), Interleukin 1β (IL-1β: $F_{(4, 31)} = 9.742$, $P < 0.001$), Tumor necrosis factor alpha (TNFα: $F_{(4, 33)} = 4.261$, $P = 0.0069$), Chemokine (C-X-C motif) ligand 1 (CXCL1, KC/Gro: $F_{(4, 30)} = 7.091$, $P < 0.001$) (**Fig. 6A-D**). Cytokine expression levels returned to normal by 48 hours post CS treatment. More modest increases in Interferon gamma (INFγ: F (4, 33) = 0.9214, $P = 0.4632$) and interleukin 10 (IL-10: $F_{(4, 32)} = 1.442$, $P = 0.2430$) were not statistically significant (**Fig. 6E-F**).

2.4 Discussion

Despite significant clinical interest in ASC as a potential therapeutic adjuvant, the role of ASC in sepsis, particularly in the brain, has not been well studied. The present study highlights the potential rapid, although modest, consumption of ASC stores during and following sepsis co-occurring with the associated inflammatory changes that occur in the brain.

Mice and most other rodent species possess the gene encoding gulonolactone oxidase, an enzyme responsible for catalyzing the final step in ASC synthesis in the liver (Gabbay *et al.* 2010; Levine and Downing 1992; Ching *et al.* 2001a; Ching *et al.* 2001b). Synthesis can be upregulated to provide higher tissue levels in liver under periods of increased physiological need, such as pregnancy (Harrison *et al.* 2010a). ASC depletion in brain is rare in non-genetically modified mice, however, increased liver levels indicate upregulation of ASC synthesis to prevent depletion. In the brain, high concentrations are critical for maintaining optimal brain function and preventing oxidative damage (Jackson *et al.* 1998; Harrison and May 2009; Harrison *et al.* 2014). CS treatment resulted in an approximately 10% decrease in ASC in cortex (**Fig. 4A**) even in this relatively mild sepsis model, and despite upregulation of synthesis in the liver. The two step transport system of ASC into the brain by SVCT2 from blood into the choroid plexus cerebral spinal fluid and then into neurons, allows for preservation of ASC at the expense of other tissues (Harrison and May 2009). It is possible that other brain regions, such as the hippocampus, may have different levels of susceptibility to ASC depletion due to varying proximity to the ventricles and choroid plexus, and future studies should address different brain areas, including hippocampus, in analysis.

Over this short time interval, we did not observe decreased ASC levels in most peripheral organs including lung and kidney (**Fig. 4C, D**) and heart, muscle, spleen, and adrenal gland (data not shown). We observed significant increase in liver ASC by 4 hours in both CS and LPS treated mice (**Fig. 4B, G**). Our data confirm results of prior work in which LPS-induced increase in liver ASC was observed from 3 hours post LPS treatment (Kuo *et al.* 2005). LPS treatment did not fully recapitulate the ASC changes we observed with CS treatment, possibly due to the dose initiating a lower neuroinflammatory effect or different pathways, although this was not directly tested. While no changes were observed in brain in that study (Kuo *et al.* 2005), the lack of cortical ASC deficiency in the LPS model may be a limitation of intraperitoneal LPS as a model

of sepsis. We hypothesize that increased synthesis in liver provided sufficient circulating levels to replenish (brain) or protect (lung, kidneys) peripheral tissues during the timeframe and dose studied. It took more than 24 hours to replete brain ASC, possibly due to slower brain uptake since ASC must first accumulate in the cerebral spinal fluid. Future experiments should be performed in transgenic mice that are, like humans, incapable of synthesizing ASC (e.g. gulonolactone oxidase knockout mice) (Harrison *et al.* 2008; Maeda *et al.* 2000), and are therefore unable to upregulate hepatic synthesis to meet increased need. Such models could also be used to establish a timeline of circulating ASC levels in plasma as well as testing whether a clinically relevant ASC pretreatment (Wilson 2013) is capable of protecting against decreased brain ASC, neuroinflammatory changes, or severity of observed sickness. If peripheral ASC administration is unable to change cortical ASC levels, this would suggest blood-brain barrier transport of ASC is limiting early in sepsis or that there is high uptake by other organs. However, if neuroinflammation is improved by pretreatment with ASC, this would suggest that ASC deficiency may be directly associated with sepsis-associated neuroinflammation.

The CS dosing regimen used (1.5 mg/g) causes a mild sickness response chosen to optimize recovery and survival to 7 days post treatment. Nevertheless, this modest insult was still sufficient to deplete ASC and increase cytokine production in the brain at 4 hours after injection (**Fig. 6**) when the mice are just starting to become systemically ill. This finding suggests that the brain is adversely affected by systemic inflammation in the earliest stages of illness. The release of cytokines in the brain at this time indicates activation of brain macrophages and resident microglia, which generate reactive oxygen species. The observed ASC depletion likely indicates ASC plays a primary role in electron donation to neutralize these free radicals, and that the oxidative stress was sufficient to overwhelm ASC recycling capacity. While future studies will need to clarify the relationship between ASC deficiency and neuroinflammation, it is most likely that ASC deficiency is driven by the acute neuroinflammatory response and associated generation of radical species. Oxidative stress is a key component of clinical sepsis (Prauchner 2017), and although the global oxidative measurements did not show elevations in brain or liver oxidative stress under these conditions, any reduction in brain ASC and especially upregulation of liver ASC synthesis indicates elevated oxidative challenge. The measures of global tissue MDA may not have been sensitive enough to detect localized increases in oxidative stress in specific cells (endothelium, for example) or tissue compartments. Despite the activated immune

response and challenge of brain ASC stores we did not observe upregulation of the sodium dependent vitamin C transporter SVCT2 in brain tissue. To confirm the association between ASC consumption and acute inflammatory challenge in a second model, we used LPS to induce endotoxemia and systemic inflammation. LPS treatment was also sufficient to upregulate liver ASC synthesis by 4 hours. Whether higher doses of CS or LPS would cause further or prolonged depletion of brain ASC in a more severe illness model should be studied in future experiments.

ASC deficiency is well defined in critical care patient populations (Borrelli *et al.* 1996; Galley *et al.* 1996; Fujii *et al.* 2019; Hudson *et al.* 2019; Carr *et al.* 2017). Many preclinical studies have shown that early ASC supplementation or IV treatment can protect against vascular and organ dysfunctions associated with sepsis (Wu *et al.* 2004; Zhou *et al.* 2012; Mckinnon *et al.* 2007). One possible explanation for the potential beneficial effects of ASC is that hospitalized patients who develop sepsis are more likely to have underlying ASC deficiency, either because of chronic illness, co-morbidities, or poor diet. However, our results and many others suggest that ASC depletion is directly caused by the illness itself, likely due to massive inflammatory challenge, endothelial breakdown, and elevated oxidative stress (Kuck *et al.* 2018; Wilson and Wu 2012). Although some clinical studies have associated lower plasma levels of ASC with increased incidence of multiple organ failure and decreased survival (Fowler *et al.* 2014), several phase I clinical studies have shown that IV administration of ASC during sepsis does not improve or worsen short term survival outcomes (Ahn *et al.* 2019; Fujii *et al.* 2019; Fowler *et al.* 2019). Overall survivability during sepsis is dependent on a variety of factors including antibiotics administration, prior health status, prior injury or illness, and age (Rhodes *et al.* 2017). While maintenance of ASC levels during sepsis may not directly impact acute survival, it may be critical to protection against inflammatory damage following sepsis, especially in the brain (Calsavara *et al.* 2018). Future studies will seek to understand how ASC is involved in the acute inflammatory response and the implications on long term cognitive dysfunction following recovery.

CHAPTER 3

Vitamin C Deficiency Does Not Exacerbate Behavioral and Cognitive Deficits in a Mouse Model of Sepsis

Abstract

The inflammatory response to infection during sepsis produces massive elevations in reactive species that break down endothelial barriers and damage vital organs including the brain. Vitamin C is a potent antioxidant that regulates reactive species signaling and protects tissues from oxidative damage. Plasma levels of ASC are decreased in septic patients, and decreased plasma ASC levels are associated with poorer patient outcomes including long-term deficits in mobility, self-care, and cognitive domains. Using gulo$^{-/-}$ mice, we modeled human ASC insufficiency and treated mice supplemented with High (1.0 g/L) or Low (0.033 g/L) ASC with cecal slurry (CS) to induce acute peritonitis. We hypothesized that prior ASC deficiency would exacerbate behavioral deficits following recovery in this model. While significant deficits were observed in locomotor activity, grip strength, spatial memory, and executive function following cecal slurry treatment, there were no additional effects of High or Low ASC supplementation on behavioral outcomes. These findings suggest that the model is sufficient to induce lasting behavioral deficits like those observed in patient populations but insufficient to increase ASC demand while providing ASC supplementation. Additional experimental modifications may be necessary to recapitulate the increased ASC demand during sepsis that is observed in patient populations and likely contributes to long-term cognitive deficits.

3.1 Introduction

Sepsis is a life-threatening illness caused by a dysregulated host response to infection (Singer *et al.* 2016b). As the immune system rallies to contain the outbreak of pathogens, excessive inflammation produces high levels of reactive oxygen and nitrogen species that contribute to endothelial and microvasculature dysfunction (Ait-Oufella *et al.* 2010; Ince *et al.* 2016; Russell *et al.* 2018). These reactive species can damage critical lipid and protein structures

and drive acute organ dysfunction in cases of severe sepsis (Angus and van der Poll 2013). Following the acute injury, up to 44% of sepsis survivors later experience severe deficits in quality of life across mobility, self-care, and cognitive domains (Yende *et al.* 2016; Iwashyna *et al.* 2010) implicating lasting oxidative damage that extends to the brain.

Vitamin C (ascorbate, ASC) is a potent antioxidant that regulates radical species within the vascular endothelium and serves critical roles in preserving brain and endothelial functions (Harrison 2012; May and Harrison 2013; Wilson 2009). Subnormal ASC levels in the plasma of septic patients are well documented (Borrelli *et al.* 1996; Galley *et al.* 1996; Carr *et al.* 2017; Prauchner 2017) and associated with greater illness severity, increased incidence of multiple organ failure, and decreased survival (Fowler *et al.* 2019; Schorah *et al.* 1996). Maintaining ASC availability during sepsis could be critical for minimizing long-term damage to vital tissues including the brain. The brain is particularly susceptible to oxidative stress because of its high energy demand, enriched lipid composition, and tight regulation at the blood brain barrier (Magistretti and Allaman 2015; Cobley *et al.* 2018). Therefore, prior ASC deficiency due to dietary or lifestyle factors could exacerbate long-term damage caused by heavy oxidative burden during illness.

Preclinical studies have shown that maintaining ASC sufficiency during sepsis has beneficial effects on preventing organ and vasculature dysfunction (Fisher *et al.* 2014; Fisher *et al.* 2011; Armour *et al.* 2001; Wu *et al.* 2004). In wild-type mice, an intravenous ASC treatment (200 mg/kg) prior to cecal ligation and puncture prevented oxidative damage and increased survival by over 50% (Wu *et al.* 2004). In gulo$^{-/-}$ mice incapable of ASC synthesis, lung, kidney, and liver injury as well as coagulation abnormalities were only observed in gulo$^{-/-}$ mice that were deficient of dietary ASC, and these injuries were attenuated by a 200 mg/kg ASC parenteral infusion during illness onset (Fisher *et al.* 2014). Few studies have investigated these protective effects on the brain. It is possible that ASC supplementation status prior to and during illness greatly contributes to development of long-term cognitive changes following sepsis. Here, we utilized gulonolactone oxidase knockout (gulo$^{-/-}$) mice dependent on dietary ASC supplementation (Maeda *et al.* 2000) to compare the effects of ASC sufficiency or ASC deficiency prior to illness on long-term behavioral outcomes following sepsis.

3.2 Methods

3.2.1. Subjects

All experiments conducted with live mice were reviewed and approved by the Vanderbilt Institutional Animal Care and Use Committee. Gulo$^{-/-}$ mice were bred in-house from founders originally obtained from the Mutant Mouse Regional Resource Centers (mmrrc.org, #000015-UCD) and maintained on a C57BL/6J background (Jackson laboratories, #000664). Like humans, gulo$^{-/-}$ mice lack the gene encoding gulonolactone oxidase, the enzyme responsible for catalyzing the final step in ASC synthesis. They depend on dietary ASC supplementation to prevent scurvy (Maeda *et al.* 2000; Harrison *et al.* 2008). Male and female mice were used in approximately equal numbers, and there were 12-16 mice per group.

3.2.2. ASC supplementation

Deficiency in ASC synthesis due to gulo$^{-/-}$ genotype does not result in a deficiency in tissue ASC levels when sufficient supplementation is provided. High (1.0 g/L) or Low (0.033 g/L) ASC was provided per cage in drinking water. High ASC supplementation maintains wild-type-equivalent tissue ASC levels and excess ASC is secreted in urine. Low ASC supplementation maintains depleted but supra-scorbutic ASC levels, and is sufficient for healthy weight gain with age and normal cognition in mice (Harrison *et al.* 2008; Harrison *et al.* 2010c). ASC was stabilized in de-ionized drinking water with 10 mM EDTA, and water was replaced at least once per week throughout experiment. Breeding pairs received High ASC supplementation and pups were weaned to High ASC supplementation until 8 weeks of age. Cages were then randomly assigned to either High (1.0 g/L) or Low (0.033 g/L) ASC supplementation until experiment completion. Mice were supplemented with High (1.0 g/L) or Low (0.033g/L) ASC for at least one month prior to experiment.

3.2.3. Cecal Slurry Treatment

To model sepsis in mice, we utilized a polymicrobial cecal slurry (CS) method as previously described (Shaver *et al.* 2019; Meegan *et al.* 2020; Kerchberger *et al.* 2019; Consoli *et al.* 2020). CS injection induces acute peritonitis which subsequently initiates a systemic inflammatory response that extends to the brain (Consoli *et al.* 2020). C57Bl/6J donor mice were

obtained at six weeks of age from Jackson Laboratory (#000664) and euthanized within 7 days of arrival. Cecal contents were collected and resuspended in 5% dextrose at 80 mg/ml, then filtered through a 100 μm filter. Aliquots were stored at -80°C until ready for use.
Mice were maintained on a consistent 12-hour light/dark cycle throughout lifetime and experimental study. Vehicle and treated mice were equally distributed across cages with 2-5 mice per cage. All mice were provided supplemental nutrition on the floor of the cage (DietGel 76A, Clear H_2O) following initial injection and throughout recovery up to 48 hours post injection to promote survival. The mice were monitored every 4-8 hours for 48 hours during onset of illness and recovery for body weight and Clinical Sickness Score evaluation (Shaver et al. 2019; Meegan et al. 2020; Kerchberger et al. 2019; Consoli et al. 2020). To optimize survival for later behavioral testing, a relatively low dose was utilized (1.5 mg/g) without use of antibiotics resulting in overall 12% mortality and 1-3 mice dying per group with no significant observable differences between High and Low ASC supplemented groups. All behavioral testing utilized facilities within the Vanderbilt Murine Neurobehavioral Core.

3.2.4. Open Field Activity

Locomotor activity was recorded by infrared beam detection using standard locomotor activity chambers (approx. 30 x 30 cm, ENV-510; MED Associates, Georgia, VT, USA). Total distance traveled during the 30-minute trial and per 5-minute bin are reported.

3.2.5. Elevated Zero Maze

Anxiety was assessed using a standard white Elevated Zero Maze (San Diego Instruments, CA). The maze consists of a circular platform equally divided into four quadrants and elevated 75 cm above the floor. Each mouse was placed into the nearest open arm of the maze and allowed to explore for 5 minutes while an experimenter monitored in an adjacent room using a camera mounted on the ceiling above the maze. Time spent in open and closed arms of the maze and distance traveled were reported using AnyMaze software (Stoelting Co. IL). One mouse jumped from the maze during this task and was excluded from analysis.

3.2.6. Y-maze alternation

A standard Y-maze made of clear acrylic tubing was used to test for spontaneous alternation as a measure of short-term memory and spatial discrimination as previously described (Harrison *et al.* 2008; Reiserer *et al.* 2007). Three arms of equal length (32 cm) radiating from the center of the maze were designated arms A, B, and C with white, gray, and striped flooring respectively to provide additional context for the mouse. The mouse was placed in the end of one of the arms and the number and sequence of entries were recorded by an experimenter using remote video monitoring as the mouse explored the maze for a single 5-minute trial. Alternations were counted when the mouse chose to move within each of the three arms in succession with all four paws without repeating entry into the same arm (e.g., ABC or BAC rather than ABA or BAB). Percent alternation was calculated as the number of alternations divided by the total number of arm entries minus two. Trials were recorded with a video camera mounted on the ceiling above the maze, and distance traveled during the task was analyzed using AnyMaze (Stoelting, Co. IL).

3.2.7. 2-trial Y-maze

For an additional assessment of spatial memory and spatial discrimination, mice underwent a second Y-maze task with two trials using a different maze, as previously described (Walker *et al.* 2017). This maze had square arms 35 cm in length and straight walls 10 cm in height. At the end of each of three arms designated A, B and C, a specific visual cue was placed to assist the mouse in spatial discrimination between the arms: a plastic ball, a water bottle, and a wire metal cup respectively. During the first trial, mice were allowed to explore two of the arms for 5 minutes while one of the arms was blocked. After an intertrial interval of less than 2 minutes, the block was removed for the second trial, and the mouse was allowed to explore all three arms of the maze for 5 minutes. Between trials, the entire maze was cleaned with 10% ethanol solution to remove odor cues. Trials were recorded with a video camera mounted on the ceiling above the maze, and exploration in each arm was analyzed using AnyMaze (Stoelting, Co. IL) including time spent in each arm and distance traveled.

3.2.8. Nest Building

Mice were singly housed overnight with two squares of pressed cotton nestlet material (Ancare Corp, New York, USA) weighing a total of 5.0 g stacked in the center of each cage.

Nests were scored the following morning using a 5-point scoring system based on nest shredded, complexity, and height (Deacon 2006; Walker *et al.* 2017).

3.2.9. Rotarod

Motor coordination and learning were assessed using a standard rotarod apparatus (Ugo Basile). Mice were placed on a ridged rubber rod 3 cm in diameter suspended 25 cm from the base of the apparatus. The rod began rotating at 4 rpm and accelerated to a final speed of 40 rpm over the course of 5 minutes. Up to five mice were run simultaneously in 6 cm wide compartments with mice separated by opaque plexiglass. The time to fall or first rotate were recorded when the mouse could not maintain pace and fell from the rod or instead gripped and rotated around with the rod. Mice completed three trials per day with approximately 30 minutes between each trial with a maximum of 5 minutes per trial. The average time to fall or rotate across all three trials was reported per day of testing.

3.2.10. Grip Strength

Grip strength was assessed using a force meter attached to a rectangular wire grid at approximately a 45-degree angle (San Diego Instruments, San Diego, CA). Mice were allowed to firmly hold onto the grid with either the front two paws or all four paws while the experimenter held the mouse by the tail. The experimenter then gently pulled the mouse back with a constant force in a horizontal plane until the grip was broken. The apparatus measured the maximum force during the pull in Newtons. Each mouse was given three trials for each 2-paw and 4-paw test, and the average force per mouse was reported.

3.2.11. Fear Conditioning

Learning and memory abilities were assessed by evaluating freezing response following fear conditioning as previously described (Dixit *et al.* 2015). Mice were placed in one of two conditioning chambers with clear plexiglass walls and a metal grid floor housed within an acoustic sound attenuating chamber (Med Associates Inc. USA). During the first day of testing, mice were trained to associate a constant 30 second 70 dB tone with a two second electrical shock (0.8 mA) by three repeated tone-shock pairings over 8 minutes. The second day of testing, mice underwent two retrieval tests. For the context retrieval test, the mice were placed within the

same testing chamber used during training and allowed to explore undisturbed for 4 minutes. Approximately one hour later, the context was changed entirely for the cue retrieval test. Context changes included using white plastic floor and curved wall inserts, adding a vanilla scent to the testing chambers, and testing mice in a different testing chamber than that used during training. The experiment also entered the room through a different door, and dimmer lighting was used in the testing rooms. Mice were placed within the testing chamber and allowed to explore the novel context undisturbed for four minutes. During the second two minutes of the trial the same tone used during training was played. During each of the trials, cameras mounted on the inside doors of the chambers and computer software scored the mice for time spent immobile, reported as time freezing. A final shock threshold test was performed to confirm equal sensitivity to the shock across groups by increasing the shock intensity in 0.02 mA increments starting at 0.075 mA until the mouse flinched, jumped, or vocalized.

3.2.12. Order of Behavioral Testing

Behavioral testing began 7 days following CS or Veh injection and was completed over the following two weeks. Testing was performed at the same time of day (12:00-16:00) and order of testing was identical across three separate cohorts of 15-22 mice (**Table 3.1**).

Table 3 – Order of behavioral testing.

Days following CS injection	Behavioral Task Performed
7	Elevated Zero Maze & Grip Strength
8	Open Field Activity
9	2-Trial Y-maze Alternation
10	Rotarod Session 1
11	Rotarod Session 2
12	Rotarod Session 3
13	No testing
14	Spontaneous Y-maze Alternation
15	Fear Conditioning (Training)
16	Fear Conditioning (Retrieval)
17	Nest Building Task (Overnight)
18	Nests Scored and Euthanasia

3.2.13. Tissue Collection

Following behavioral testing, mice were anesthetized with isoflurane then euthanized by decapitation at 21 days post treatment. For the acute follow-up study, additional mice were euthanized at 4, 24, 48 hrs or 7 days post-injection, and vehicle treated mice were distributed across each timepoint and data from all control animals were collapsed into one group. Tissue samples were collected, flash frozen on dry ice, and stored at -80°C for further analysis.

3.2.14. High Performance Liquid Chromatography

Tissue ASC concentrations were measured by ion-pair high performance liquid chromatography as described previously (Consoli *et al.* 2020; Harrison *et al.* 2008; May *et al.* 1998). Sample extracts were normalized by weight by adding 10 µl extraction buffer (7:2 25% *w/v* metaphosphoric acid: 100 mM sodium phosphate, 0.05 mM EDTA pH 8.0) per mg of wet tissue. Following tissue homogenization and centrifugation, the supernatant was diluted 1:100 in deionized water and measured in triplicate.

3.2.15. Statistics

Data shown in figures and text are reported as mean +/- S.E.M. All statistical analyses were performed using GraphPad Prism (version 9.1.1). All groups were equally balanced with male and female mice, and analyses were first run with sex as a fixed variable. There were no significant differences according to sex, and male and female groups were subsequently combined and analyzed together. Data were first checked for normality with an Anderson Darling test (alpha = 0.05), and data with normal distribution were subsequently analyzed using parametric statistical analyses. Behavioral data were compared using two-way analysis of variance with ASC supplementation (High 1.0g/L or Low 0.033g/L) and treatment (vehicle or CS) as the independent variables and main effects of ASC, CS, or interaction (Int) are reported as noted in the text. Significant main effects following ANOVA ($p<0.05$) were followed by Tukey's multiple comparisons post hoc tests. Where behavior data utilized repeated measurements (weights, sickness scores, rotarod), a repeated measures three-way ANOVA included time as an additional independent variable and following significant results a Sidak's multiple comparison test was used to compare effects of ASC treatment specifically within CS treated mice. Nest building data were not normally distributed and were analyzed using a

nonparametric Mann-Whitney test corrected for multiple comparisons using the Holm-Sidak method ($p<0.05$).

3.3 Results

3.3.1. Weight loss and sickness scores were not affected by Low ASC supplementation.

At 12-weeks of age, High- and Low-ASC supplemented mice were injected with CS (1.5 mg/g, i.p.) or vehicle (5% dextrose, i.p.). One week after injection, approximately 5 days after recovery from illness, a behavioral battery was performed with tasks distributed over the following two weeks (**Fig. 7A**). During illness, weights of CS treated mice decreased over time by up to 15% at 48 hours post injection (CS: $F_{1,55}=77.07$, $p=0.0001$; Time: $F_{3,111}=19.86$, $p<0.0001$, **Fig. 7B**). Male mice in general weigh more than female mice, so percent weight change from starting weight was utilized to compare differences between groups. Weights recovered to previous body weights by 7 days when behavior testing began (7-day post-hoc p's>0.3864). Illness was observable by clinical sickness score at 4 hours and persisted until approximately 48 hours following injection (CS: $F_{1,68}=271.9$, $p<0.0001$, **Fig. 7C**). Weights and sickness scores did not significantly differ between High and Low ASC supplemented groups (ASC: F's<0.2148, p's>0.6455) and there were no significant interactions between CS and ASC (CS x ASC Int: F's<1.636, p's>0.2062).

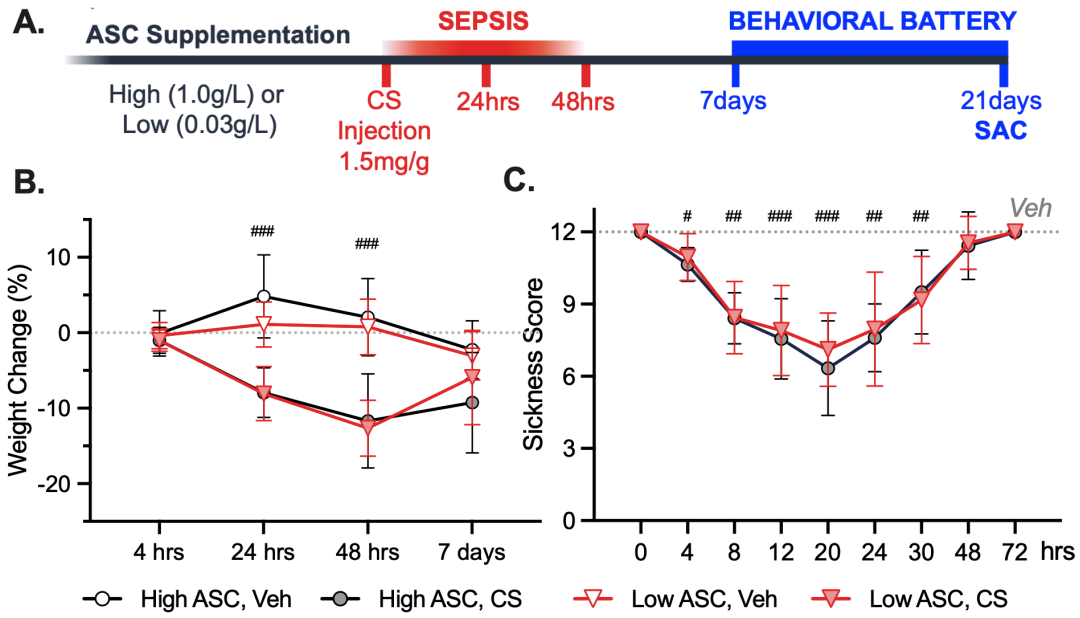

Figure 7 – Experimental design and CS treatment in gulo$^{-/-}$ mice.
(**A**) Experimental timeline. (**B**) Weights, dotted line represents zero change from weight at time of injection. (**C**) Sickness scores, dotted line in represents maximum score of 12 recorded in all vehicle treated mice. $^{\#}p<0.05$, $^{\#\#}p<0.01$, $^{\#\#\#}p<0.001$ vehicle (Veh) vs. CS treated within High and Low ASC supplementation by Sidak's post-hoc following significant ANOVA.

3.3.2. Persistent hypoactivity and normal anxiety following illness

CS treated mice explored less than vehicle treated mice 8 days during the 30-minute trial following CS treatment in both High and Low ASC supplemented groups (CS: $F_{1,52}=31.56$, $p<0.0001$, **Fig. 8A-B**). Mice supplemented with Low ASC had marginally increased activity regardless of CS treatment although this effect appears to be mainly driven by vehicle supplemented animals (ASC: $F_{1,52}=5.113$, $p=0.0280$; Int: $F_{1,52}=2.223$, $p=0.1420$).

All groups spent a similar amount of time (50-60%) in the closed arms during the Elevated Zero Maze task indicating no differences in anxiety-like behavior between groups (F's<2.326, p's>0.1334, **Fig. 8Ci**). Decreased exploration was observed again in CS treated mice in the Elevated Zero Maze (CS: $F_{1,51}=10.62$, $p=0.0020$, **Fig. 8Cii**) and further confirmed by decreased transitions between zones in CS treated mice (CS: $F_{1,51}=16.94$, $p=0.0001$, **Fig. 8Ciii**). Effects in distance and entries due to CS treatment in the Elevated Zero Maze were not affected by ASC supplementation or interaction effects (F's<2.016, p's>0.1618).

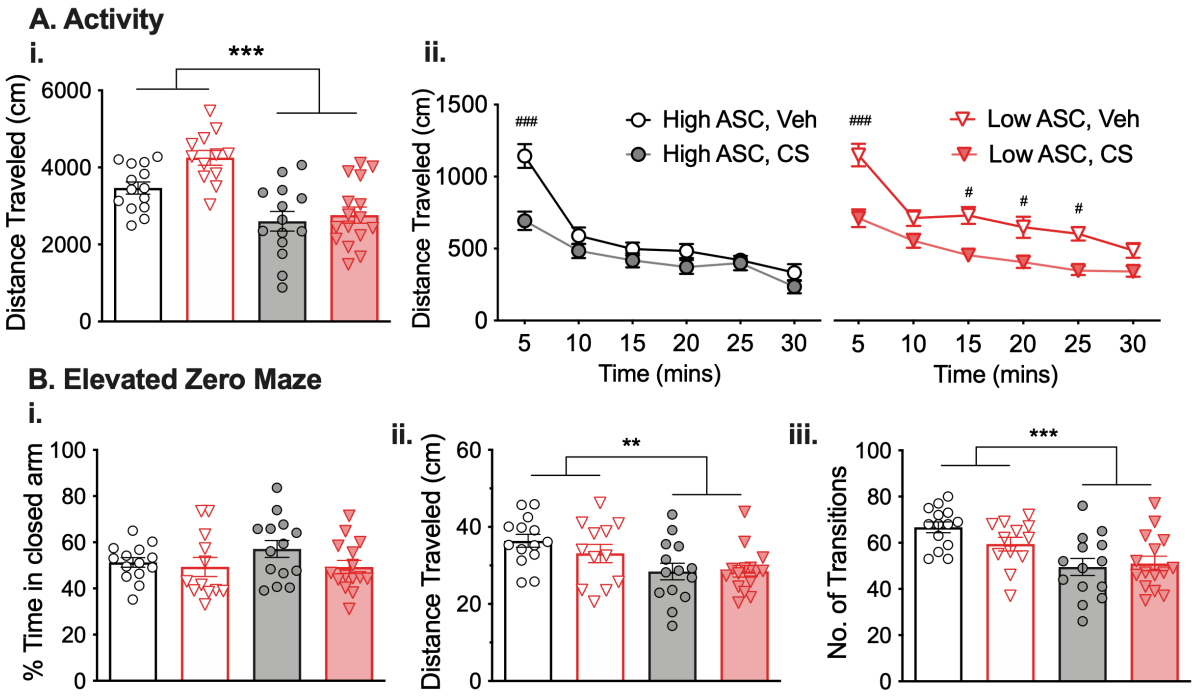

Figure 8 – Activity and anxiety.
(**A**) Total activity (i) and activity per 5-minute bin (ii) during open field test. (**B**) Time in closed arm (i), distance traveled (ii), and number of transitions between open and closed arms (iii) during Elevated Zero Maze test. **p<0.01, ***p<0.001 Main effect of CS treatment by two-way ANOVA. $^{\#}$p<0.05, $^{\#\#\#}$p<0.001 vehicle (Veh) vs. CS treated within High and Low ASC supplementation by Sidak's post-hoc following significant ANOVA.

3.3.3. Decreased spatial memory and executive function following illness.

Spontaneous Y-maze alternation assessed short-term memory and spatial discrimination indicated by a preference for alternating between arms rather than entering an arm more recently explored. Mice did not show any difference in percent alternation between the arms of the maze due to CS treatment or ASC supplementation (F's<1.501, p's>0.2261, **Fig. 9Ai**). However, persistent hypoactivity was observed in CS treated mice by decreased distance traveled (CS: $F_{1,52}$=8.8.093, p=0.0063, **Fig. 9Aii**) and decreased number of entries (CS: $F_{1,52}$=8.625, p=0.0049, **Fig. 9Aiii**). There were no additional effects of ASC supplementation or interactions (F's<1.073, p's>0.3051).

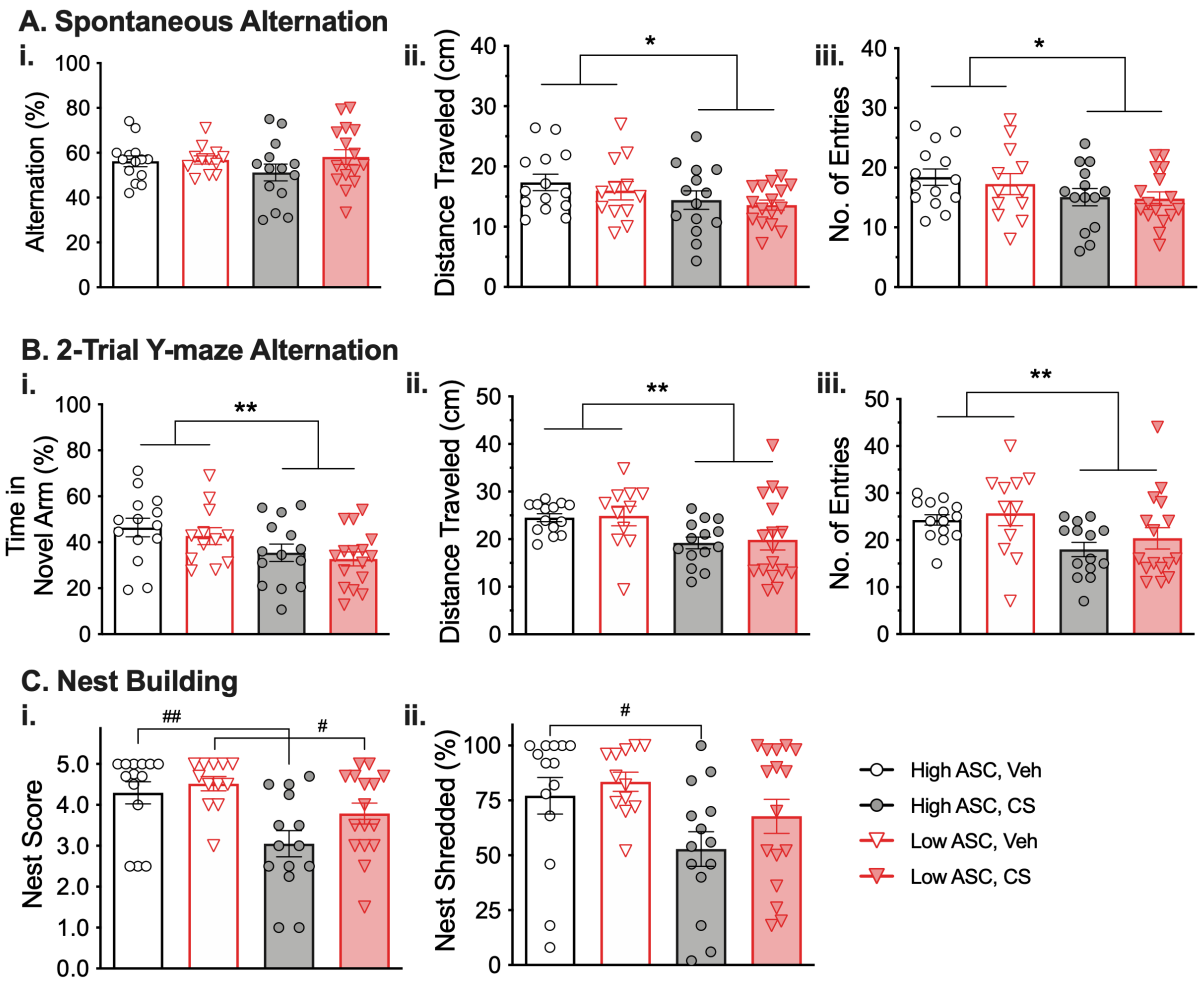

Figure 9 – Spatial memory and executive function.
(**A**) Percent alternation (i), distance traveled (ii), and number of entries (iii) during spontaneous Y-maze alternation task. (**B**) Time in novel arm (i), distance traveled (ii), and number of entries (iii) during 2-Trial Y-maze task. (**C**) Nest building score (i) and percent nestlet shredded (ii). *p<0.05, **p<0.01, ***p<0.001 main effect of CS treatment by two-way ANOVA. $^{\#}$p<0.05, $^{\#\#}$p<0.01 by nonparametric Mann-Whitney test corrected for multiple comparisons.

The evaluation of short-term memory and spatial discrimination was extended using a more complex 2-trial Y-maze task. During the first trial the mouse was allowed to explore two of the arms while a third arm was blocked. In the second trial, the block was removed, and the time spent in the novel arm was used to indicate preference for a novel environment. CS treated mice showed decreased time exploring the novel arm compared to vehicle treated mice (CS: $F_{1,52}$=8.171, p=0.0061, **Fig. 9Bi**) indicating decreased short term memory recall and spatial discrimination ability. Lower percentage of time spent in novel arm is independent of observed hypoactivity (CS: $F_{1,52}$=4.111, p=0.0477, **Fig. 9Bii**) and lower zone entries (CS: $F_{1,52}$=8.625,

p=0.0049, **Fig. 9Biii**) due to CS treatment. Alternation preferences for both tasks were not affected by ASC supplementation or interaction effects (F's<1.501, p's>0.2261).

The nest building task evaluated deficits in executive function and engagement in rewarding, survival-promoting behavior. CS treated mice in both High and Low ASC supplemented groups showed overall lower nest scores than vehicle treated mice (High ASC: U=35.50, p=0.0028; Low ASC: U=54.00, p=0.0483, **Fig. 9Ci**). Lower percent nestlet shredded was only statistically significant in mice supplemented with High ASC (High ASC: U=48.50, p=0.0021; Low ASC: U=74.00, p=0.3162, **Fig. 9Cii**).

3.3.4. Decreased motor coordination in low ASC mice and decreased grip strength following illness.

All mice showed normal motor learning capability with improvement in latency to fall over the 3 days of training on the rotarod task (Time: $F_{2,104}$=27.56, p<0.0001, **Fig. 10A**). Differences in overall motor coordination indicated by lower time to fall or rotate were not distinguishable between CS and vehicle treated mice (CS: $F_{1,52}$=0.2769, p=0.1021). Mice supplemented with Low ASC showed lower overall performance on the rotarod compared to mice supplemented with High ASC (ASC: $F_{1,52}$=5.207, p=0.0266) similar to observations in previous studies (Harrison *et al.* 2008). CS treated mice showed significantly decreased grip strength in the 4-paw task (CS: $F_{1,52}$=31.43, p<0.0001, **Fig. 10Bi**) and only marginally decreased grip strength in the 2-paw task (CS: $F_{1,52}$=3.630, p=0.0623, **Fig. 10Bii**). Grip strength was not affected by ASC supplementation (ASC: F's<0.4240, p's>0.5178).

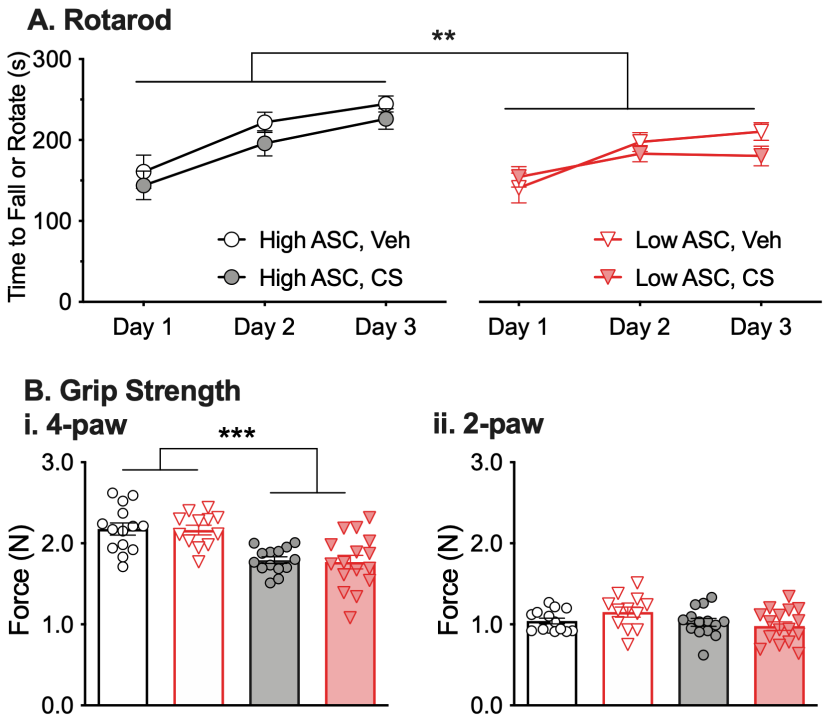

Figure 10 – Motor coordination and grip strength.
(**A**) Time to fall or rotate per day of testing during rotarod task. (**B**) 4-paw (i) and 2-paw (ii) grip strength. **p<0.01, ***p<0.001 Main effect of CS treatment by ANOVA.

3.3.5. Normal learning and memory in fear conditioning and retrieval tasks following illness.

All mice had similar increases in freezing post-training than at baseline (Time: $F_{1,52}$=310.2, p<0.0001, **Fig. 11A** right) with no additional impacts of ASC or CS (F's<0.7727, p's>0.3843). There were differences in freezing at baseline reflecting lower activity in the first 2 minutes (CS: $F_{1,52}$=17.25, p<0.0001, **Fig. 11A** left). We therefore used percent increase in freezing time relative to baseline as the primary index of memory in retrieval tasks. During context retrieval the following day of testing, all mice exhibited freezing behavior indicating recollection of the shock-context pairing. Greater freezing was observed in CS treated mice (CS: $F_{1,52}$=14.53, p=0.0004, **Fig. 11Bi**) compared to vehicle treated controls with no additional effect of ASC or interactions (F's<3.229, p's>0.0781). However, percent change from first two minutes of baseline was significantly lower in CS-treated animals suggesting possible impaired spatial memory (CS: $F_{1,52}$=7.089, p=0.0103, **Fig. 11Bii**).

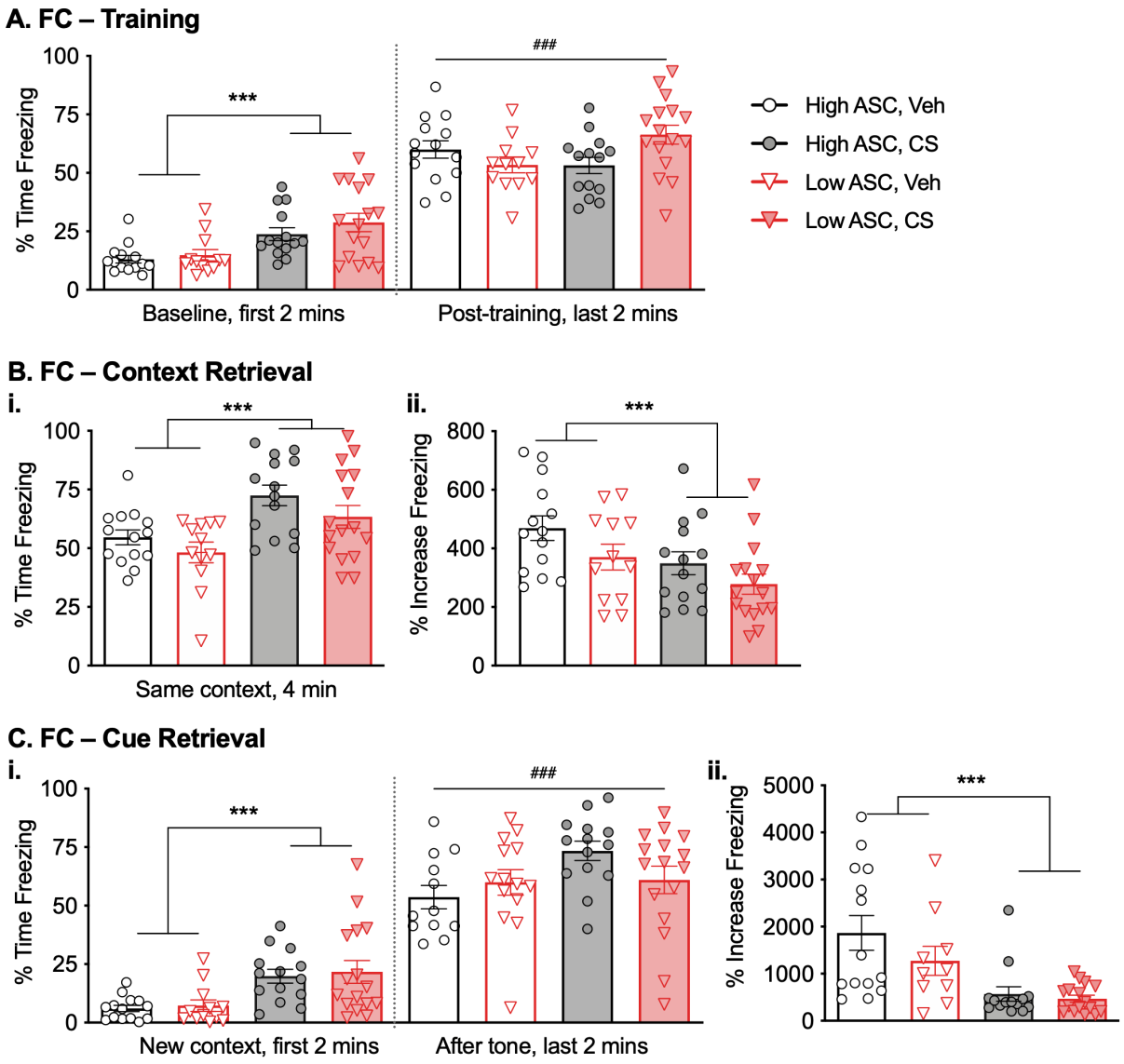

Figure 11 – Fear Conditioning (FC).
(**A**) Time freezing before and after shock training (i) and percent increase in time freezing during training (ii). (**B**) Time freezing during context retrieval test (i) and percent increase from baseline (ii). (**C**) Time freezing in a new context and after tone during cue retrieval test (i) and percent increase following tone (ii). ***p<0.001 main effect of CS by two-way ANOVA. $^{###}$p<0.001 main effect of time by repeated measure three-way ANOVA.

Mice placed in a new context showed normal exploratory behavior and low time freezing similarly to baseline although CS-treated animals moved less than controls as in the previous two trials (CS: $F_{1,52}$= 17.04, p=0.0001, **Fig. 11Ci** left). Following the tone, all mice exhibited increased freezing behavior compared to the previous 2 mins indicating recollection of the tone-shock pairing (Time: $F_{1,52}$=422.3, p<0.0001, **Fig. 11Ci** right). Again because of higher freezing

in the novel context in CS treated mice, we used percent increase in freezing before and after the tone as an index of memory. A significantly lower percent increase in freezing behavior following the tone in CS treated animals suggest poorer recall in that group ($F_{1,52}$=18.66, p<0.0001, **Fig. 11Cii**).

3.3.6. Tissue ASC levels reflect supplementation and were not changed during or following illness.

Mice were maintained on their respective High or Low ASC supplementation throughout illness, recovery, and behavioral experiments. Tissue ASC levels following the behavioral battery showed those anticipated based on ASC supplementation, with lower ASC observed in cortex ($F_{1,25}$=339.0, p<0.0001, **Fig. 12A**) and liver ($F_{1,25}$=126.3, p<0.0001, **Fig. 12B**) in mice supplemented with Low ASC and no further effect of CS at this timepoint 18 days following CS treatment (F's<1.873, p's>0.1833). We hypothesized that ASC levels could deplete during acute illness, when elevated inflammation could challenge antioxidant reserves or lethargy and decreased food and water intake could cause insufficient hydration and supplementation. Surprisingly, ASC levels did not change due to CS treatment during the acute illness at 4-, 24-, or 48-hours post injection in cortical tissue (F's<0.2899, p's>0.8820, **Fig. 12C**). In liver, ASC levels were marginally elevated in CS treated mice ($F_{4,31}$=3.086, p=0.0300, **Fig. 12D**), though these changes were not statistically distinguishable across timepoints in post-hoc analysis (High ASC: p's>0.0545, Low ASC: p's>0.1243).

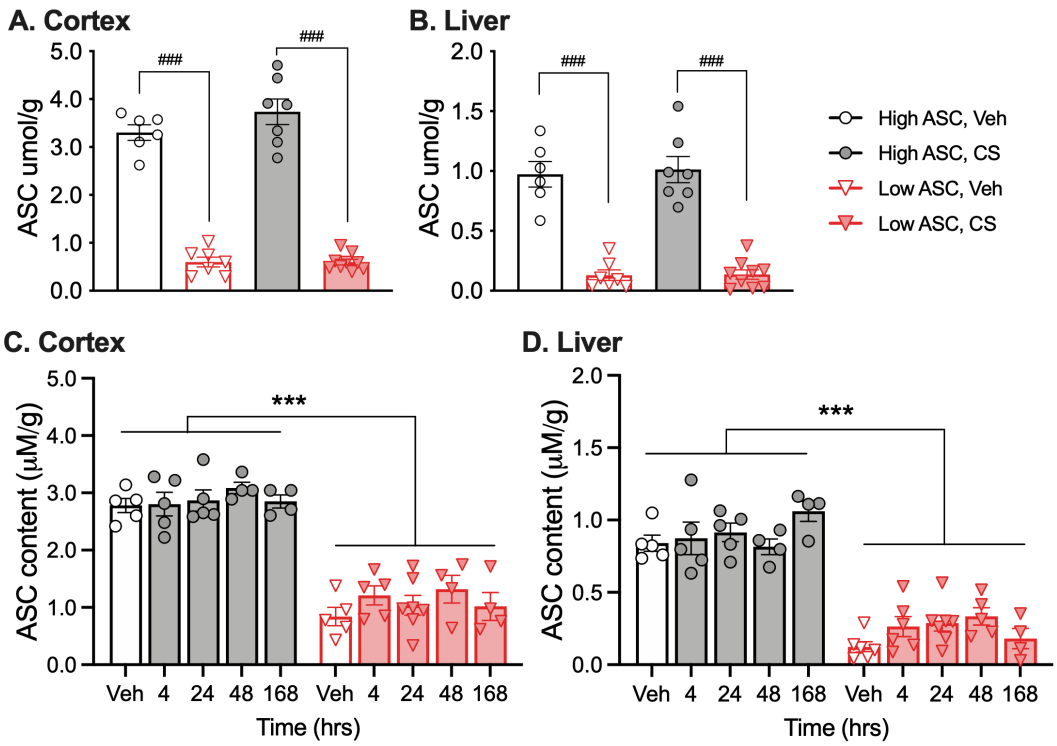

Figure 12 – Tissue ASC levels following behavior and throughout illness. ASC levels following behavior in cortex (**A**) and liver (**B**) and tissue ASC levels during or following illness in cortex (**C**) and liver (**D**). $^{###}p<0.001$ by Tukey's post-hoc following significant two-way ANOVA. ***$p<0.001$ Main effect of ASC by repeated measures three-way ANOVA.

3.4 Discussion

In this study, we observed extensive behavioral deficits following CS-induced sepsis in gulo$^{-/-}$ mice including deficits in locomotor activity, grip strength, spatial discrimination, and executive function. Gulo$^{-/-}$ mice, like humans, cannot synthesize ASC and therefore depend on dietary supplementation to maintain adequate tissue levels (Maeda *et al.* 2000; Harrison *et al.* 2008). In wild-type mice, this dose of CS led to acute depletion of ASC in the brain and upregulated synthesis of ASC in the liver indicating significant demand for ASC during illness (Consoli *et al.* 2020). We hypothesized that prior ASC deficiency would predispose mice to greater cognitive deficits following increased ASC demand during illness, especially considering the severe cognitive deficits we have observed previously in gulo$^{-/-}$ mice following an acute scorbutic period (Ward *et al.* 2013). However, at this dose, there were no significant differences between CS treated High and Low ASC supplemented groups.

Interestingly, the gulo$^{-/-}$ mice showed longer sickness duration than previously observed in their wild-type counter parts. Wild-type mice at this CS dose recovered by approximately 24 hours (Consoli *et al.* 2020) while the gulo$^{-/-}$ mice in this study had observable illness nearly twice as long. This longer illness duration was independent of High or Low ASC supplementation, suggesting that the specific ability to synthesize ASC endogenously is associated with shorter illness duration. This key difference may be impacting studies of septic injury or long-term cognitive damage which are most performed in wild-type mice. Whether the ability of wild-type mice to synthesize ASC is consequently more protective of long-term cognitive and behavioral changes in this model should be determined in future studies.

Persistent hypoactivity following illness was observed in several of the behavior tasks performed. Decreased exploratory behavior indicates that mice have not fully recovered from sepsis in the weeks following illness even though they apparently resemble vehicle treated mice by Clinical Sickness Score. It is interesting to note that lasting hypoactivity was not observed in wild-type mice treated at the same dose, though this may not be directly comparable since the wild-type animals in that study were treated with antibiotics and underwent surgery prior to injection (see Chapter 4). Hypoactivity observed during the Y-maze tasks does not explain the decreased percentage of time spent in the novel arm during the 2-trial Y-maze task, which instead indicates CS treated mice have lasting impaired spatial memory.

Hypoactivity observed during fear conditioning may change interpretation of fear conditioning data. All mice in the fear conditioning trials were observed to learn the tone-shock association and recall the context and cue the following day despite higher baseline freezing due to hypoactivity in CS treated mice. Lower percent increases in freezing behavior in the retrieval tasks due to CS treatment may reflect impaired spatial memory as observed in the 2-trial Y-maze task. Alternatively, these differences may be driven by the hypoactivity at baseline. In this case, it is possible that the relatively high shock amplitude elicits an extensive fear response that masks more subtle differences in learning and memory, such as those observed in the 2-trial Y-maze. Future studies may utilize a lower shock during training to allow greater ability to distinguish more subtle differences between groups.

Nest building deficits were also observed in CS treated mice. Mice readily engage in nest building when the material is provided such that the behavior is assumedly rewarding. It is a hippocampal mediated task that demonstrates the ability of a mouse to exhibit self-care and carry

out a task as a measure of overall cognitive well-being (Deacon 2006; Deacon *et al.* 2002; Walker *et al.* 2017; Dixit *et al.* 2015). It is possible, in this study, that the nest building deficits could partly be attributed to hypoactivity or decreased grip strength. However, the deficits observed in this study support the findings of many other studies that behavioral deficits can be observed in mice following various models of sepsis (Schwalm *et al.* 2014; Qin *et al.* 2007; Semmler *et al.* 2007; Skelly *et al.* 2019; Hippensteel *et al.* 2019). Specific to this study, we showed deficits in impaired mobility, short-term memory, and executive function that directly translate to the deficits that up to 44% of human sepsis survivors experience in quality of life across mobility, daily activities, and self-care domains (Yende *et al.* 2016).

Low ASC supplementation did not exacerbate any of the deficits observed following CS treatment. Likewise, High ASC supplementation did not attenuate any of the deficits observed following CS treatment. These findings were surprising given the protective effects of ASC sufficiency in other mouse models of sepsis on organ damage and overall survival (Fowler *et al.* 2019; Fisher *et al.* 2011; Fisher *et al.* 2014). If organ damage during illness was indeed improved in this model as in similar previous models, it is possible that peripheral organ damage may be independent of cerebral damage that contributes to the long-term cognitive deficits observed in this study. It is also possible that if this study were extended to several months following CS treatment, mice supplemented with High ASC would recover these behavioral deficits faster than mice maintained on Low ASC.

No changes in tissue ASC levels were observed during sepsis in this model. Mice with Low ASC supplementation maintained consistently low ASC in cortex and liver, and mice with High ASC supplementation maintained consistently saturated ASC levels in cortex and liver. Again, this was surprising due to the acute depletion we observed in wild-type mice (Consoli *et al.* 2020). We hypothesize these findings could be attributable to alterations in drinking behavior due to illness, which would disrupt anticipated ASC supplementation rates. In the gulo$^{-/-}$ model, ASC is depleted under the assumption that mice drink approximately the same amount of water each day. It is possible that during sepsis, either prior to or immediately following the period of acute lethargy, mice drink more water to replenish fluids lost during illness. This would explain the marginal elevations in ASC observed in the liver of CS treated mice on Low ASC supplementation or the lack of an observable ASC depletion in any tissue entirely. It may be relevant to restrict ASC supplementation prior to CS injection and specifically administer ASC

only to the High ASC group during illness to compare the effects of total ASC depletion. However, such changes to the experimental design would diminish the translational relevancy of this model and instead force the mice into scorbutic conditions driven primarily by insufficient ASC supplementation rather than by sepsis. One study indeed evaluated the survivability of septic mice under such forced conditions and unsurprisingly found that mice with undetectable tissue levels of ASC suffered increased mortality from sepsis likely due to comorbid scurvy (Gaut *et al.* 2006). High survival in this study was achieved by maintaining supra-scorbutic ASC levels and utilizing a relatively low CS dose to optimize for long-term behavioral testing. It is certainly possible that in conditions with lower survivability, mice supplemented with Low ASC would exhibit worsened cognitive deficits.

ASC is regularly given enterally or parenterally to septic patients with the intention to improve immune function and prevent oxidative damage (Chan *et al.* 1999; Yamazaki *et al.* 2011; Wintergerst *et al.* 2007). Given the potentially beneficial antioxidant and protective roles of ASC in sepsis, there is significant interest in high-dose intravenous vitamin C in clinical trials (Marik *et al.* 2017; Lindsell *et al.* 2019). Maintaining sufficient ASC levels in the plasma of septic patients is challenging and requires significantly higher doses than those expected with modeled normal uptake (Long *et al.* 2003; Baines and Shenkin 2002). This is presumably due to enhanced metabolic demands for ASC amidst inflammatory or infectious processes (Carr *et al.* 2017) or circulation dysfunction preventing proper distribution of ASC using multi-step and endothelial mediated transport systems (Wilson 2009; May and Harrison 2013). The lack of difficulty in maintaining adequate tissue ASC levels in this model, suggests that the oxidative burden inflicted by this CS method, while sufficient to inflict lasting behavioral deficits, is insufficient to model the severe oxidative stress and subsequent ASC demand experienced by patients in critical care. Age is a significant factor in the outcome of sepsis in clinical populations (Martin *et al.* 2006), and notably these studies were conducted in young mice. Decreased mitochondrial function with aging leads to age-related accumulation of oxidative stress and exponentially increased ASC demand (Cui *et al.* 2012). Given that ASC status correlates with healthy markers of metabolic and cognitive health in aged populations (Pearson *et al.* 2017) and has protective therapeutic potential in the prevention of neurodegeneration (Harrison and May 2009; Dixit *et al.* 2017; Harrison 2012), it is likely that prior ASC deficiency would have a greater effect on the long-term cognitive decline following sepsis in aged animals.

CHAPTER 4

Slow-Wave EEG Activity and Neurobehavioral Deficits Implicate Delirium in a Mouse Model of Sepsis Associated Encephalopathy

Abstract

Sepsis is often accompanied with severe encephalopathy and delirium that strongly correlate with poor clinical outcomes including long-term cognitive deficits. Delirium is diagnosed primarily through inattention during interactive tasks with critically ill patients making preclinical studies of delirium in mouse models challenging. We utilized concurrent measures of telemetry electroencephalography (EEG) recordings and neurobehavioral tasks to characterize inattention and long-term cognitive deficits in a mouse model of polymicrobial sepsis. During the first 24 hours of critical illness in this model, EEG activity was dominated by slow-wave frequencies that resembled those observed in delirious patients. We also measured pre-pulse inhibition of startle response, a phenomenon that is translatable across species, to measure inattention during illness and found that mice are hypersensitive to the pre-pulse stimulus. Following recovery, persistent poorer cognitive function determined by nest building evaluation correlated with greater delta power, lower beta power during illness, and molecular deficits in hippocampal long-term potentiation compared to mice that returned to baseline cognitive performance. EEG profiling using this experimental setup offers a robust biomarker of a delirium-like state during sepsis associated encephalopathy in mice and presents an important new tool to investigate therapeutic strategies for improving delirium and subsequent cognitive outcomes in patients.

4.1 Introduction

Of the more than 48 million estimated annual sepsis cases globally, approximately 37 million will survive and subsequently experience increased risk for long-term cognitive impairment (Rudd *et al.* 2020; Rengel *et al.* 2019). Organ dysfunction during the acute critical illness extends to the brain, driving acute encephalopathy through cardiovascular dysregulation,

respiratory distress, microvasculature hypoperfusion, metabolic crisis, toxin accumulation, and endothelial breakdown (Bauer *et al.* 2018; Mazeraud *et al.* 2016; Hughes *et al.* 2013). This acute cerebral pathophysiology is defined as sepsis associated encephalopathy and manifests clinically as delirium (Slooter *et al.* 2020; Zampieri *et al.* 2011; Remick 2007). Delirium is reported in up to 82% of patients in intensive care units, and its duration and severity strongly correlate with mortality and long-term cognitive deficits in survivors (Sasannejad *et al.* 2019; Pandharipande *et al.* 2013; Atterton *et al.* 2020; Ely *et al.* 2004). Optimizing patient care during delirium in critical illness has improved survivorship from sepsis, but survivors still face lasting functional and cognitive deficits including decreased executive function, global cognition, and memory (Wolters *et al.* 2013; Rengel *et al.* 2019; Iwashyna *et al.* 2010). Changes are comparable to mild cognitive impairment in many with the greatest deficits resembling Alzheimer's disease in up to 24% of patients at one year (Pandharipande *et al.* 2013).

Classic descriptions of delirium include disruptions of awareness and inattention that can be observed by generalized electroencephalography (EEG) slowing (Engel and Romano 1959). EEG has been used for decades to monitor delirium in critically ill patients, culminating in reports of slow-wave dominance, disrupted alpha rhythms (Jacobson *et al.* 1993; Koponen *et al.* 1989; Atterton *et al.* 2020) and a series of increasingly well-defined EEG abnormalities (Palanca *et al.* 2017; Hirsch *et al.* 2021). More recently, slow-wave EEG activity has been shown to corelate specifically with delirium severity and be predictive of long-term cognitive impairment (Roberson *et al.* 2020; Kimchi *et al.* 2019).

Delirium is typically diagnosed using a confusion assessment method (CAM-ICU) that evaluates the patient's ability to understand and act on instructions (Ely *et al.* 2001). Mouse models, therefore, have limited means to test therapeutic strategies that specifically target delirium to improve cognitive outcomes. While mouse models of sepsis have demonstrated long-term cognitive deficits across many different cognitive and behavioral tasks including support with molecular markers of neuronal degeneration (Schwalm *et al.* 2014; Qin *et al.* 2007; Semmler *et al.* 2007; Skelly *et al.* 2019; Hippensteel *et al.* 2019), studies investigating acute sepsis associated encephalopathy during illness and its association with delirious mental status in mice are sparse. Efforts to measure EEG in rodent models of sepsis have been limited to tethered EEG systems preventing long-term recording or the synchronization of behavioral assessment and EEG metrics during and following illness (Trzepacz *et al.* 1992; Leavitt *et al.* 1994; Kimchi

et al. 2017). In this study, we utilized wireless surgically implanted telemetry devices in a cecal slurry mouse model of sepsis to characterize EEG profiles throughout critical illness onset and recovery. During recording, we utilized nest building as a simple neurobehavioral assessment of executive function and global cognition to determine individual EEG metric contributions to long-term cognitive outcome following illness. We supplemented our findings with an attention based neurobehavioral task during illness and an electrophysiological measure of learning and memory following recovery. Together, these studies outline a comprehensive mouse model of sepsis associated encephalopathy that closely resembles patient delirium and subsequent cognitive decline with predictive validity to differentiate between cognitive outcomes.

4.2 Methods

4.2.1. Subjects & Treatment

All experiments conducted with live mice were reviewed and approved by the Vanderbilt Institutional Animal Care and Use Committee. To model sepsis-associated encephalopathy in mice, we utilized a polymicrobial cecal slurry (CS) method of sepsis induction as previously described (Shaver et al. 2019; Meegan et al. 2020; Kerchberger et al. 2019; Consoli et al. 2020). CS injection induces acute peritonitis which subsequently initiates a systemic inflammatory response that extends to the brain (Consoli et al. 2020). C57Bl/6J donor mice were obtained at six weeks of age from Jackson Laboratory (#000664) and euthanized within 7 days of arrival. Cecal contents were collected and resuspended in 5% dextrose at 80 mg/ml, then filtered through a 100 µm filter. Aliquots were stored at -80°C until ready for use.

All mice were bred in house from C57Bl/6J mice originally obtained from Jackson Laboratory. Mice were maintained on a consistent 12-hour light/dark cycle (light from 06:00-18:00, dark from 18:00-06:00) throughout lifetime and experimental study. For EEG studies, mice at 10-12 weeks of age underwent telemetry device implantation surgery (see Section 2.3). Approximately 5-7 days following surgery, mice were treated with CS (1.5 mg/g; i.p.) or the vehicle (Veh, 5% dextrose, i.p.). For LTP studies, mice received CS treatment at 8-10 weeks of age. At 8 and 20 hours following initial injection, all mice received antibiotics and fluid resuscitation in the form of 1.5 mg imipenem stabilized in cilastatin and suspended in 300 µl of 0.9% NaCl saline (Steele et al. 2017). Imipenem is a carbapenem class beta lactam antibiotic that

has no association with delirium severity during critical illness (Grahl et al. 2018). For EEG studies, mice were singly housed following EEG surgeries and for all other studies, control and treated mice were equally distributed across cages with 2-5 mice per cage. All mice were provided supplemental nutrition on the floor of the cage (DietGel 76A, Clear H_2O) following initial injection and throughout recovery up to 48 hours post injection to promote survival. The mice were monitored every 4-8 hours for 24 hours during onset of illness and recovery for body weight and Clinical Sickness Score evaluation (Shaver et al. 2019; Meegan et al. 2020; Kerchberger et al. 2019; Consoli et al. 2020).

The EEG study used 26 mice that underwent telemetry device surgery and recording across four separate cohorts. Two mice were excluded, because they died during illness prior to completion of recovery trajectory. Three additional mice were excluded, because they did not exhibit sufficient signs of behavioral illness (indicated by receiving a Clinical Sickness Score less than 10 likely due to failed injection). The LTP study used 30 mice across five separate cohorts. Five mice that did not exhibit sufficient signs of illness and one mouse that died during illness were excluded from all analysis.

4.2.2. Nest Building

Mice were singly housed overnight with two squares of pressed cotton nestlet material weighing a total of 5.0 g stacked in the center of each cage. Nests were scored the following morning based on three primary criteria adapted from (Deacon 2006) (**Table 4**). First, 0-1 point were given based on the presence of a clear nest site (0 points for no site, 0.5 point for slightly moving the nestlets, and 1 point for a clear nest site). Next, 0-2 points were given based on extent of nestlet shredded and utilization of un-shredded nestlet (0 points for little to no shredded, 0.5 point for at least 25% shredded, 1 point for at least 50% shredded, 1.5 points for at least 75% shredded, and 2 points for 100% shredded). If less than 50% was shredded, but a largely un-shredded piece was utilized structurally as a wall or roof, an additional point was given. Lastly, 0-2 points were given based on overall nest height (0 points for flat, 0.5 point for low, 1 point for medium height, 1.5 points for medium high, and 2 points for high coverage or dome structure). If nest criteria were deemed between two score designations scores were made with 0.25-point increments. Graphical representations of nests of varying complexity are illustrated in **Figure 13B**.

Table 4 – Nest building behavioral task scoring criteria.

Nest Site	+0 No site	+0.5 Moved	+1 Clear site		
Nestlet Shredded	+0 <25%	+0.5 25%	+1 50%	+1.5 75%	+2 100%
	+1 Un-shredded nestlet utilized structurally as wall or roof				
Nest Height	+0 Flat	+0.5 Low	+1 Medium	+1.5 Med-High	+2 Dome

4.2.3. EEG Telemetry

Telemetry Device Implantation Surgery

To record electroencephalogram (EEG) activity in mice while minimizing disturbance to normal behavior, we utilized a wireless EEG telemetry system (PhysioTel HD-X02; Data Sciences International, DSI, St. Paul, MN) as previously described (Gould *et al.* 2020). In brief, a wireless telemetry device was implanted in each mouse subcutaneously between the left shoulder and hip according to DSI protocol and under anesthesia (isoflurane 2-5%). Four wires (0.3 mm diameter helix of stainless-steel coils protected with silastic coating 0.63 mm in diameter) connected the device to the recording and reference sites in the neck muscle for electromyograph (EMG) recording and to the skull for EEG recording. EEG leads were inserted into two burr holes 1-mm in diameter exactly +1.0 mm anterior-posterior, -1.0 mm medial-lateral from bregma for reference and -3.0 mm anterior posterior, +3.0 mm medial-lateral from bregma for recording. The skull was covered with dental cement and the incision site was sutured. Immediately following surgery and every 24 hours for 48 hours, mice received analgesic (ketoprofen, 10 mg/kg, i.p.). Mice were allowed 4-6 days of recovery prior to beginning baseline data acquisition.

Telemetry Device Data Acquisition

Following telemetry device implantation surgeries, individual cages of singly housed mice were placed on a PhysioTel receiver plate (model RPC-1) that transmitted data in real time from the wireless implant to a computer using the MX2 data exchange matrix and Dataquest ART software (DSI, St. Paul, MN). Data were collected using Ponemah Physiology Platform version 5.20 software (DSI, St. Paul, MN). Single channel EEG and EMG were sampled at a rate

of 500 Hz, and activity counts were sampled at 50 Hz. Video (20 frames/sec) of each mouse was recorded using Axis cameras (M1145-L) and MediaRecorder 2.6 (Noldus) and synchronized to physiologic measurements. Approximately one week following completion of surgeries and prior to CS or vehicle treatment, 24 hours of baseline telemetry data including EEG, EMG, and activity were recorded for all mice. After treatment injections, telemetry data were collected in 24 hour increments up to 72 hours post injection and then again 7 days post injection for a total of five, 24-hour periods as depicted in **Figure 13A**.

Prior to injections, mice were briefly anesthetized with isoflurane to avoid displacing the EMG and EEG leads during handling, requiring temporary removal of the mice from the plate reader for less than one minute. During Clinical Sickness Scoring, mice were scored in their cages on the receiver and weighed by removal from the cage onto a scale near the plate reader with minimal disruption of data acquisition.

Telemetry Device Data Analysis

Telemetry data were analyzed using NeuroScore (version 3.3.0, DSI, St. Paul, MN). To determine global changes in EEG independent of behavioral vigilance state, spectral power band analyses separated the EEG signal into relative power percentages using 10 second epochs across different frequencies (delta 0.5-4 Hz, theta 4-8 Hz, alpha 8-12 Hz, sigma 12-16 Hz, beta 16-24 Hz, and gamma 24-50 Hz). The averaged power percentages for each hour were normalized to the average baseline value. The theta ratio is reported as relative theta power divided by relative delta power normalized to the average baseline value. For telemetry activity data, the maximum activity count per 10 second epoch was determined, and the sum of activity counts per hour and total activity per 24-hour period are reported.

To determine changes in EEG within behavioral vigilance states, data were visualized and scored within 10 second epoch windows according to DSI instructions for Sleep Scoring in Neuroscore. Periodograms ranging from 0 to 25 Hz were viewed in 10 second epochs alongside continuous plots of EEG theta ratio, EEG number of crossings, EEG and EMG raw traces, and activity counts. The behavioral state for each 10 second epoch was scored as non-rapid eye movement (NREM, slow-wave sleep), REM (paradoxical sleep), or wake. High delta power, low theta ratio and number of crossings, low EMG muscle tone, and low activity counts were scored as NREM. High theta power and theta ratio, low number of crossings, low EMG muscle tone,

and low activity were scored as REM. High EMG muscle tone and high activity counts with low to medium delta and theta power were scored as wake. Micro-wakes and quiet wakes were included as wake. Sleep stages were scored for one hour at the same time of day (17:00-18:00) at baseline (Day 0), during illness (Day 1), following acute recovery (Day 2), and following long-term recovery (Day 7). The relative power for each 1 Hz frequency within each sleep stage was averaged and reported.

4.2.5. Locomotor Activity

Open-field activity was recorded by infrared beam detection using standard locomotor activity chambers (approx. 30 x 30 cm, ENV-510; MED Associates, Georgia, VT, USA). Total activity travelled during the 30-minute trial is reported.

4.2.6. Pre-pulse Inhibition of Acoustic Startle Response

Mice were placed in a small, clear acrylic animal holder, cylindrical in shape and mounted on a white acrylic base. The holder was secured to a startle platform detector housed within an acoustic chamber insulated with 2 cm sound attenuating foam (ENV-022S, MED Associates). Various startle and pre-pulse stimuli were delivered using Startle-PPI Pro Series software (SOF-826, MED Associates). Testing consisted of six different trials (null, 0 dB; startle only, 120 dB; pre-pulse at 72, 76, 82, 88 dB each followed by startle at 120 dB) repeated nine times in a pseudo-random order for a total of 54 trials. The mice were allowed an acclimation period of 5 minutes before trials began, and time between trials was 30 seconds. In trials with a pre-pulse, the pre-pulse stimulus was delivered 50 ms before startle stimulus. The highest and lowest values for each trial type were excluded, and the average response per trial type was determined. The percent pre-pulse inhibition was calculated at each pre-pulse amplitude using the difference between the pre-pulse trials and the startle only trial.

4.2.7. Long-Term Potentiation

Hippocampal slices were prepared from 8-10-week-old mice treated with CS or Veh. Mice were briefly anesthetized and then sacrificed by decapitation. The brain was quickly removed into an ice-cold solution of sucrose-rich artificial cerebrospinal fluid (aCSF) containing 85 mM NaCl, 2.5 mM KCl, 1.25 mM NaH_2PO_4, 25 mM $NaHCO_3$, 75 mM sucrose, 25 mM

glucose, 10 µM DL-APV (NMDA antagonist), 100 uM kynurenate, 0.5 mM sodium L-ascorbate, 0.5 mM $CaCl_2$, and 4 mM $MgCl_2$ oxygenated and equilibrated with 95%O_2/5%CO_2 and titrated to a pH of 7.4. The brain was mounted on a slicing stage ventral side up, and 300µm horizontal slices were prepared using a Leica VT-1200S vibratome (Leica Biosystems) in sucrose-aCSF. Slices from both hemispheres were micro-dissected before transferring to a holding chamber containing sucrose-aCSF warmed to 32ºC that slowly returned to room temperature over the course of 30 minutes. Slices were then transferred to a second holding chamber containing room temperature aCSF containing 125 mM NaCl, 2.4 mM KCl, 1.2 mM NaH_2PO_4, 25 mM $NaHCO_3$, 25 mM glucose, 2 mM $CaCl_2$, and 1 mM $MgCl_2$ oxygenated and equilibrated with 95%O_2/5%CO_2 and titrated to a pH of 7.4. Slices were maintained under these conditions until transferred into a submerged recording chamber (Scientifica SliceScope Pro 2000, Scientific UK) flowing warmed (in-line heater temperature set at 36ºC) oxygenated aCSF at approximately 6 ml/min.

Field excitatory postsynaptic potentials (fEPSPs) were recorded by stimulating along the Schaffer collaterals in the stratum radiatum and recording the response from the Cornu ammonis 1 (CA1) region of the hippocampus at a rate of 0.05 Hz. An input-output relationship was determined for each slice, plotting the peak amplitude of the fiber volley against the slope of the fEPSP. For LTP experiments, the baseline recordings used a stimulus intensity that produced ~40% of the maximum response and were recorded for at least 20 min before tetanizing the slice. LTP was induced using theta-burst stimulation (5 bursts at 100 Hz, repeated at 5 Hz over 5 seconds, with each tetanus including four of these burst trains separated by 10 seconds, totaling 100 bursts). Experiments in which the fiber volley amplitude changed by >20% post-tetanus were discarded. Recordings were continued for at least 60 mins post-tetanus. The magnitude of LTP was measured in the last 5 minutes of the 60 minutes post tetanus recording. There were 5-8 slices in each group from 2-3 mice.

4.2.8. Statistics

Data shown in figures and text are reported as mean +/- S.E.M. unless otherwise stated. Bar graph data were analyzed using GraphPad Prism (version 9.1.1). All groups were equally balanced male and female mice, and analyses were first run with sex as a fixed variable. There were no significant meaningful differences according to sex, thus all data were collapsed and

analyzed together. All data were first checked for normality with an Anderson Darling test (alpha = 0.05), and all data with normal Gaussian distribution were subsequently analyzed using parametric statistical analyses. Nest building data were not normally distributed and were instead analyzed per day of scoring using the non-parametric Kruskal-Wallis test, and the Kruskal-Wallis statistic (KW) is reported. Following significant results, nest building scores for each group were compared with Dunn's test for nonparametric comparisons. Activity data were analyzed using a two-way repeated measures ANOVA with time and treatment as dependent variables. Following significant results, activity data were compared to baseline activity levels using a Dunnett's multiple comparisons test. Periodogram data were analyzed using an ordinary two-way ANOVA with treatment and frequency as dependent variables. Tukey's multiple comparison test was used to compare differences between treatment groups within each frequency. PPI data were analyzed using a two-way repeated measures ANOVA, with treatment and pre-pulse amplitude as dependent variables. To compare means across vehicle and CS treated mice specifically within each pre-pulse amplitude, treatment groups were compared using a Šídák's multiple comparisons test.

We conducted statistical analyses of EEG theta ratio and power bands using R Statistical Software version 4.0.3 (R Foundation for Statistical Computing, Vienna, Austria). To assess the difference in the change of each EEG metric over time between CS and vehicle during the first and final 24-hour periods following injection, we used a linear mixed-effects model with a random intercept in which the EEG metric was the dependent variable and the group indicator (i.e., CS vs. Veh), time, and the interaction term between the group and time were the explanatory variables. To capture the nonlinear trend of the EEG metric over time, we employed natural splines of time variable, while the underlying temporal correlation was modeled by an autoregressive temporal process with order one, i.e., AR(1). The statistical significance (p-value < 0.05) was tested by comparing the model with the interaction terms to the model without them by a likelihood ratio (LR) test. For each model, we tested for the effect of sex on the association of interest, i.e., the association between Theta ratio and the interaction between time and group (e.g., CS vs. Veh). There was no significant sex effect in any of the models.

4.3 Results

4.3.1. CS treatment causes EEG slowing during illness and long-term cognitive impairments.

Throughout EEG data acquisition, we used nest building (designated NB in the figures) to measure lasting changes in cognitive ability following recovery from CS treatment (**Fig. 13A-B, D**). All CS treated mice showed similar illness trajectory based on Clinical Sickness Score evaluation (p's>0.2912, **Fig. 13C**). Nest building was performed at three timepoints: baseline (prior to injection), following illness on Day 2 (acute recovery), and again on Day 7 (long-term recovery). Nest building scores did not vary in vehicle treated mice up to Day 7 following injection (KW=1.269, p=0.5302), but nest building scores were significantly decreased following illness in CS treated mice (KW's>11.26, p's<0.0009). These deficits were most apparent on Day 2 following illness and were more variable on Day 7, which permitted subdivision of CS-treated animals into two distinct groups based on nest building score at 7 days. CS treated mice that had nest building scores equivalent to pre-CS levels (score > 3.0) were designated "recovered" whereas mice that built poor nests (score < 3.0) were placed in the "persistent deficits" group. The criteria were based on the lowest baseline score observed in vehicle treated mice (**Fig. 13D**). Differential long-term recovery in CS-treated mice was distinguishable on Day 7 (p=0.0072) but the two groups did not differ on Day 2 (p>0.9999). This separation of CS treated mice based on long-term recovery was utilized throughout remaining data analysis to explore individual metric contributions to long-term cognitive deficits.

Total activity per day was compared across groups and time. Changes in activity of CS treated mice during and following illness drove a significant interaction between time and treatment ($F_{8,72}$=9.691, p<0.0001). As expected, total activity did not change in vehicle treated mice throughout the experiment (p's>0.6987), and all CS treated mice had decreased activity during illness on Day 1 (p's<0.0001). Hypoactivity in CS treated mice persisted following acute recovery only until Day 3 (p's<0.0033), and by Day 7 activity had gradually returned to baseline levels (p's>0.9217) in all groups (**Fig. 13E**). Normal activity levels on Day 7 in all CS treated mice indicated that persistent nest building deficits on Day 7 were not due to persistent hypoactivity and thus more likely reflect cognitive rather than locomotor deficits.

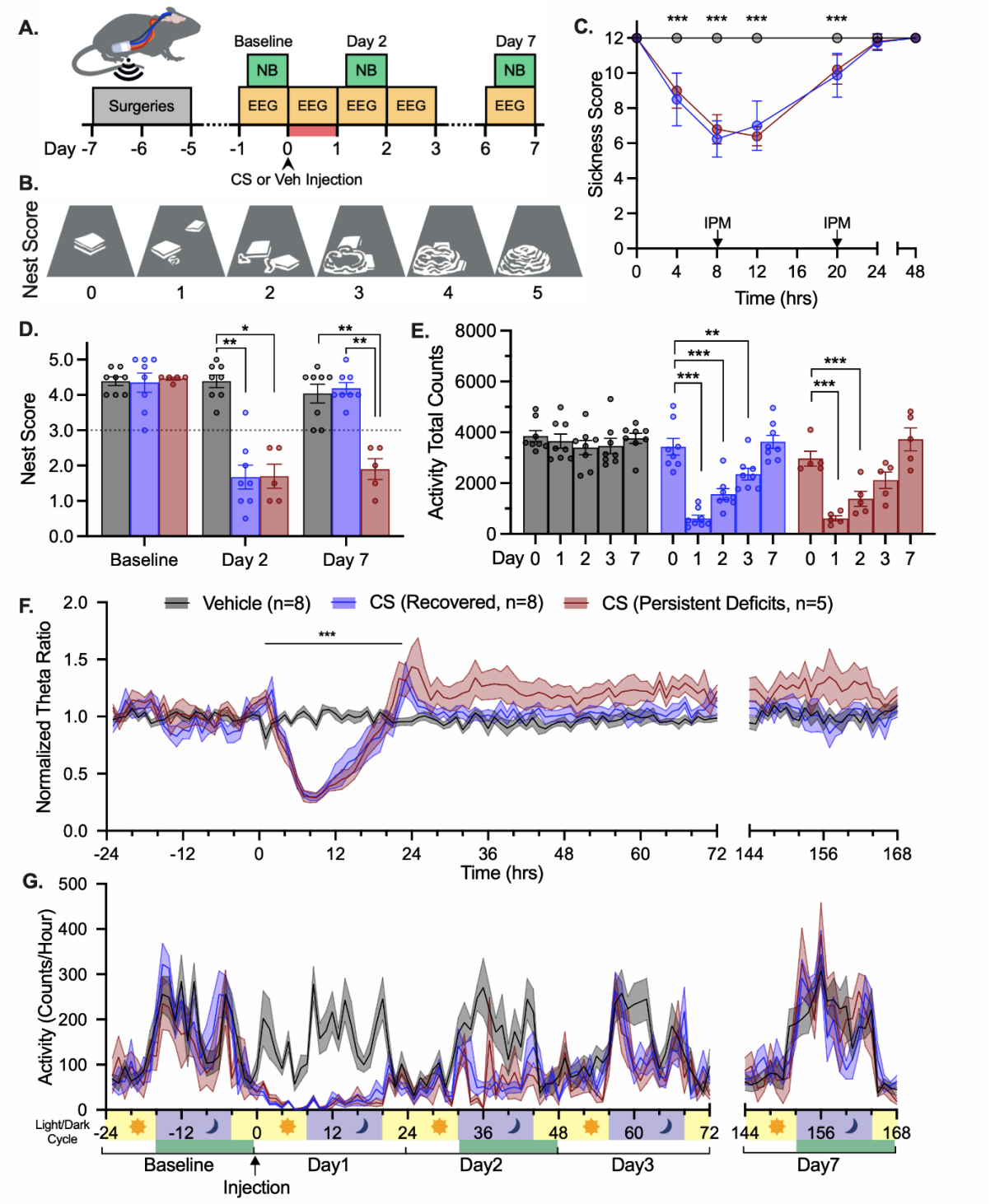

Figure 13 – Nest building, EEG, and activity.
(**A**) EEG and behavior experimental timeline. Nest building (NB) task shown in green boxes were performed at baseline and on Days 2 and 7 following the illness period highlighted in red. Telemetry data were recorded in 24-hour increments as indicated in yellow boxes. (**B**) Illustrations of nests representing a range of scores in order of increasing complexity, cage floor shown in grey, nestlet material in white. (**C**) Clinical Sickness Scores. IPM – imipenem (i.p. 1.5

mg/300cc saline). (**D**) Nest scores following CS treatment and separation into groups based on recovery on Day 7. (**E**) Total activity counts per day. (**F**) Normalized theta ratio synchronized to (**G**) activity counts per hour shown with light/dark cycle. Nest building task performed during times highlighted in green. ***p<0.001, **p<0.01, *p<0.05.

To compare global changes in EEG frequencies during and following illness, we first examined the average theta ratio per hour throughout the experiment. During illness, CS treated mice elicited a dramatic decrease in theta ratio that persisted until no longer observably ill at approximately 24 hours (LR=99.1052, p<0.0001, **Fig. 13F**). Decreased theta ratio persisted marginally longer in the CS group with persistent impairments at 7 days (LR=7.7511, p=0.0514). Theta ratio was not significantly different between any groups on Day 7 (LR=6.7642, p=0.0798). Closer analysis of activity per hour within light/dark cycles showed normal activity across all groups at baseline were greatly disrupted during illness on Day 1 and following acute recovery. Decreased activity per hour gradually recovered to resemble those of vehicle treated mice by Day 7 regardless of NB outcome on Day 7 (**Fig. 13G**).

4.3.2. Power band analysis

Global changes in EEG signatures were further investigated by dividing the data into six functionally distinct power bands of differing frequency ranges. Average power percent per hour was reported for delta (0.5-4 Hz), theta (4-8 Hz), alpha (8-12 Hz), sigma (12-16 Hz), beta (16-24 Hz), and gamma (25-50 Hz) (**Fig. 14A-F**). Changes in power band composition in CS treated mice were most apparent from 0-24 hours. During illness onset, delta power increased (LR=104.6962, p<0.0001, **Fig. 14A**) as theta power decreased (LR=78.8804, p<0.0001, **Fig. 14B**) compared to vehicle. Following illness, delta power returned to baseline as theta power increased (**Fig. 14A-B**). Increased theta power gradually returned to normal levels by Day 3. Alpha power decreased during illness and returned to normal upon recovery (LR=54.8937, p<0.0001, **Fig. 14C**). There were no changes in sigma power during illness (LR=4.3151, p=0.2294, **Fig. 14D**). Higher frequency ranges including beta and gamma power were increased during illness (Beta: LR=12.1489, p=0.0069; Gamma: LR=27.8134, p<0.0001 **Fig. 14E-F**). There were no significant differences between CS treated mice with variable nest building recovery during illness or on Day 7 (LR's<2.9358, p's>0.4016).

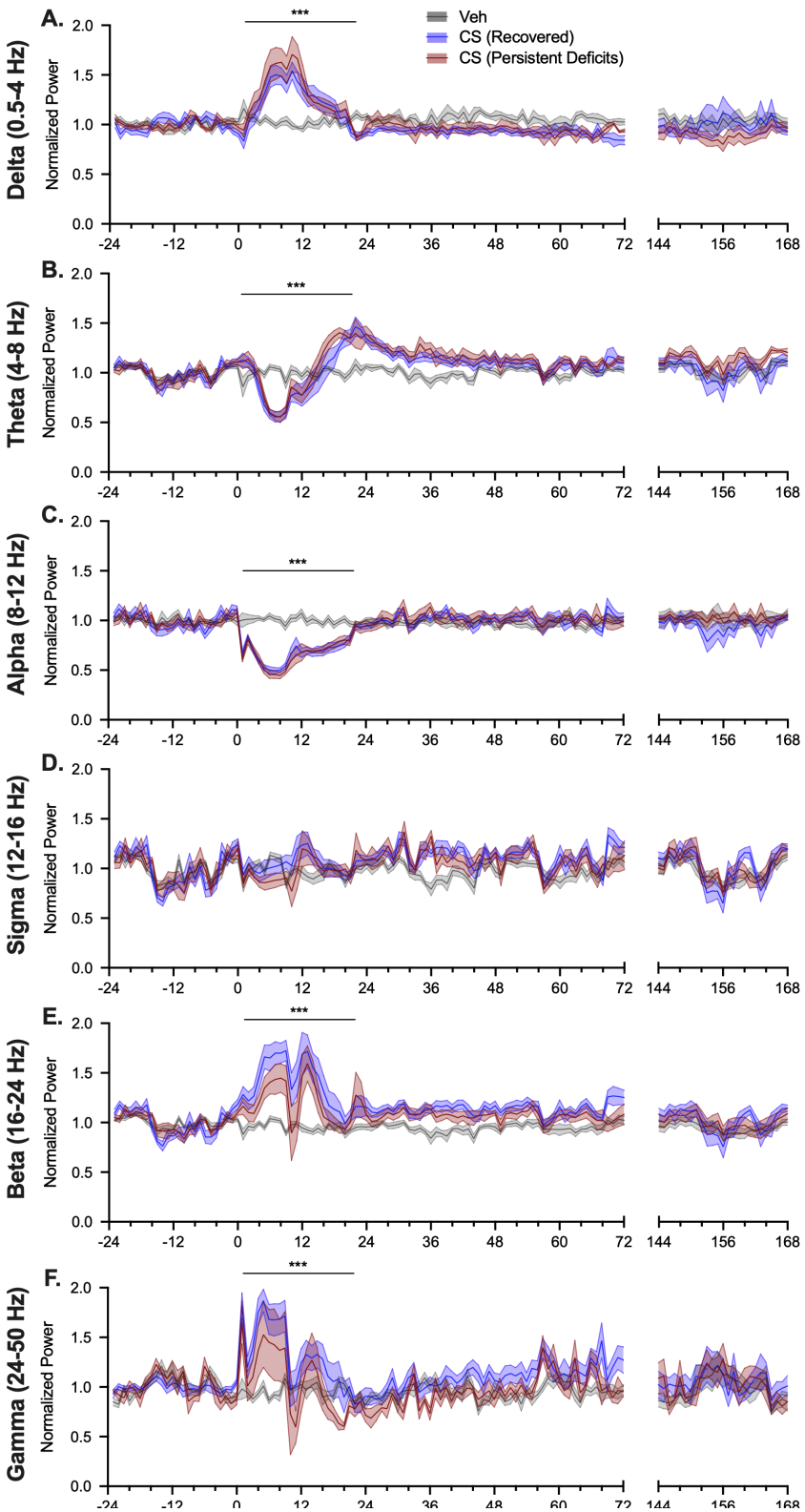

Figure 14 – Power band analysis.
Average normalized power per hour for (**A**) delta (0.5-4 Hz), (**B**) theta (4-8 Hz), (**C**) alpha (8-12 Hz), (**D**) sigma (12-16 Hz), (**E**) beta (16-24 Hz), and (**F**) gamma (25-50 Hz). ***p<0.001 vehicle vs. CS, #p<0.05 CS persistent deficits vs. CS recovered

4.3.3. Periodograms within Sleep Stages show generalized EEG slowing during illness.

Using the same EEG dataset, we generated spectral periodograms to visualize and compare changes in EEG within sleep stages. EEG activity in CS treated mice was broadly dominated by slower EEG frequencies during illness (**Fig. 15A**). The timeframe shown is hour 7-8 (17:00-18:00) following vehicle or CS injection, during peak critical illness, prior to antibiotic injection, and just prior to light-cycle change. Slow-wave dominance is even more apparent when these periodograms were compared across sleep stages to vehicle treated mice. Periodograms scored as NREM and wake had greatly increased delta power and did not resemble normal NREM and wake (**Fig 15Biv** NREM p's<0.0095; **Fig. 15Bvi** wake p's<0.0029). Vehicle treated mice showed normal variation in sleep stages by exhibiting wake, NREM, and REM sleep stages within each hour scored. Interestingly, CS treated mice showed no observable REM sleep during illness though as expected showed increased NREM and decreased wake (**Fig. 15Bv, C**).

Subtle changes in power frequencies were observed across sleep stages following illness. During the acute and long-term recovery periods scored immediately prior to initiation of the nest building task, CS treated mice had altered NREM, REM, and wake periodograms (**Fig. 15Bvii-xii)**. During wake, CS treated mice had decreased delta power and increased theta power compared to vehicle treated mice (p's<0.0128). Most notably, during REM in the long-term recovery period, CS treated mice with persistent deficits had significantly decreased theta power compared to CS mice who recovered (**Fig. 15Bxi**, p=0.0313) suggesting that a lack of normal restorative REM sleep may contribute to the long-term cognitive deficits observed in the nest building task.

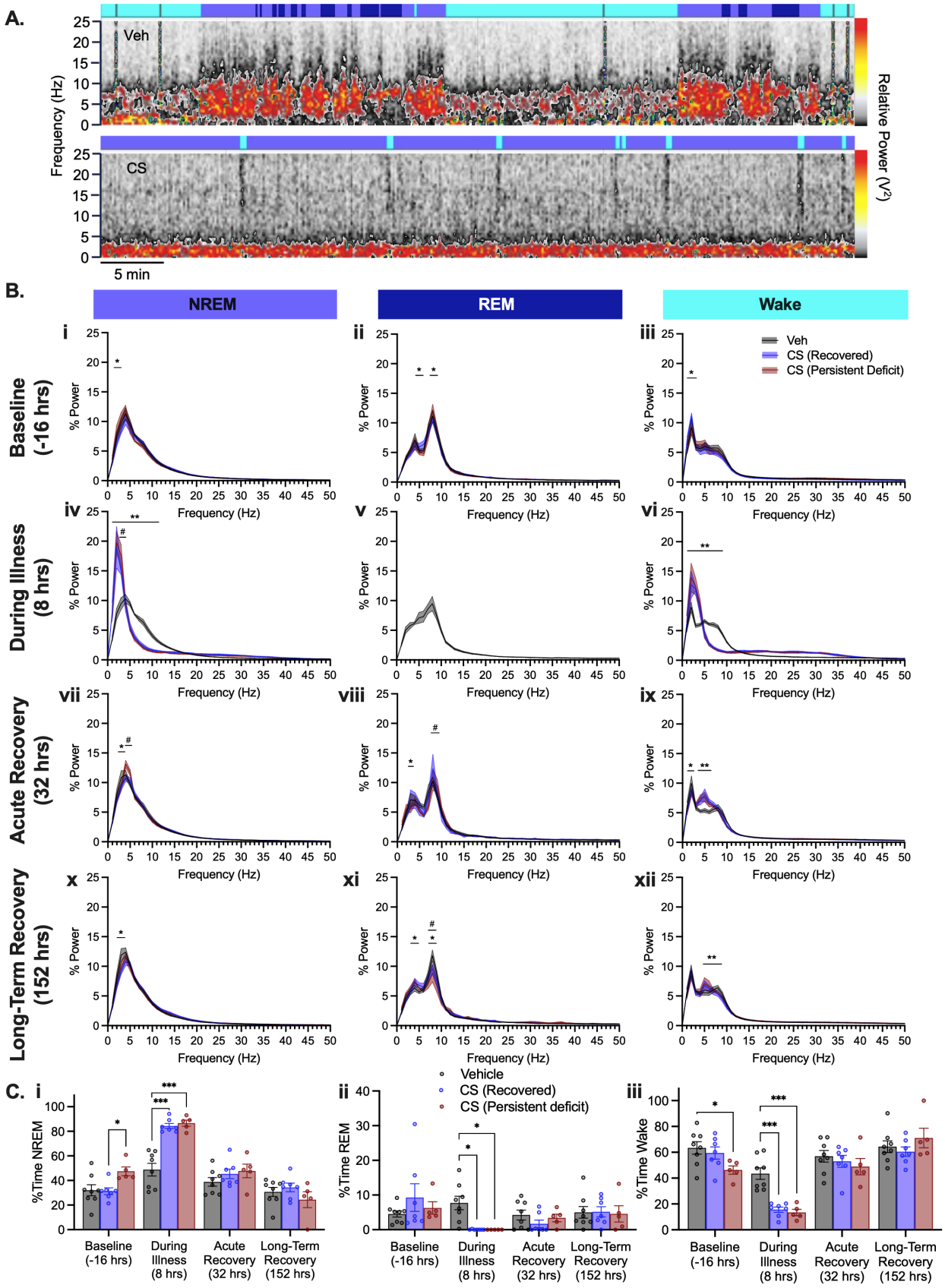

Figure 15 – Sleep score analysis.

(**A**) Representative one-hour spectral periodograms for Vehicle(top) and CS (bottom) groups 8 hours following injection. Top colored ribbons indicate scored sleep stage for each 10 second epoch: blue – NREM, dark blue – REM, cyan – wake, gray – artifact/excluded. (**B**) Periodograms within sleep stages NREM (left), REM (middle) and wake (right) at baseline (**i-iii**), during illness (**iv-vi**), acute recovery (**vii-ix**), and long-term recovery (**x-xii**). (**C**) Duration spent in each sleep stage across scored timepoints. ***p<0.001, **p<0.01, *p<0.05 CS vs Veh; #p<0.01 CS Recovered vs. CS Persistent Deficits

4.3.4. Elevated PPI implicates hypersensitivity to stimulus.

We performed a second experiment in mice destined for ex vivo electrophysiology following CS treatment (**Fig. 16A**). A parallel behavioral paradigm utilized nest building and locomotor activity chambers to determine long-term cognitive deficits, and data were again analyzed based on long-term cognitive outcome on Day 7 post CS treatment. During illness, we used pre-pulse inhibition (PPI) of startle response as a behavioral measure of attention and awareness during illness. No changes were observed in startle response during illness (Time: $F_{2,42}$=2.718, p=0.0776; Treatment: $F_{1,21}$=0.2477, p=0.6238, **Fig. 16B**). At 4- and 8-hours post treatment, CS treated mice showed an unexpected increase in PPI (**Fig. 4C, 16E** 4 hrs: Treatment, $F_{1,22}$=6.992, p=0.0148; 8 hrs: Treatment, $F_{1,22}$=15.95, p=0.0007) indicating a greater inhibition of startle response and hypersensitivity to the pre-pulse stimulus during illness. This effect was exaggerated when compared as a change from baseline measures for each mouse (**Fig. 16D, F** 4 hrs: Treatment, $F_{1,22}$=16.08, p=0.0006; 8 hrs: Treatment, $F_{1,22}$=15.01, p=0.0008). This analysis was only performed for mice that completed testing to Day 7 (n=3-4 mice per group). However, there were no significant differences in PPI response between CS groups with differential long-term NB outcome (p's>0.9991).

Nest building behavior in this experiment resembled those observed previously in telemetry implanted mice. CS treated mice showed poor nest building ability on Day 2 following illness (KW=9.806, p=0.0006), but on Day 7 mice showed differential recovery (KW=8.723, p=0.0009, **Fig. 16G**). Activity data also recapitulated findings from the previous telemetry experiment, showing significant effects of time driven by hypoactivity on Day 2 ($F_{2,29}$=4.477, p=0.0202). Activity returned to normal exploration levels on Day 7 regardless of Day 7 NB outcome (p's>0.3502, **Fig. 16H**).

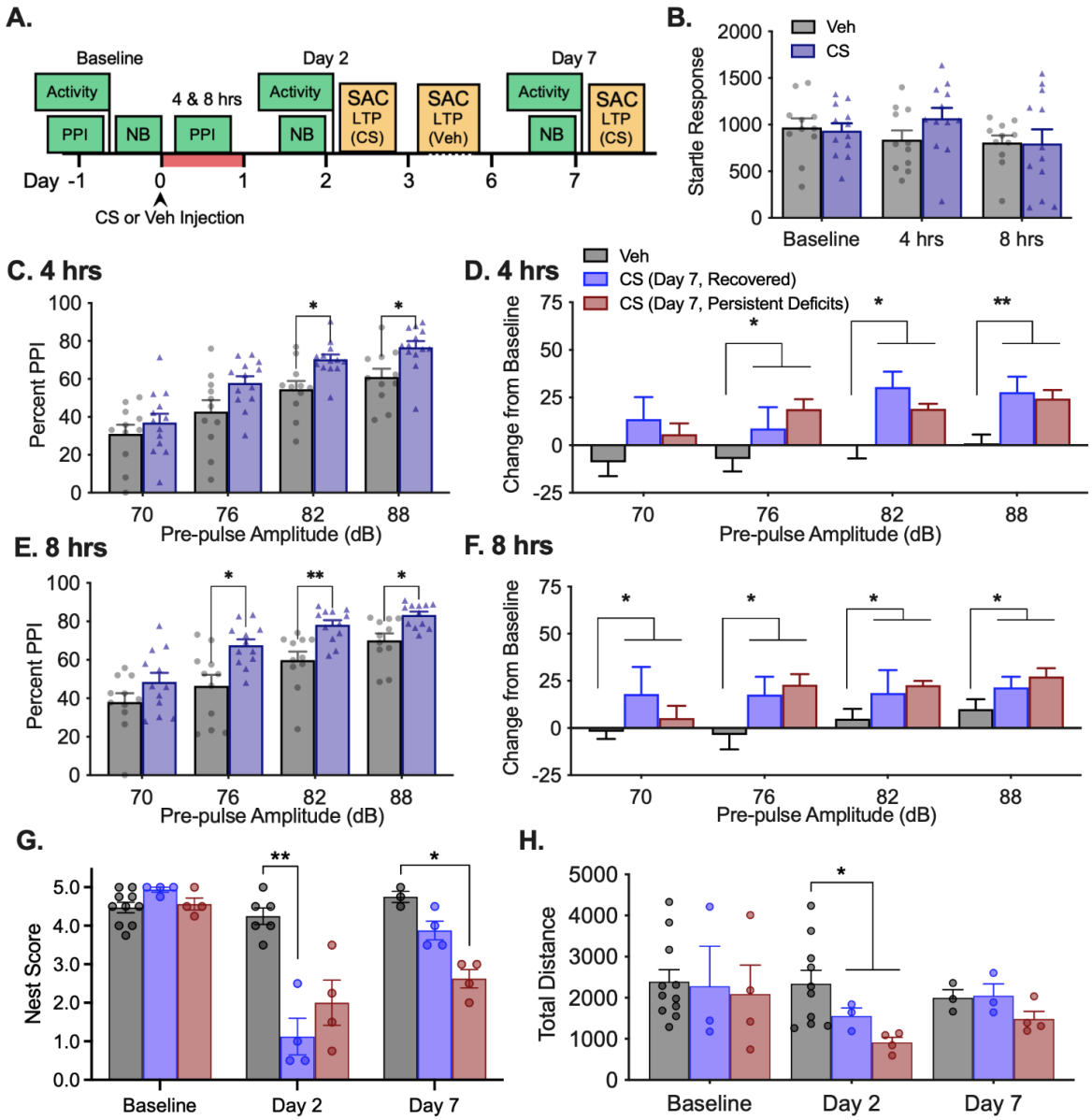

Figure 16 – Pre-pulse inhibition during illness.
(**A**) Experimental timeline. NB, PPI, and activity behavioral tasks were performed at timepoints indicated by green boxes. After NB scoring, CS treated mice were euthanized for LTP recording on Days 2 and 7 while vehicle treated mice were distributed between Days 2-7 as indicated in yellow boxes. Illness period is highlighted in red. **(B)** Startle response during 120 dB startle only trial. (**C**) PPI at 4 hours and (**E**) 8 hours post injection comparing all CS to Veh during illness. (**D**) PPI change from baseline at 4 hours and (**F**) 8 hours split by NB groups on Day 7 (n=3-4 mice per group). (**G**) NB scores for each group prior to SAC for LTP recording. (**H**) Total locomotor activity during 30 min open field exploration task.

4.3.5. Deficits in Long-term Potentiation implicate long-term cognitive deficits following CS treatment.

To support the hypothesis that nest building deficits indicate long-term cognitive damage, we measured long-term potentiation (LTP) in mice that recovered from CS treatment by recording local field excitatory post-synaptic potentials (EPSPs) in ex-vivo hippocampal slices before and after theta-burst stimulation (**Fig. 17A-B**). We observed normal input-output responses and fiber volley to excitatory post-synaptic potential (EPSP) relationships in the slices (**Fig. 17C-E**, Time and Treatment, F's<2.022, p's>0.1449). LTP was impaired by roughly 50% in CS treated mice on Day 2 following illness (p=0.0229, **Fig. 17F-G**). On Day 7, mice that had recovered NB ability also showed recovered LTP (p>0.9999, **Fig. 17F-G**), however, mice with persistent NB deficits on Day 7 showed deficits in LTP (p=0.0056, **Fig. 17F-G**). We observed no changes in paired pulse ratios between groups (**Fig. 17H**, F's<06069, p's>0.4451).

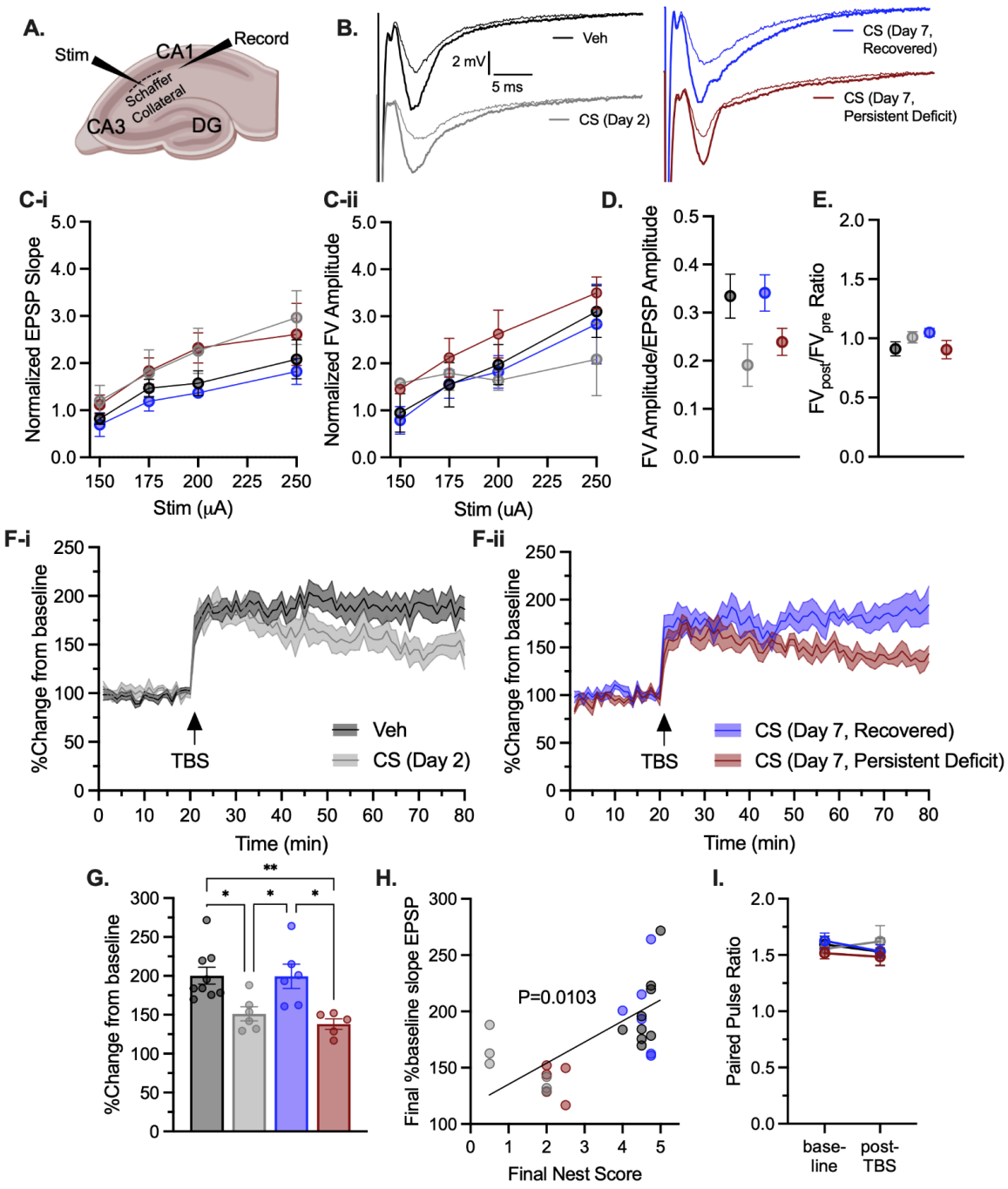

Figure 17 – Evaluation of long-term potentiation (LTP).
(**A**) Stimulation and recording setup. (**B**) Representative EPSP traces after first pulse prior to (thin line) and post (thick line) TBS. (**C**) Input-output curves. (**D**) Fiber volley to EPSP ratio. (**E**) Fiber volley ratio pre/post TBS. (**F**) EPSP slope percent change from baseline and (**G**) final EPSP slope percent change from baseline in last 5 min. (**H**) Correlation with nest building. (**I**) Paired pulse ratio. TBS – theta burst stimulation.

4.4 Discussion

Difficulty measuring behavioral deficits in mice during critical illness has previously limited preclinical studies of delirium and its correlation with poor cognitive outcomes. Using an innovative combination of behavior and electrophysiological techniques, we built an animal model that quantifies delirium-like mental status in mice. We observed dramatic decreases in theta ratio during illness (**Fig. 13D**) indicating a shift towards slow-wave delta EEG activity confirmed by individual power band analyses (**Fig. 14A-B**). Similar slow-wave EEG activity is well-documented in delirious patients and is strongly related to cognitive deficits following illness (Mart *et al.* 2020; Roberson *et al.* 2020; Engel and Romano 1959; Kimchi *et al.* 2019). We also observed global decreases in alpha power during illness (**Fig. 14C**), indicating decreases in active attention. Regular alpha rhythm demonstrates normal responsiveness and is disrupted in delirium (Hirsch *et al.* 2021; Jacobson *et al.* 1993; Mulkey *et al.* 2019).

Delirious patients exhibit markedly decreased beta power relative to controls (Roberson *et al.* 2020; Hirsch *et al.* 2021), and patients with preserved higher-frequency activity including beta power have lower incidence of delirium (Nielsen *et al.* 2019). Surprisingly, we observed elevations in beta and gamma powers in CS treated mice during illness (**Fig. 14E-F**). We did not observe significant differences in power bands between CS treated groups separated by long-term recovery, however, power band analysis may still be an appropriate signal of brain dysfunction during illness that put 38% of mice at risk of later cognitive decline. We postulate that the differences in cognitive outcomes between the groups could be driven by greater beta activity during illness indicating greater arousal, though these differences were not directly observable in the current analysis. Elevated beta frequencies are observed in sedated patients due to sedative-hypnotic drugs, particularly barbiturates and benzodiazepines (Van Lier *et al.* 2004; Satapathy *et al.* 2019). The increases in beta waves we observed during illness could also be attributable to stress, anxiety, and higher arousal (Abhang *et al.* 2016; Satapathy *et al.* 2019). This explanation would suggest a greater arousal during illness, indicated by greater relative beta power, is protective of long-term cognitive damage regardless of the extent of overall EEG slowing.

During illness, CS treated mice showed periodograms that were dramatically shifted towards slower (delta, 0.5-4 Hz) frequencies and did not resemble normal wake or sleep (**Fig.**

15A-B). Due to these dramatic shifts, CS treated mice showed no identifiable REM sleep during illness, increased NREM sleep, and decreased wake consistent with another study of sleep following cecal ligation and puncture to induce sepsis in rats (Baracchi *et al.* 2011). Following illness, at both the acute and long-term recovery timepoints we observed decreased theta power intensity during REM sleep, suggesting that sleep may be perpetually altered following illness. Disruptions in normal sleep-wake cycles during illness and lasting neuroimmune dysregulation following illness could contribute to lasting cognitive deficits (Opp *et al.* 2015).

At 8 hours immediately following antibiotic administration, beta and gamma power were noticeably decreased while delta and theta were marginally increased (**Fig. 14**). These alterations following injection were contrary to what we expected, because interacting with a sick mouse should intuitively increase arousal. Subsequent antibiotic interactions on the system, such as comprehensive lysis of bacteria or indirect cerebral drug interactions could contribute to the raising of beta and gamma and dropping of excess delta and theta. Subsequently increased LPS accumulation and inflammatory signaling could decrease arousal driving these observations. Imipenem is also a beta-lactam antibiotic belonging to the class of carbapenems, which have a proconvulsant nature through inhibitory receptor antagonism that could be driving changes in EEG or LTP (Miller *et al.* 2011). We did not observe any drastic EEG or LTP changes in the control mice that also received antibiotics. However, differences in drug concentrations are possible during illness due to impaired renal function in septic mice. Perhaps in mice with renal failure secondary to sepsis, a carbapenem can contribute to EEG abnormalities that impair learning and hippocampal LTP. This potential mechanism of action should be investigated in future studies and would have important implications for the therapeutic mechanisms of long-term cognitive impairment in septic patients receiving antibiotics.

Although we did not observe any significant differences in hypersensitivity during illness within CS treated groups in the PPI task, we hypothesize that greater inattention during illness is indicative of greater neuropathological and neuroinflammatory damage that contribute to long term cognitive decline in this model. Deficits in PPI are usually discussed in the context of schizophrenia, observed as decreased PPI relative to healthy controls (Mena *et al.* 2016). Decreased PPI is greatly associated with prefrontal cortical dysfunction (Kumari *et al.* 2003; Hammer *et al.* 2013). Contrary to our initial predictions, during illness we found elevated PPI, indicating hypersensitivity to the pre-pulse stimulus that may be indicative of a hyperadrenergic

state (Hinson and Sheth 2012). This would further explain elevations in beta and gamma powers relative to controls. Elevated PPI has been observed in children with autism spectrum disorder and attributed to high stress and anxiety (Madsen *et al.* 2014). Contributions of hyperadrenergic signaling to long term cognitive deficits is differential across different mouse models of sepsis (O'Neill *et al.* 2021; Field *et al.* 2012). If hypersensitive PPI is indicative of a hyperadrenergic state that correlates with higher beta and gamma powers, this model would suggest that proper adrenergic regulation could be protective of later cognitive dysfunction.

Nest building ability is a hippocampal dependent task associated with executive function, and deficits in nest building ability are associated with cognitive decline (Walker *et al.* 2017; Deacon 2006; Deacon *et al.* 2002). Neurocognitive deficits assessed by decreased nest building ability were supported by deficits in hippocampal LTP, an important molecular foundation of learning and memory (Lynch 2004). We found similar deficits in LTP in our CS model of sepsis as those reported in two other mouse models of sepsis using lipopolysaccharide and cecal ligation and puncture 7 days following acute illness (Hippensteel *et al.* 2019). CS was a preferable tool for this study over other such alternative methods of sepsis induction due to its translationally relevant microbial diversity, precise dose control of illness severity and tight temporal control of illness onset which was necessary for circadian rhythm synchronization. Cortical and hippocampal dysfunction is intimately linked via neural disinhibition (McGarrity *et al.* 2017; Bast *et al.* 2017; Moretti *et al.* 2012), so it is likely that the hippocampal dysfunction we observed in LTP is driven by the cortical dysfunction we observed using EEG. Further, molecular deficits in the hippocampus in sepsis models are reported to require acute brain injury and associated neuroinflammation and do not occur due to systemic inflammation alone (Skelly *et al.* 2019).

Fewer mice that were utilized in the LTP experiments showed a persistent nest building deficit compared to those observed in the EEG study (24% of mice had observed nest building deficits on Day 7 in the EEG study compared to 13% in the LTP study). Given the extensive research on post-op surgery, delirium, and cognitive decline (Illendula *et al.* 2020; Crosby and Culley 2011; Crosby *et al.* 2010), the insult of surgery and anesthesia in the EEG study likely contributed to the severity of illness we observed. Singly housing the mice in the EEG study could also have contributed to delirium and cognitive deficit severity, as mice in the second

study were also housed 3-5 mice per cage and social isolation is known to greatly increase risk of delirium (Pun *et al.* 2021; Kotfis *et al.* 2020).

EEG slowing is a strong indicator of delirium and is associated with cognitive deficits following critical illness. The recapitulation of patient EEG metrics in a mouse model of sepsis demonstrates occurrence of a translationally relevant sepsis associated encephalopathy in mice. In line with the higher prevalence of delirium and greater risk for cognitive decline following critical illness in older patients (Pandharipande *et al.* 2013; Rengel *et al.* 2019), these approaches all lend themselves to testing across the lifespan in mice. Characterization of this acute encephalopathy with EEG and neurobehavioral tasks implicates a delirium-like mental status and allows the exploration of therapeutic strategies to target delirium in preclinical studies.

CHAPTER 5

Discussion

Overview

To characterize outcomes of sepsis on the brain in the CS mouse model of sepsis, we performed three main studies. These studies investigated the effects of sepsis specifically on ASC regulation, neuroinflammation, acute changes in cognition, and long-term cognitive outcomes. The results outline a comprehensive mouse model of sepsis associated encephalopathy that is directly translatable to patient studies of delirium and long-term cognitive decline.

5.1 CS treatment depletes ASC and activates an inflammatory response in the brain.

We treated wild-type mice with CS and defined a timeline for inflammatory and oxidative changes throughout illness. At 4- and 24-hours post injection, we observed pro-inflammatory profiles in cortical tissue that coincided with an acute depletion of ASC. Simultaneously, ASC synthesis was upregulated in the liver, likely elevating circulating ASC and restoring cortical ASC levels by 48 hours post injection. Decreased cortical ASC and increased upregulation of ASC synthesis in the liver suggest that an activated inflammatory response during illness increases ASC demand particularly in the brain. In the absence of sufficient ASC repletion, such demand could drive oxidative stress changes that contribute to organ and cerebral dysfunction.

Humans are not capable of synthesizing their own ASC and must obtain ASC through dietary intake (Harrison and May 2009). ASC depletion is commonly observed in plasma of sepsis patients (Wilson and Wu 2012; Carr *et al.* 2017), and patients require significant ASC supplementation to maintain adequate circulating levels (Baines and Shenkin 2002; Long *et al.* 2003). While we did not collect plasma in these studies, it is likely that ASC depletion occurs briefly in circulation, as we observed in the brain, before liver upregulation of ASC synthesis repletes circulating levels. Given the important roles for ASC in regulating the endothelium, inflammatory response, and oxidative stress during sepsis (May and Harrison 2013; Wilson

2013), the ability for wild-type mice to upregulate ASC synthesis as early as 4 hours into the onset of illness is an important limitation to sepsis models utilizing wild-type mice.

While ASC is the first line of antioxidant defense due to its availability, water-solubility, and low-reduction potential, ASC is not the only antioxidant mechanism in the body or brain. ASC often functions in conjunction with another antioxidant glutathione. Unlike ASC, glutathione is synthesized in most mammalian cells, including neurons (Aoyama *et al.* 2008), and synthesis of glutathione in liver is required for survival in mice (Chen *et al.* 2007). Glutathione is less susceptible to spontaneous oxidation than ASC, however, glutathione will react readily with hydroxyl radicals and peroxynitrite, key oxidative products in endothelial dysfunction (Griffith 1999). ASC is essential for glutathione recycling, and the availability of ASC and glutathione are often coordinated. In the glutathione-ascorbate cycle, ascorbate and glutathione can neutralize hydrogen peroxide at the expense of NADPH without consuming glutathione or ASC (Noctor and Foyer 1998). In the absence of ASC, glutathione synthesis is often upregulated resulting in new metabolic demand and oxidative changes (Harrison *et al.* 2010d). Glutathione metabolism could be an important contributor to ASC regulation during sepsis especially in this model.

Data on glutathione levels in septic patients are limited (Biolo *et al.* 2007), though one study in septic pediatric patients noted decreased glutathione synthesis in blood (Lyons *et al.* 2001). Rodent studies have shown variable regulation of glutathione synthesis depending on the model and duration of septic insult (Biolo *et al.* 2007). In a CLP model, sepsis depleted glutathione levels and led to increased neutrophil infiltration and worsened survival that was augmented when glutathione levels were repleted (Villa *et al.* 2002). These findings resemble studies showing attenuation of septic injury using ASC administration. The dependency of glutathione on ASC for recycling coupled with the metabolic requirements for glutathione synthesis are limitations that could drive oxidative imbalance during sepsis when nutrient demand is high. In the current studies, it is likely that ASC depletion in the brain coincides with glutathione depletion, though future studies will need to confirm this.

5.2 CS treatment leads to cognitive deficits not affected by pre-septic ASC deficiency.

Given the acute ASC depletion we observed in wild-type mice amidst upregulation of ASC synthesis in the liver, we sought to assess behavioral and cognitive impairments in mice that like humans are incapable of ASC synthesis. We treated gulo$^{-/-}$ mice maintained on either wild-type-equivalent or depleted ASC and following recovery mice underwent behavioral testing. CS treatment led to significant behavioral and cognitive deficits up to 18 days following insult. Persistent deficits due to CS treatment in spatial memory were observed in the 2-trial Y-maze alternation task, and deficits in executive function were observed in the nest building task. Additionally, we observed persistent hypoactivity and decreased grip strength indicating lasting physical impairments like those observed in patient studies. These results in these tasks resemble prior studies of cognition following sepsis in wild-type mice (See **Table 1**).

In these tasks, there were no differences between groups due to pre-septic ASC supplementation likely due to the lack of observable changes in tissue ASC levels during and following CS treatment. Two main conclusions can be drawn from these findings. First, pre-septic ASC sufficiency at least in the liver and brain, did not protect against the development of cognitive deficits. We considered adding a treatment group where gulo$^{-/-}$ mice on Low ASC supplementation received a dose of high ASC (intraperitoneal, 200 mg/kg) during the onset of illness. However, since we observed consistently repleted ASC levels in septic mice supplemented with High ASC, it is likely that such a treatment group would be analogous to the mice on High ASC supplementation. It is possible that such a treatment could attenuate tissue damage by other means without affecting tissue levels. An intraperitoneal high dose of ASC could interact directly with the bacterial slurry or contribute to neutralization of the immediate neutrophil response specifically within the peritoneum, protecting organ damage from external endothelial damage. Such a scenario would not support therapies targeting repletion of tissue ASC but would instead support roles for ASC in protecting localized injury from inflammatory damage regardless of tissue levels.

The second conclusion that can be drawn from this study is that pre-existing ASC deficiency did not lead to worsened cognitive deficits following illness. We expected that due to the acute cortical ASC depletion we observed in wild-type mice, pre-septic ASC deficiency would lead to greater ASC depletion in the brain during illness driving greater cognitive deficits. However, we observed no acute depletion amidst ASC supplementation and equal behavioral differences in CS mice across High and Low supplemented groups. This may be due to a floor

effect where further behavioral deficits cannot be observed in the current model. It is also possible that these cognitive deficits were only similar between ASC supplemented groups within the tested time interval, and gulo$^{-/-}$ mice supplemented on Low ASC could take longer to recover from these deficits if tested at later behavioral timepoints such as 2- or 6-months following illness. A high dose of ASC during illness could also contribute to such hypothesized differences in longer-term recovery, but future studies will be necessary to characterize these recovery trajectories.

Deficits in motor coordination by rotarod were not driven by CS treatment as in the other behavioral tasks. Instead, we observed decreased motor coordination driven by Low ASC supplementation consistent with our previous reports in gulo$^{-/-}$ mice (Harrison *et al.* 2008). In a separate study in gulo$^{-/-}$ mice, we showed that prolonged ASC deficiency decreases striatal dopamine release *ex vivo* (Consoli *et al.* 2021). Interestingly, in a study in mice with dysfunctional dopamine transporters, prolonged dopamine presence in the synapse led to increased motor coordination in the same rotarod task (DiCarlo *et al.* 2019). In ASC deficient gulo$^{-/-}$ mice, decreased dopaminergic signaling could be responsible for the decreased motor coordination we observe.

The neuroinflammatory response we observed by elevated cortical cytokine levels in the study in wild-type mice could be responsible for long-term cognitive changes in the gulo$^{-/-}$ mice. Activation of microglia is associated with cognitive impairments. In a study that modulated microglial inflammatory phenotypes, deficits in step down inhibitory avoidance task and open-field assessment were ameliorated following CLP when pro-inflammatory microglia were depleted with $GdCl_2$ administration and also independently when anti-inflammatory microglia were promoted with IL-4 administration (Michels *et al.* 2019). Activated microglia are also implicated in synaptic damage after CLP by elevated amyloid beta and decreased synaptophysin (Schwalm *et al.* 2014). We have some preliminary immunohistochemistry data (*not shown*) showing microglial activation in the hippocampus persists up to 21 days following CS treatment, findings that are consistent with other models of sepsis (Hoogland *et al.* 2015). Such data support the hypothesis that persistent pro-inflammatory microglial status contributes to persistent cognitive deficits.

Elevated inflammation is associated with poorer performance on general cognition tests in normal functioning adults (Sartori *et al.* 2012). Increased levels of IL-6, TNF-α, and CRP

predicted cognitive decline measured by poorer memory performance in the Modified Mini-Mental State Examination over 8 years of follow up in adult subjects with healthy cognition at baseline (Yaffe *et al.* 2009). Similar studies show ASC status correlates with markers of metabolic and cognitive health and maintenance of healthy cognition amidst age-related accumulation of oxidative stress (Pearson *et al.* 2017; Travica *et al.* 2017). Such studies suggest maintenance of healthy ASC levels even without septic insult serves a critical role in prevention of inflammatory driven cognitive decline.

5.3 Cognitive deficits following CS treatment can be predicted by EEG slowing.

Because we did not observe any robust effects of ASC in behavior following the cecal slurry model, we decided to focus on characterizing the acute brain dysfunction that is a key driver of long-term cognitive deficits, delirium. Using surgically implanted telemetry devices, we observed dramatic EEG slowing following CS treatment in wild-type mice that resembles the EEG slowing observed in sepsis patients with delirium (Engel and Romano 1959; Roberson *et al.* 2020; Atterton *et al.* 2020). Interestingly, this shift towards slower EEG frequencies was also associated with relative increases in beta and gamma frequencies indicating higher arousal during illness. Increased arousal by EEG was coupled with behavioral hypersensitivity measured by PPI. Measuring delirium-like behavior in mice is difficult due to lethargy during illness. PPI was a practical task to overcome this challenge as it does not require conscious movement. Increased sensitivity to the pre-pulse stimulus indicates increased attentional awareness during illness that resembles that observed in septic patients with agitation or hypervigilant levels of consciousness as evaluated by CAM-ICU (Ely *et al.* 2001). Detecting this hypervigilant state in CS treated mice coupled with the EEG data strongly supports a delirium-like mental status in mice with sepsis associated encephalopathy.

We utilized nest building as a behavioral measure of long-term cognitive recovery. Many models of sepsis investigate long term deficits utilizing the inhibitory avoidance task or fear conditioning (Atucha and Roozendaal 2015; Zhao *et al.* 2019; Semmler *et al.* 2007; Hippensteel *et al.* 2019; Michels *et al.* 2019; Singer *et al.* 2016a). Both these tests examine learning and memory utilizing shock training. Nest building has several strong advantages over such tasks because it does not require training, shock ingraining, or fear driven components. It is sensitive

to hippocampal lesions (Deacon *et al.* 2002), and is a naturally occurring behavior in mice and is presumably rewarding since mice readily engage in the behavior when the material is provided (Walker *et al.* 2017; Deacon 2006). As a more comprehensive assessment of physical, emotional, and cognitive well-being, coupled with the simplicity in setup of the task, nest building is an excellent tool for assessment of rodent behavior and was well suited for this experimental design given the required individual housing of the mice following surgeries.

Two mice died prior to 24 hours after CS treatment. EEG traces immediately preceding death showed repeated spike trains of abnormal epileptiform activity resembling seizures that were not readily observed in mice that survived. These seizures were confirmed by synchronized video and occurred shortly following scoring and weighing by the experimenter. Agitation during the critical illness period could have provoked kindling activity in predisposed mice. Abnormal epileptiform activity including seizures are reported in up to 15% of critical care patient populations (Hassett and Frontera 2021; Nielsen et al. 2019), and slow-wave EEG activity in epilepsy (Holler and Trinka 2015) particularly during sleep (Rossi 2017; Boly et al. 2017) greatly contributes to long term cognitive impairments. Similarities between delirium and epilepsy driven cognitive damage should be explored in future studies.

These studies to date were performed in young (12-16 weeks) mice. Age greatly predisposes delirium severity in other mouse models of sepsis (Kimchi et al. 2017). In aged animals the long-term deficits we observed will likely have greater occurrence or extended duration beyond 7 days post CS treatment. Similar studies using this telemetry system have already been performed successfully in older mice up to 26 months of age, though not during critical illness (Gould et al. 2020). A CLP mouse model of sepsis in aged animals showed elevated amyloid beta peptides and decreased synaptic markers correlated with poorer performance in cognitive tasks following recovery from sepsis (Schwalm et al. 2014). Given that advanced age is a significant risk factor for cognitive impairment including Alzheimer's disease following delirium (Rengel et al. 2019; Sasannejad et al. 2019; Pandharipande et al. 2013), future studies should explore this model in aged animals.

Mice were housed 2-5 mice per cage in all the studies performed except the EEG study which required singly housing the mice due to the surgically implanted telemetry devices. Social isolation is a strong risk factor for delirium (Kotfis *et al.* 2020), and family visitation greatly lowers risk of delirium (Pun *et al.* 2021). In this model, social isolation during illness likely

intensifies illness severity and duration due to decreased social interaction and increased difficulty in maintaining adequate body temperature without shared body heat from vehicle treated mice. The additional burden of isolation coupled with the burdens of surgery and anesthesia, prompted the decision to administer antibiotics in the EEG experiments. Antibiotic administration was likely critical in maintaining high survival rates comparable to those observed in the other studies without surgery, anesthesia, or social isolation.

The microbiome is emerging as a significant factor in development of sepsis associated encephalopathy through the gut-brain axis. In one study in mice, fecal microbiome transplantation greatly improved long-term cognitive deficits determined by number of EEG abnormalities and performance in Morris water maze behavioral task 7 days following intravenous treatment with LPS (Li *et al.* 2018). The presence of persistent EEG abnormalities including absence of reactivity, seizures, triphasic waves, periodic discharges, and delta or theta dominance indicated lasting brain dysfunction that was ameliorated by vagus nerve mediated signaling from prior fecal microbiome transplantation. This study emphasizes the importance of preparing cecal slurry with mice ordered from an outside vendor, in this case Jackson Laboratories, within 7 days of arrival. After this time, the microbiome could change to resemble those of in-house mice which could significantly impact cecal slurry effectiveness in inducing septic illness.

5.4 ASC dysregulation during sepsis may contribute to delirium severity.

Clinical and preclinical evidence suggest that ASC regulation plays a critical role in mitigating acute organ dysfunction including sepsis associate encephalopathy. Our observation of cortical ASC depletion in wild-type mice suggested that in this CS model of sepsis, ASC demand is increased amidst the acute oxidative challenge. This depletion occurs during sepsis associated encephalopathy that we observed using EEG. Given the tripartite role of ASC in neuroprotection, neuroinflammation, and neuromodulation (**Fig. 1**), acute ASC depletion in the brain could contribute to underlying cerebral dysfunction driving generalized slowing of EEG metrics. When gulo$^{-/-}$ mice are maintained on Low ASC supplementation, we have observed baseline EEG differences in preliminary studies. We have also noted increased susceptibility to anesthesia in gulo$^{-/-}$ mice supplemented on Low ASC through more frequent unexpected deaths

during survival surgical procedures. Future EEG studies that investigate sepsis associated encephalopathy in gulo$^{-/-}$ mice could identify differences in acute cerebral pathology due to ASC supplementation that we have yet to identify in the present studies and could affect long-term cognitive outcomes.

A recent clinical study investigated the effects of intravenous ASC administration specifically on delirium incidence in critically ill patients (Park *et al.* 2020). A significant decrease in the number of days with delirium driven by ASC treatment was unfortunately not significant when patients were paired using propensity matched scoring. This early evidence supports ongoing clinical trials that suggest intravenous ASC administration has no effect on improving acute survival rates from sepsis (Lindsell *et al.* 2019; Fujii *et al.* 2020). However, it remains possible that intravenous ASC treatment during delirium affects long-term cognitive deficits following recovery. Single nucleotide polymorphisms in both ASC transporters have been identified and associated with decreases in circulating ASC levels and presumably brain levels (Duell *et al.* 2013). Such predispositions to impairments in ASC distribution could exacerbate inflammatory pathology including endothelial, microvascular, and cerebral dysfunction or contribute to controversial findings in intravenous ASC studies. Effects of intravenous ASC on neuromodulation of delirium during critical illness should be explored in future studies.

Conclusions

Estimated global sepsis related deaths surpassed 11.0 million in 2017. Most of these deaths occurred in low to middle income countries that lack proper resources to address the acute organ failure and are concurrently limited in their capacity to treat long-term physical impairments (Rudd *et al.* 2018). Inadequate access to staffing and facilities including physical therapy, rehabilitation medicine, and nursing care contribute to poor patient outcomes. In the current studies, we explored two relatively inexpensive and accessible interventions for managing sepsis severity and long-term complications: ASC regulation and EEG recording. First, we investigated the potential benefit of ASC maintenance on long-term behavioral outcomes in the CS mouse model of sepsis. ASC demand is increased during illness as evidenced by the studies in wild-type mice. However, high ASC supplementation is likely sufficient to cover this increased ASC demand since ASC depletion was not observed when High ASC

supplementation was provided. Maintained ASC levels did not prevent development of behavioral deficits, nor did depleted ASC levels exacerbate behavioral deficits. ASC therapeutic strategies could still provide inexpensive and easily accessible interventions to reduce organ injury during sepsis and attenuate long-term cognitive complications following survival. Second, we showed that sepsis associated encephalopathy and delirium-like mental status can be extensively characterized using EEG in this model. The EEG slowing that has been extensively observed in septic patients was recapitulated in the CS model of sepsis along with increased arousal and cognitive deficits in nest building and long-term potentiation. EEG monitoring is an easily accessible biomarker for managing sepsis severity, and the development of this translational mouse model of delirium will allow preclinical exploration of new therapeutic strategies to minimize sepsis associated encephalopathy driven long-term cognitive impairments.

REFERENCES

Abhang P. A., Gawali B. W., Mehrotra S. C. (2016) *Introduction to EEG- and Speech-Based Emotion Recognition*. Elsevier Inc.

Ahn J. H., Oh D. K., Huh J. W., Lim C. M., Koh Y., Hong S. B. (2019) Vitamin C alone does not improve treatment outcomes in mechanically ventilated patients with severe sepsis or septic shock: A retrospective cohort study. *J. Thorac. Dis.* **11**, 1562–1570.

Ait-Oufella H., Maury E., Lehoux S., Guidet B., Offenstadt G. (2010) *The endothelium: Physiological functions and role in microcirculatory failure during severe sepsis*. Intensive Care Med.

Aksenov M. Y., Markesbery W. R. (2001) Changes in thiol content and expression of glutathione redox system genes in the hippocampus and cerebellum in Alzheimer's disease. *Neurosci. Lett.* **302**, 141–145.

Aktas O., Ullrich O., Infante-Duarte C., Nitsch R., Zipp F. (2007) *Neuronal damage in brain inflammation*. American Medical Association.

Anderson S. T., Commins S., Moynagh P. N., Coogan A. N. (2015) Lipopolysaccharide-induced sepsis induces long-lasting affective changes in the mouse. *Brain. Behav. Immun.* **43**, 98–109.

Angus D. C., Poll T. van der (2013) Severe Sepsis and Septic Shock. *N. Engl. J. Med.* **369**, 840–851.

Annane D., Sharshar T. (2015) *Cognitive decline after sepsis*. Lancet Publishing Group.

Aoyama K., Watabe M., Nakaki T. (2008) *Regulation of neuronal glutathione synthesis*. J Pharmacol Sci.

Armour J., Tyml K., Lidington D., Wilson J. X. (2001) Ascorbate prevents microvascular dysfunction in the skeletal muscle of the septic rat. *J. Appl. Physiol.* **90**, 795–803.

Atterton B., Paulino M. C., Povoa P., Martin-Loeches I. (2020) *Sepsis associated delirium*. Multidisciplinary Digital Publishing Institute (MDPI).

Atucha E., Roozendaal B. (2015) The inhibitory avoidance discrimination task to investigate accuracy of memory. *Front. Behav. Neurosci.* **9**, 60.

Baines M., Shenkin A. (2002) Lack of effectiveness of short-term intravenous micronutrient nutrition in restoring plasma antioxidant status after surgery. *Clin. Nutr.* **21**, 145–150.

Ballaz S. J., Rebec G. V. (2019) *Neurobiology of vitamin C: Expanding the focus from antioxidant to endogenous neuromodulator*.

Banks W. A., Farr S. A., Morley J. E. (2002) *Entry of blood-borne cytokines into the central nervous system: Effects on cognitive processes*.

Banks W. A., Kastin A. J., Broadwell R. D. (1995) *Passage of cytokines across the blood-brain barrier*. Karger Publishers.

Baracchi F., Ingiosi A. M., Raymond R. M., Opp M. R. (2011) Sepsis-induced alterations in sleep of rats. *Am. J. Physiol. - Regul. Integr. Comp. Physiol.* **301**.

Bast T., Pezze M., McGarrity S. (2017) *Cognitive deficits caused by prefrontal cortical and hippocampal neural disinhibition*. Wiley-Blackwell.

Bastarache J. A., Koyama T., Wickersham N. E., Ware L. B. (2014) Validation of a multiplex electrochemiluminescent immunoassay platform in human and mouse samples. *J. Immunol. Methods* **408**, 13–23.

Bauer M., Coldewey S. M., Leitner M., Löffler B., Weis S., Wetzker R. (2018) Deterioration of organ function as a hallmark in sepsis: The cellular perspective. *Front. Immunol.* **9**, 1460.

Biesalski H. K., McGregor G. P. (2007) Antioxidant therapy in critical care - Is the microcirculation the primary target?, in *Crit. Care Med.*, Vol. 35, pp. S577–S583.

Biolo G., Antonione R., Cicco M. De (2007) Glutathione metabolism in sepsis, in *Crit. Care Med.*, Vol. 35.

Blaschke K., Ebata K. T., Karimi M. M., Zepeda-Martínez J. a, Goyal P., Mahapatra S., Tam A., et al. (2013) Vitamin C induces Tet-dependent DNA demethylation and a blastocyst-like state in ES cells. *Nature* **500**, 222–226.

Boly M., Jones B., Findlay G., Plumley E., Mensen A., Hermann B., Tononi G., Maganti R. (2017) Altered sleep homeostasis correlates with cognitive impairment in patients with focal epilepsy. *Brain* **140**, 1026–1040.

Bone R. C., Sibbald W. J., Sprung C. L. (1992) *The ACCP-SCCM consensus conference on sepsis and organ failure*. Elsevier.

Borrelli E., Roux-Lombard P., Grau G. E., Girardin E., Ricou B., Dayer J. M., Suter P. M. (1996) Plasma concentrations of cytokines, their soluble receptors, and antioxidant vitamins can predict the development of multiple organ failure in patients at risk. *Crit. Care Med.* **24**, 392–397.

Bozza F. A., Salluh J. I., Japiassu A. M., Soares M., Assis E. F., Gomes R. N., Bozza M. T., Castro-Faria-Neto H. C., Bozza P. T. (2007) Cytokine profiles as markers of disease severity in sepsis: A multiplex analysis. *Crit. Care* **11**, R49.

Calsavara A. J. C., Costa P. A., Nobre V., Teixeira A. L. (2018) Factors Associated with Short and Long Term Cognitive Changes in Patients with Sepsis. *Sci. Rep.* **8**, 4509.

Cao C., Yu M., Chai Y. (2019) *Pathological alteration and therapeutic implications of sepsis-induced immune cell apoptosis*. Nature Publishing Group.

Cárcamo J. M., Pedraza A., Bórquez-Ojeda O., Zhang B., Sanchez R., Golde D. W. (2004) Vitamin C Is a Kinase Inhibitor: Dehydroascorbic Acid Inhibits IκBα Kinase β. *Mol. Cell. Biol.* **24**, 6645–6652.

Carr A. C., Frei B. (1999) *Toward a new recommended dietary allowance for vitamin C based on antioxidant and health effects in humans*.

Carr A. C., Maggini S. (2017) *Vitamin C and immune function*. MDPI AG.

Carr A. C., Rosengrave P. C., Bayer S., Chambers S., Mehrtens J., Shaw G. M. (2017) Hypovitaminosis C and vitamin C deficiency in critically ill patients despite recommended enteral and parenteral intakes. *Crit. Care* **21**.

Carr A. C., Shaw G. M., Fowler A. A., Natarajan R. (2015) *Ascorbate-dependent vasopressor synthesis: A rationale for vitamin C administration in severe sepsis and septic shock?* Crit Care.

Chan S., McCowen K. C., Blackburn G. L. (1999) Nutrition management in the ICU, in *Chest*, Vol. 115, pp. 145S-148S. Chest.

Chavan S. S., Huerta P. T., Robbiati S., Valdes-Ferrer S. I., Ochani M., Dancho M., Frankfurt M., Volpe B. T., Tracey K. J., Diamond B. (2013) Response to "HMGB1 Mediates Cognitive Impairment in Sepsis Survivors." *Mol. Med.* **18**, 1359–1359.

Chen L., Deng H., Cui H., Fang J., Zuo Z., Deng J., Li Y., Wang X., Zhao L. (2018) Inflammatory responses and inflammation-associated diseases in organs. *Oncotarget* **9**, 7204–7218.

Chen Y., Yang Y., Miller M. L., Shen D., Shertzer H. G., Stringer K. F., Wang B., Schneider S. N., Nebert D. W., Dalton T. P. (2007) Hepatocyte-specific Gclc deletion leads to rapid onset of steatosis with mitochondrial injury and liver failure. *Hepatology* **45**, 1118–1128.

Ching S., Mahan D. C., Dabrowski K. (2001a) Liver L-Gulonolactone Oxidase Activity and

Tissue Ascorbic Acid Concentrations in Nursing Pigs and the Effect of Various Weaning Ages. *J. Nutr.* **131**, 2002–2006.

Ching S., Mahan D. C., Ottobre J. S., Dabrowski K. (2001b) Ascorbic Acid Synthesis in Fetal and Neonatal Pigs and in Pregnant and Postpartum Sows. *J. Nutr.* **131**, 1997–2001.

Cobley J. N., Fiorello M. L., Bailey D. M. (2018) *13 reasons why the brain is susceptible to oxidative stress*. Elsevier B.V.

Consoli D. C., Brady L. J., Bowman A. B., Calipari E. S., Harrison F. E. (2021) Ascorbate deficiency decreases dopamine release in gulo–/– and APP/PSEN1 mice. *J. Neurochem.* **157**, 656–665.

Consoli D. C., Jesse J. J., Klimo K. R., Tienda A. A., Putz N. D., Bastarache J. A., Harrison F. E. (2020) A Cecal Slurry Mouse Model of Sepsis Leads to Acute Consumption of Vitamin C in the Brain. *Nutrients* **12**, 911.

Crosby G., Culley D. J. (2011) *Surgery and anesthesia: Healing the body but harming the brain?* Anesth Analg.

Crosby G., Culley D. J., Marcantonio E. R. (2010) *Delirium: A cognitive cost of the comfort of procedural sedation in elderly patients?* Mayo Clin Proc.

Cui H., Kong Y., Zhang H. (2012) Oxidative Stress, Mitochondrial Dysfunction, and Aging. *J. Signal Transduct.* **2012**, 1–13.

Daubner S. C., Le T., Wang S. (2011) *Tyrosine hydroxylase and regulation of dopamine synthesis*. NIH Public Access.

Deacon R. M. J. (2006) Assessing nest building in mice. *Nat. Protoc.* **1**, 1117–1119.

Deacon R. M. J., Croucher A., Rawlins J. N. P. (2002) Hippocampal cytotoxic lesion effects on species-typical behaviours in mice. *Behav. Brain Res.* **132**, 203–213.

Dejager L., Pinheiro I., Dejonckheere E., Libert C. (2011) *Cecal ligation and puncture: The gold standard model for polymicrobial sepsis?* Trends Microbiol.

DiCarlo G. E., Aguilar J. I., Matthies H. J. G., Harrison F. E., Bundschuh K. E., West A., Hashemi P., et al. (2019) Autism-linked dopamine transporter mutation alters striatal dopamine neurotransmission and dopamine-dependent behaviors. *J. Clin. Invest.* **129**, 3407–3419.

Dixit S., Bernardo A., Walker J. M., Kennard J. A., Kim G. Y., Kessler E. S., Harrison F. E. (2015) Vitamin C Deficiency in the Brain Impairs Cognition, Increases Amyloid

Accumulation and Deposition, and Oxidative Stress in APP/PSEN1 and Normally Aging Mice. *ACS Chem. Neurosci.* **6**, 570–581.

Dixit S., Fessel J. P., Harrison F. E. (2017) Mitochondrial dysfunction in the APP/PSEN1 mouse model of Alzheimer's disease and a novel protective role for ascorbate. *Free Radic. Biol. Med.* **112**, 515–523.

Duell E. J., Lujan-Barroso L., Llivina C., Muñoz X., Jenab M., Boutron-Ruault M. C., Clavel-Chapelon F., et al. (2013) Vitamin C transporter gene (SLC23A1 and SLC23A2) polymorphisms, plasma vitamin C levels, and gastric cancer risk in the EPIC cohort. *Genes Nutr.* **8**, 549–560.

Ely E. W., Bernard G. R., Speroff T., Gautam S., Dittus R., May L., Truman B., et al. (2001) Delirium in mechanically ventilated patients: Validity and reliability of the Confusion Assessment Method for the intensive care unit (CAM-ICU). *J. Am. Med. Assoc.* **286**, 2703–2710.

Ely E. W., Shintani A., Truman B., Speroff T., Gordon S. M., Harrell F. E., Inouye S. K., Bernard G. R., Dittus R. S. (2004) Delirium as a Predictor of Mortality in Mechanically Ventilated Patients in the Intensive Care Unit. *J. Am. Med. Assoc.* **291**, 1753–1762.

Engel G. L., Romano J. (1959) Delirium, a syndrome of cerebral insufficiency. *J. Chronic Dis.* **9**, 260–277.

Engelmann C., Weih F., Haenold R. (2014) Role of nuclear factor kappa B in central nervous system regeneration. *Neural Regen. Res.* **9**, 707–711.

Ferrada L., Magdalena R., Barahona M. J., Ramírez E., Sanzana C., Gutiérrez J., Nualart F. (2021) *Two distinct faces of vitamin c: Aa vs. dha*. Antioxidants (Basel).

Field R. H., Gossen A., Cunningham C. (2012) Prior pathology in the basal forebrain cholinergic system predisposes to inflammation-induced working memory deficits: Reconciling inflammatory and cholinergic hypotheses of delirium. *J. Neurosci.* **32**, 6288–6294.

Fisher B. J., Kraskauskas D., Martin E. J., Farkas D., Puri P., Massey H. D., Idowu M. O., et al. (2014) Attenuation of sepsis-induced organ injury in mice by vitamin C. *J. Parenter. Enter. Nutr.* **38**, 825–839.

Fisher B. J., Seropian I. M., Kraskauskas D., Thakkar J. N., Voelkel N. F., Fowler A. A., Natarajan R. (2011) Ascorbic acid attenuates lipopolysaccharide-induced acute lung injury. *Crit. Care Med.* **39**, 1454–1460.

Fleischmann C., Scherag A., Adhikari N. K. J., Hartog C. S., Tsaganos T., Schlattmann P., Angus D. C., Reinhart K. (2016) Assessment of global incidence and mortality of hospital-treated sepsis current estimates and limitations. *Am. J. Respir. Crit. Care Med.* **193**, 259–272.

Fowler A. A., Syed A. A., Knowlson S., Sculthorpe R., Farthing D., DeWilde C., Farthing C. A., et al. (2014) Phase I safety trial of intravenous ascorbic acid in patients with severe sepsis. *J. Transl. Med.* **12**, 32.

Fowler A. A., Truwit J. D., Hite R. D., Morris P. E., Dewilde C., Priday A., Fisher B., et al. (2019) Effect of Vitamin C Infusion on Organ Failure and Biomarkers of Inflammation and Vascular Injury in Patients with Sepsis and Severe Acute Respiratory Failure: The CITRIS-ALI Randomized Clinical Trial, in *JAMA - J. Am. Med. Assoc.*, Vol. 322, pp. 1261–1270. American Medical Association.

Fujii T., Luethi N., Young P. J., Frei D. R., Eastwood G. M., French C. J., Deane A. M., et al. (2020) Effect of Vitamin C, Hydrocortisone, and Thiamine vs Hydrocortisone Alone on Time Alive and Free of Vasopressor Support among Patients with Septic Shock: The VITAMINS Randomized Clinical Trial, in *JAMA - J. Am. Med. Assoc.*, Vol. 323, pp. 423–431. American Medical Association.

Fujii T., Udy A. A., Deane A. M., Luethi N., Bailey M., Eastwood G. M., Frei D., et al. (2019) Vitamin C, Hydrocortisone and Thiamine in Patients with Septic Shock (VITAMINS) trial: study protocol and statistical analysis plan. *Crit. Care Resusc.* **21**, 119–125.

Fujinami Y., Inoue S., Ono Y., Miyazaki Y., Fujioka K., Yamashita K., Kotani J. (2021) Sepsis Induces Physical and Mental Impairments in a Mouse Model of Post-Intensive Care Syndrome. *J. Clin. Med.* **10**, 1593.

Gabbay K. H., Bohren K. M., Morello R., Bertin T., Liu J., Vogel P. (2010) Ascorbate synthesis pathway: Dual role of ascorbate in bone homeostasis. *J. Biol. Chem.* **285**, 19510–19520.

Gaieski D. F., Edwards J. M., Kallan M. J., Carr B. G. (2013) Benchmarking the incidence and mortality of severe sepsis in the united states. *Crit. Care Med.* **41**, 1167–1174.

Galley H. F., Davies M. J., Webster N. R. (1996) Ascorbyl radical formation in patients with sepsis: Effect of ascorbate loading. *Free Radic. Biol. Med.* **20**, 139–143.

Gao Y.-L., Lu B., Zhai J.-H., Liu Y.-C., Qi H.-X., Yao Y., Chai Y.-F., Shou S.-T. (2017) The Parenteral Vitamin C Improves Sepsis and Sepsis-Induced Multiple Organ Dysfunction

Syndrome via Preventing Cellular Immunosuppression. *Mediators Inflamm.* **2017**, 4024672.

Gaut J. P., Belaaouaj A., Byun J., Roberts L. J., Maeda N., Frei B., Heinecke J. W. (2006) Vitamin C fails to protect amino acids and lipids from oxidation during acute inflammation. *Free Radic. Biol. Med.* **40**, 1494–1501.

Gofton T. E., Bryan Young G. (2012) *Sepsis-associated encephalopathy*. Nature Publishing Group.

Gould R. W., Russell J. K., Nedelcovych M. T., Bubser M., Blobaum A. L., Bridges T. M., Newhouse P. A., et al. (2020) Modulation of arousal and sleep/wake architecture by M1 PAM VU0453595 across young and aged rodents and nonhuman primates. *Neuropsychopharmacology* **45**, 2219–2228.

Grahl J. J., Stollings J. L., Rakhit S., Person A. K., Wang L., Thompson J. L., Pandharipande P. P., Wesley Ely E., Patel M. B. (2018) Antimicrobial exposure and the risk of delirium in critically ill patients 11 Medical and Health Sciences 1103 Clinical Sciences. *Crit. Care* **22**.

Griffith O. W. (1999) Biologic and pharmacologic regulation of mammalian glutathione synthesis, in *Free Radic. Biol. Med.*, Vol. 27, pp. 922–935. Pergamon.

Hammer T. B., Oranje B., Skimminge A., Aggernæs B., Ebdrup B. H., Glenthøj B., Baaré W. (2013) Structural brain correlates of sensorimotor gating in antipsychotic-naive men with first-episode schizophrenia. *J. Psychiatry Neurosci.* **38**, 34–42.

Han M., Pendem S., Teh S. L., Sukumaran D. K., Wu F., Wilson J. X. (2010) Ascorbate protects endothelial barrier function during septic insult: Role of protein phosphatase type 2A. *Free Radic. Biol. Med.* **48**, 128–135.

Han Z., Zhang Z., Guan Y., Chen B., Yu M., Zhang L., Fang J., Gao Y., Guo Z. (2021) New insights into Vitamin C function: Vitamin C induces JAK2 activation through its receptor-like transporter SVCT2. *Int. J. Biol. Macromol.* **173**, 379–398.

Harrison F. E. (2012) A critical review of vitamin C for the prevention of age-related cognitive decline and Alzheimer's disease. *J. Alzheimers. Dis.* **29**, 711–26.

Harrison F. E., Bowman G. L., Polidori M. C. (2014) *Ascorbic acid and the brain: Rationale for the use against cognitive decline*. Multidisciplinary Digital Publishing Institute (MDPI).

Harrison F. E., Dawes S. M., Meredith M. E., Babaev V. R., Li L., May J. M. (2010a) Low vitamin C and increased oxidative stress and cell death in mice that lack the sodium-dependent vitamin C transporter SVCT2. *Free Radic. Biol. Med.* **49**, 821–829.

Harrison F. E., Green R. J., Dawes S. M., May J. M. (2010b) Vitamin C distribution and retention in the mouse brain. *Brain Res.* **1348**, 181–186.

Harrison F. E., Hosseini A. H., McDonald M. P., May J. M. (2009) Vitamin C reduces spatial learning deficits in middle-aged and very old APP/PSEN1 transgenic and wild-type mice. *Pharmacol. Biochem. Behav.* **93**, 443–450.

Harrison F. E., May J. M. (2009) *Vitamin C function in the brain: vital role of the ascorbate transporter SVCT2*. NIH Public Access.

Harrison F. E., May J. M., McDonald M. P. (2010c) Vitamin C deficiency increases basal exploratory activity but decreases scopolamine-induced activity in APP/PSEN1 transgenic mice. *Pharmacol. Biochem. Behav.* **94**, 543–552.

Harrison F. E., Meredith M. E., Dawes S. M., Saskowski J. L., May J. M. (2010d) Low ascorbic acid and increased oxidative stress in gulo (-/-) mice during development. *Brain Res.* **1349**, 143–152.

Harrison F. E., Yu S. S., Bossche K. L. Van Den, Li L., May J. M., McDonald M. P. (2008) Elevated oxidative stress and sensorimotor deficits but normal cognition in mice that cannot synthesize ascorbic acid. *J. Neurochem.* **106**, 1198–1208.

Hart R. P., Levenson J. L., Sessler C. N., Best A. M., Schwartz S. M., Rutherford L. E. (1996) Validation of a cognitive test for delirium in medical ICU patients. *Psychosomatics* **37**, 533–546.

Hassett C. E., Frontera J. A. (2021) *Neurologic aspects of coronavirus disease of 2019 infection*. Curr Opin Infect Dis.

He Y. J., Xu H., Fu Y. J., Lin J. Y., Zhang M. W. (2018) Intraperitoneal hypertension, a novel risk factor for sepsis-associated encephalopathy in sepsis mice. *Sci. Rep.* **8**, 1–10.

Hinson H. E., Sheth K. N. (2012) *Manifestations of the hyperadrenergic state after acute brain injury*. Curr Opin Crit Care.

Hippensteel J. A., Anderson B. J., Orfila J. E., McMurtry S. A., Dietz R. M., Su G., Ford J. A., et al. (2019) Circulating heparan sulfate fragments mediate septic cognitive dysfunction. *J. Clin. Invest.* **129**, 1779–1784.

Hirsch L. J., Fong M. W. K., Leitinger M., LaRoche S. M., Beniczky S., Abend N. S., Lee J. W., et al. (2021) American Clinical Neurophysiology Society's Standardized Critical Care EEG Terminology: 2021 Version. *J. Clin. Neurophysiol.* **38**, 1–29.

Holford P., Carr A. C., Jovic T. H., Ali S. R., Whitaker I. S., Marik P. E., Smith A. D. (2020) *Vitamin C—An adjunctive therapy for respiratory infection, sepsis and COVID-19*. Nutrients.

Holler Y., Trinka E. (2015) Is there a relation between eeg-slow waves and memory dysfunction in epilepsy? A critical appraisal. *Front. Hum. Neurosci.* **9**, 341.

Hoogland I. C. M., Houbolt C., Westerloo D. J. van, Gool W. A. van, Beek D. van de (2015) *Systemic inflammation and microglial activation: Systematic review of animal experiments*. BioMed Central.

Hudson E. P., Collie J. T., Fujii T., Luethi N., Udy A. A., Doherty S., Eastwood G., et al. (2019) Pharmacokinetic data support 6-hourly dosing of intravenous vitamin C to critically ill patients with septic shock. *Crit. Care Resusc.* **21**, 236–42.

Hughes C. G., Morandi A., Girard T. D., Riedel B., Thompson J. L., Shintani A. K., Pun B. T., Wesley Ely E., Pandharipande P. P. (2013) Association between endothelial dysfunction and acute brain dysfunction during critical illness. *Anesthesiology* **118**, 631–639.

Illendula M., Osuru H. P., Ferrarese B., Atluri N., Dulko E., Zuo Z., Lunardi N. (2020) Surgery, Anesthesia and Intensive Care Environment Induce Delirium-Like Behaviors and Impairment of Synaptic Function-Related Gene Expression in Aged Mice. *Front. Aging Neurosci.* **12**.

Ince C., Mayeux P. R., Nguyen T., Gomez H., Kellum J. A., Ospina-Tascón G. A., Hernandez G., Murray P., Backer D. De (2016) *The endothelium in sepsis*. Lippincott Williams and Wilkins.

Iwashyna T. J., Ely E. W., Smith D. M., Langa K. M. (2010) Long-term cognitive impairment and functional disability among survivors of severe sepsis. *JAMA - J. Am. Med. Assoc.* **304**, 1787–1794.

Jackson T. S., Xu A., Vita J. A., Keaney J. F. (1998) Ascorbate prevents the interaction of superoxide and nitric oxide only at very high physiological concentrations. *Circ. Res.* **83**, 916–922.

Jacobson S. A., Leuchter A. F., Walter D. O. (1993) Conventional and quantitative EEG in the diagnosis of delirium among the elderly. *J. Neurol. Neurosurg. Psychiatry* **56**, 153–158.

Jäkel S., Dimou L. (2017) Glial Cells and Their Function in the Adult Brain: A Journey through the History of Their Ablation. *Front. Cell. Neurosci.* **11**, 24.

Kaukonen K. M., Bailey M., Suzuki S., Pilcher D., Bellomo R. (2014) Mortality related to severe sepsis and septic shock among critically ill patients in Australia and New Zealand, 2000-2012. *JAMA - J. Am. Med. Assoc.* **311**, 1308–1316.

Kerchberger E. V., Bastarache J. A., Shaver C. M., Nagata H., Brennan McNeil J., Landstreet S. R., Putz N. D., et al. (2019) Haptoglobin-2 variant increases susceptibility to acute respiratory distress syndrome during sepsis. *JCI Insight* **4**.

Kimchi E., Coughlin B., Cash S. (2017) Rodent models of delirium and encephalopathy: Behavioral and neurophysiological studies in aging (P5.090). *Neurology* **88**.

Kimchi E. Y., Neelagiri A., Whitt W., Sagi A. R., Ryan S. L., Gadbois G., Groothuysen D., Westover M. B. (2019) Clinical EEG slowing correlates with delirium severity and predicts poor clinical outcomes. *Neurology* **93**, E1260–E1271.

Knowles R. G., Moncada S. (1994) *Nitric oxide synthases in mammals*. Portland Press Ltd.

Konsman J. P., Parnet P., Dantzer R. (2002) Cytokine-induced sickness behaviour: mechanisms and implications. *Trends Neurosci.* **25**, 154–9.

Koponen H., Partanen J., Pääkkönen A., Mattila E., Riekkinen P. J. (1989) EEG spectral analysis in delirium. *J. Neurol. Neurosurg. Psychiatry* **52**, 980.

Kotfis K., Williams Roberson S., Wilson J. E., Dabrowski W., Pun B. T., Ely E. W. (2020) *COVID-19: ICU delirium management during SARS-CoV-2 pandemic*. Crit Care.

Kuck J. L., Bastarache J. A., Shaver C. M., Fessel J. P., Dikalov S. I., May J. M., Ware L. B. (2018) Ascorbic acid attenuates endothelial permeability triggered by cell-free hemoglobin. *Biochem. Biophys. Res. Commun.* **495**, 433–437.

Kuhn S. O., Meissner K., Mayes L. M., Bartels K. (2018) *Vitamin C in sepsis*. Lippincott Williams and Wilkins.

Kumari V., Gray J. A., Geyer M. A., Ffytche D., Soni W., Mitterschiffthaler M. T., Vythelingum G. N., Simmons A., Williams S. C. R., Sharma T. (2003) Neural correlates of tactile prepulse inhibition: A functional MRI study in normal and schizophrenic subjects. *Psychiatry Res. - Neuroimaging* **122**, 99–113.

Kuo S.-M., Tan C.-H., Dragan M., Wilson J. X. (2005) Endotoxin Increases Ascorbate Recycling and Concentration in Mouse Liver. *J. Nutr.* **135**, 2411–2416.

Leavitt M. L., Trzepacz P. T., Ciongoli K. (1994) Rat model of delirium: Atropine dose-response relationships. *J. Neuropsychiatry Clin. Neurosci.* **6**, 279–284.

Levine M., Conry-Cantilena C., Wang Y., Welch R. W., Washko P. W., Dhariwal K. R., Park J. B., et al. (1996) Vitamin C pharmacokinetics in healthy volunteers: Evidence for a recommended dietary allowance. *Proc. Natl. Acad. Sci. U. S. A.* **93**, 3704–3709.

Levine M., Downing D. (1992) New Concepts in the Biology and Biochemistry of Ascorbic Acid. *J. Nutr. Med.* **3**, 361–362.

Lewis A. J., Seymour C. W., Rosengart M. R. (2016) Current Murine Models of Sepsis. *Surg. Infect. (Larchmt).* **17**, 385–393.

Li S., Lv J., Li J., Zhao Z., Guo H., Zhang Y., Cheng S., et al. (2018) Intestinal microbiota impact sepsis associated encephalopathy via the vagus nerve. *Neurosci. Lett.* **662**, 98–104.

Liang L., Moore B., Soni A. (2020) *National Inpatient Hospital Costs: The Most Expensive Conditions by Payer, 2017*.

Liddelow S. A., Guttenplan K. A., Clarke L. E., Bennett F. C., Bohlen C. J., Schirmer L., Bennett M. L., et al. (2017) Neurotoxic reactive astrocytes are induced by activated microglia. *Nature* **541**, 481–487.

Lier H. Van, Drinkenburg W. H. I. M., Eeten Y. J. W. Van, Coenen A. M. L. (2004) Effects of diazepam and zolpidem on EEG beta frequencies are behavior-specific in rats. *Neuropharmacology* **47**, 163–174.

Lin J. L., Huang Y. H., Shen Y. C., Huang H. C., Liu P. H. (2010) Ascorbic acid prevents blood-brain barrier disruption and sensory deficit caused by sustained compression of primary somatosensory cortex. *J. Cereb. Blood Flow Metab.* **30**, 1121–1136.

Lindsell C. J., McGlothlin A., Nwosu S., Rice T. W., Hall A., Bernard G. R., Busse L. W., et al. (2019) The Vitamin C, Thiamine and Steroids in Sepsis (VICTAS) Protocol: A prospective, multi-center, double-blind, adaptive sample size, randomized, placebo-controlled, clinical trial. *Trials* **20**, 4–7.

Lobo-Silva D., Carriche G. M., Castro A. G., Roque S., Saraiva M. (2016) *Balancing the immune response in the brain: IL-10 and its regulation*. BioMed Central.

Lobo S. M. A., Lobo F. R. M., Peres Bota D., Lopes-Ferreira F., Soliman H. M., Mélot C., Vincent J. L. (2003) C-reactive protein levels correlate with mortality and organ failure in critically III patients. *Chest* **123**, 2043–2049.

Long C. L., Maull K. I., Krishnan R. S., Laws H. L., Geiger J. W., Borghesi L., Franks W., Lawson T. C., Sauberlich H. E. (2003) Ascorbic acid dynamics in the seriously ill and

injured. *J. Surg. Res.* **109**, 144–148.

Louis E. K. St., Frey L. C. (2016) *Electroencephaolgraphy - An introductory text*. American Epilepsy Society.

Lynch M. A. (2004) *Long-Term Potentiation and Memory*. Physiol Rev.

Lyons J., Rauh-Pfeiffer A., Ming-Yu Y., Lu X. M., Zurakowski D., Curley M., Collier S., et al. (2001) Cysteine metabolism and whole blood glutathione synthesis in septic pediatric patients. *Crit. Care Med.* **29**, 870–877.

Madsen G. F., Bilenberg N., Cantio C., Oranje B. (2014) Increased prepulse inhibition and sensitization of the startle reflex in autistic children. *Autism Res.* **7**, 94–103.

Maeda N., Hagihara H., Nakata Y., Hiller S., Wilder J., Reddick R. (2000) Aortic wall damage in mice unable to synthesize ascorbic acid. *Proc. Natl. Acad. Sci. U. S. A.* **97**, 841–6.

Magistretti P. J., Allaman I. (2015) *A Cellular Perspective on Brain Energy Metabolism and Functional Imaging*. Cell Press.

Manley M. O., O'Riordan M. A., Levine A. D., Latifi S. Q. (2005) Interleukin 10 extends the effectiveness of standard therapy during late sepsis with serum interleukin 6 levels predicting outcome. *Shock* **23**, 521–6.

Mantzarlis K., Tsolaki V., Zakynthinos E. (2017) *Role of Oxidative Stress and Mitochondrial Dysfunction in Sepsis and Potential Therapies*. Hindawi Limited.

Marechal X., Favory R., Joulin O., Montaigne D., Hassoun S., Decoster B., Zerimech F., Neviere R. (2008) Endothelial glycocalyx damage during endotoxemia coincides with microcirculatory dysfunction and vascular oxidative stress. *Shock* **29**, 572–576.

Marik P. E., Khangoora V., Rivera R., Hooper M. H., Catravas J. (2017) Hydrocortisone, Vitamin C, and Thiamine for the Treatment of Severe Sepsis and Septic Shock: A Retrospective Before-After Study. *Chest* **151**, 1229–1238.

Mart M. F., Williams Roberson S., Salas B., Pandharipande P. P., Ely E. W. (2020) Prevention and Management of Delirium in the Intensive Care Unit. *Semin. Respir. Crit. Care Med.*

Martin G. S., Mannino D. M., Moss M. (2006) The effect of age on the development and outcome of adult sepsis. *Crit. Care Med.* **34**, 15–21.

Matsumoto H., Ogura H., Shimizu K., Ikeda M., Hirose T., Matsuura H., Kang S., Takahashi K., Tanaka T., Shimazu T. (2018) The clinical importance of a cytokine network in the acute phase of sepsis. *Sci. Rep.* **8**, 1–11.

May J. M. (2012) Vitamin C transport and its role in the central nervous system. *Subcell. Biochem.* **56**, 85–103.

May J. M., Harrison F. E. (2013) *Role of vitamin C in the function of the vascular endothelium*. Antioxid Redox Signal.

May J. M., Qu Z. C., Mendiratta S. (1998) Protection and recycling of α-tocopherol in human erythrocytes by intracellular ascorbic acid. *Arch. Biochem. Biophys.* **349**, 281–289.

Mazeraud A., Pascal Q., Verdonk F., Heming N., Chrétien F., Sharshar T. (2016) *Neuroanatomy and Physiology of Brain Dysfunction in Sepsis*. Elsevier.

McGarrity S., Mason R., Fone K. C., Pezze M., Bast T. (2017) Hippocampal neural disinhibition causes attentional and memory deficits. *Cereb. Cortex* **27**, 4447–4462.

McKim D. B., Weber M. D., Niraula A., Sawicki C. M., Liu X., Jarrett B. L., Ramirez-Chan K., et al. (2018) Microglial recruitment of IL-1β-producing monocytes to brain endothelium causes stress-induced anxiety. *Mol. Psychiatry* **23**, 1421–1431.

Mckinnon R. L., Lidington D., Tyml K. (2007) Ascorbate inhibits reduced arteriolar conducted vasoconstriction in septic mouse cremaster muscle. *Microcirculation* **14**, 697–707.

Medina E. (2010) Murine model of polymicrobial septic peritonitis using Cecal Ligation and Puncture (CLP). *Methods Mol. Biol.* **602**, 411–415.

Meegan J. E., Shaver C. M., Putz N. D., Jesse J. J., Landstreet S. R., Lee H. N. R., Sidorova T. N., et al. (2020) Cell-free hemoglobin increases inflammation, lung apoptosis, and microvascular permeability in murine polymicrobial sepsis. *PLoS One* **15**, e0228727.

Mena A., Ruiz-Salas J. C., Puentes A., Dorado I., Ruiz-Veguilla M., la Casa L. G. De (2016) Reduced prepulse inhibition as a biomarker of schizophrenia. *Front. Behav. Neurosci.* **10**, 202.

Mi D. J., Dixit S., Warner T. A., Kennard J. A., Scharf D. A., Kessler E. S., Moore L. M., et al. (2018) Altered glutamate clearance in ascorbate deficient mice increases seizure susceptibility and contributes to cognitive impairment in APP/PSEN1 mice. *Neurobiol. Aging* **71**, 241–254.

Michels M., Ávila P., Pescador B., Vieira A., Abatti M., Cucker L., Borges H., et al. (2019) Microglial Cells Depletion Increases Inflammation and Modifies Microglial Phenotypes in an Animal Model of Severe Sepsis. *Mol. Neurobiol.*

Miller A. D., Ball A. M., Bookstaver P. B., Dornblaser E. K., Bennett C. L. (2011) *Epileptogenic*

potential of carbapenem agents: Mechanism of action, seizure rates, and clinical considerations. John Wiley & Sons, Ltd.

Monacelli F., Acquarone E., Giannotti C., Borghi R., Nencioni A. (2017) Vitamin C, Aging and Alzheimer's Disease. *Nutrients* **9**.

Moretti D. V., Prestia A., Fracassi C., Binetti G., Zanetti O., Frisoni G. B. (2012) *Specific EEG changes associated with atrophy of hippocampus in subjects with mild cognitive impairment and Alzheimer's disease*. Hindawi Limited.

Mulkey M. A., Everhart D. E., Kim S., Olson D. W. M., Hardin S. R. (2019) Detecting delirium using a physiologic monitor. *Dimens. Crit. Care Nurs.* **38**, 241–247.

Nemeroff C. B., Weinberger D., Rutter M., MacMillan H. L., Bryant R. A., Wessely S., Stein D. J., et al. (2013) DSM-5: A collection of psychiatrist views on the changes, controversies, and future directions. *BMC Med.* **11**.

Nielsen R. M., Urdanibia-Centelles O., Vedel-Larsen E., Thomsen K. J., Møller K., Olsen K. S., Lauritsen A. Ø., Eddelien H. S., Lauritzen M., Benedek K. (2019) Continuous EEG Monitoring in a Consecutive Patient Cohort with Sepsis and Delirium. *Neurocritical Care 2019 321* **32**, 121–130.

Niki E., Yoshida Y., Saito Y., Noguchi N. (2005) *Lipid peroxidation: Mechanisms, inhibition, and biological effects*.

Noctor G., Foyer C. H. (1998) Ascorbate and Glutathione: Keeping Active Oxygen under Control. *Annu. Rev. Plant Biol.* **49**, 249–279.

O'Neill E., Griffin É. W., O'Sullivan R., Murray C., Ryan L., Yssel J., Harkin A., Cunningham C. (2021) Acute neuroinflammation, sickness behavior and working memory responses to acute systemic LPS challenge following noradrenergic lesion in mice. *Brain. Behav. Immun.* **94**, 357–368.

Opmeer E. M., Kortekaas R., Aleman A. (2010) *Depression and the role of genes involved in dopamine metabolism and signalling*. Pergamon.

Opp M. R., George A., Ringgold K. M., Hansen K. M., Bullock K. M., Banks W. A. (2015) Sleep fragmentation and sepsis differentially impact blood-brain barrier integrity and transport of tumor necrosis factor-α in aging. *Brain. Behav. Immun.* **50**, 259–265.

Palanca B. J. A., Wildes T. S., Ju Y. S., Ching S., Avidan M. S. (2017) *Electroencephalography and delirium in the postoperative period*. Elsevier.

Pandharipande P. P., Girard T. D., Jackson J. C., Morandi A., Thompson J. L., Pun B. T., Brummel N. E., et al. (2013) Long-Term Cognitive Impairment after Critical Illness. *N. Engl. J. Med.* **369**, 1306–1316.

Park J. E., Shin T. G., Jo I. J., Jeon K., Suh G. Y., Park M., Won H., Chung C. R., Hwang S. Y. (2020) Impact of Vitamin C and Thiamine Administration on Delirium-Free Days in Patients with Septic Shock. *J. Clin. Med.* **9**, 193.

Pearson J. F., Pullar J. M., Wilson R., Spittlehouse J. K., Vissers M. C. M., Skidmore P. M. L., Willis J., Cameron V. A., Carr A. C. (2017) Vitamin C status correlates with markers of metabolic and cognitive health in 50-year-olds: Findings of the CHALICE cohort study. *Nutrients* **9**.

Pierrakos C., Vincent J. L. (2010) Sepsis biomarkers: A review. *Crit. Care* **14**, R15.

Prauchner C. A. (2017) *Oxidative stress in sepsis: Pathophysiological implications justifying antioxidant co-therapy*. Burns.

Pun B. T., Badenes R., Heras La Calle G., Orun O. M., Chen W., Raman R., Simpson B. G. K., et al. (2021) Prevalence and risk factors for delirium in critically ill patients with COVID-19 (COVID-D): a multicentre cohort study. *Lancet Respir. Med.* **9**, 239–250.

Qin L., Wu X., Block M. L., Liu Y., Breese G. R., Hong J. S., Knapp D. J., Crews F. T. (2007) Systemic LPS causes chronic neuroinflammation and progressive neurodegeneration. *Glia* **55**, 453–462.

Raetz C. R. H., Whitfield C. (2002) Lipopolysaccharide Endotoxins. *Annu. Rev. Biochem.* **71**, 635–700.

Rebec G. V, Christopher Pierce R. (1994) *A vitamin as neuromodulator: Ascorbate release into the extracellular fluid of the brain regulates dopaminergic and glutamatergic transmission*.

Reiserer R. S., Harrison F. E., Syverud D. C., McDonald M. P. (2007) Impaired spatial learning in the APPSwe + PSEN1ΔE9 bigenic mouse model of Alzheimer's disease. *Genes, Brain Behav.* **6**, 54–65.

Remick D. G. (2007) Pathophysiology of sepsis. *Am. J. Pathol.* **170**, 1435–1444.

Remick D. G., Ward P. A. (2005) *Evaluation of endotoxin models for the study of sepsis*. Shock.

Rengel K. F., Hayhurst C. J., Pandharipande P. P., Hughes C. G. (2019) *Long-term Cognitive and Functional Impairments After Critical Illness*. NLM (Medline).

Rhodes A., Evans L. E., Alhazzani W., Levy M. M., Antonelli M., Ferrer R., Kumar A., et al.

(2017) *Surviving Sepsis Campaign: International Guidelines for Management of Sepsis and Septic Shock: 2016*. Lippincott Williams and Wilkins.

Rice M. E. (2000) *Ascorbate regulation and its neuroprotective role in the brain*. Elsevier.

Rittirsch D., Huber-Lang M. S., Flierl M. A., Ward P. A. (2009) Immunodesign of experimental sepsis by cecal ligation and puncture. *Nat. Protoc.* **4**, 31–36.

Roberson S. W., Azeez N. A., Taneja R., Pun B. T., Pandharipande P. P., Jackson J. C., Ely E. W. (2020) Quantitative EEG During Critical Illness Correlates With Patterns of Long-Term Cognitive Impairment: *https://doi.org/10.1177/1550059420978009*.

Rossi M. A. (2017) Epileptic activity and cognitive impairment: Hijacking plasticity during sleep. *Epilepsy Curr.* **17**, 227–228.

Rubio-Gayosso I., Platts S. H., Duling B. R. (2006) Reactive oxygen species mediate modification of glycocalyx during ischemia-reperfusion injury. *Am. J. Physiol. - Hear. Circ. Physiol.* **290**.

Rudd K. E., Johnson S. C., Agesa K. M., Shackelford K. A., Tsoi D., Kievlan D. R., Colombara D. V., et al. (2020) Global, regional, and national sepsis incidence and mortality, 1990–2017: analysis for the Global Burden of Disease Study. *Lancet* **395**, 200–211.

Rudd K. E., Kissoon N., Limmathurotsakul D., Bory S., Mutahunga B., Seymour C. W., Angus D. C., West T. E. (2018) *The global burden of sepsis: Barriers and potential solutions*. BioMed Central.

Russell J. A., Rush B., Boyd J. (2018) *Pathophysiology of Septic Shock*. Crit Care Clin.

Salazar K., Martínez F., Pérez-Martín M., Cifuentes M., Trigueros L., Ferrada L., Espinoza F., et al. (2018) SVCT2 Expression and Function in Reactive Astrocytes Is a Common Event in Different Brain Pathologies. *Mol. Neurobiol.* **55**, 5439–5452.

Sartori A. C., Vance D. E., Slater L. Z., Crowe M. (2012) *The impact of inflammation on cognitive function in older adults: Implications for healthcare practice and research*. NIH Public Access.

Sasannejad C., Ely E. W., Lahiri S. (2019) *Long-term cognitive impairment after acute respiratory distress syndrome: A review of clinical impact and pathophysiological mechanisms*. Crit Care.

Satapathy S. K., Dehuri S., Jagadev A. K., Mishra S. (2019) *EEG Brain Signal Classification for Epileptic Seizure Disorder Detection*. Elsevier.

Schleicher R. L., Carroll M. D., Ford E. S., Lacher D. A. (2009) Serum vitamin C and the prevalence of vitamin C deficiency in the United States: 2003-2004 National Health and Nutrition Examination Survey (NHANES). *Am. J. Clin. Nutr.* **90**, 1252–1263.

Schorah C. J., Downing C., Piripitsi A., Gallivan L., Al-Hazaa A. H., Sanderson M. J., Bodenham A. (1996) Total vitamin C, ascorbic acid, and dehydroascorbic acid concentrations in plasma of critically ill patients. *Am. J. Clin. Nutr.* **63**, 760–765.

Schuler A., Wulf D. A., Lu Y., Iwashyna T. J., Escobar G. J., Shah N. H., Liu V. X. (2018) The impact of acute organ dysfunction on long-term survival in sepsis. *Crit. Care Med.* **46**, 843–849.

Schwalm M. T., Pasquali M., Miguel S. P., Santos J. P. A. Dos, Vuolo F., Comim C. M., Petronilho F., et al. (2014) *Acute brain inflammation and oxidative damage are related to long-term cognitive deficits and markers of neurodegeneration in sepsis-survivor rats*. Mol Neurobiol.

Seif F., Khoshmirsafa M., Aazami H., Mohsenzadegan M., Sedighi G., Bahar M. (2017) *The role of JAK-STAT signaling pathway and its regulators in the fate of T helper cells*. BioMed Central.

Semmler A., Frisch C., Debeir T., Ramanathan M., Okulla T., Klockgether T., Heneka M. T. (2007) Long-term cognitive impairment, neuronal loss and reduced cortical cholinergic innervation after recovery from sepsis in a rodent model. *Exp. Neurol.* **204**, 733–740.

Sgaravatti Â. M., Magnusson A. S., Oliveira A. S., Mescka C. P., Zanin F., Sgarbi M. B., Pederzolli C. D., et al. (2009) Effects of 1,4-butanediol administration on oxidative stress in rat brain: Study of the neurotoxicity of γ-hydroxybutyric acid in vivo. *Metab. Brain Dis.* **24**, 271–282.

Shaver C. M., Paul M. G., Putz N. D., Landstreet S. R., Kuck J. L., Scarfe L., Skrypnyk N., et al. (2019) Cell-free hemoglobin augments acute kidney injury during experimental sepsis. *Am. J. Physiol. Physiol.* **317**, F922–F929.

Singer B. H., Newstead M. W., Zeng X., Cooke C. L., Thompson R. C., Singer K., Ghantasala R., et al. (2016a) Cecal ligation and puncture results in long-term central nervous system myeloid inflammation. *PLoS One* **11**, e0149136.

Singer M., Deutschman C. S., Seymour C., Shankar-Hari M., Annane D., Bauer M., Bellomo R., et al. (2016b) *The third international consensus definitions for sepsis and septic shock*

(sepsis-3). JAMA.

Skelly D. T., Griffin É. W., Murray C. L., Harney S., O'Boyle C., Hennessy E., Dansereau M.-A., et al. (2019) Acute transient cognitive dysfunction and acute brain injury induced by systemic inflammation occur by dissociable IL-1-dependent mechanisms. *Mol. Psychiatry* **24**, 1533.

Slooter A. J. C., Otte W. M., Devlin J. W., Arora R. C., Bleck T. P., Claassen J., Duprey M. S., et al. (2020) Updated nomenclature of delirium and acute encephalopathy: statement of ten Societies. *Intensive Care Med.* **46**, 1020–1022.

Spector R., Johanson C. E. (2014) *The nexus of vitamin homeostasis and DNA synthesis and modification in mammalian brain*. BioMed Central.

Sram R. J., Binkova B., Rossner P. (2012) Vitamin C for DNA damage prevention. *Mutat. Res. - Fundam. Mol. Mech. Mutagen.* **733**, 39–49.

Starr M. E., Steele A. M., Saito M., Hacker B. J., Evers B. M., Saito H., Raju R. (2014) A new cecal slurry preparation protocol with improved long-term reproducibility for animal models of sepsis. *PLoS One* **9**.

Steele A. M., Starr M. E., Saito H. (2017) Late Therapeutic Intervention with Antibiotics and Fluid Resuscitation Allows for a Prolonged Disease Course with High Survival in a Severe Murine Model of Sepsis. *Shock* **47**, 726–734.

Su G., Atakilit A., Li J. T., Wu N., Luong J., Chen R., Bhattacharya M., Sheppard D. (2013) Effective treatment of mouse sepsis with an inhibitory antibody targeting integrin αvβ5. *Crit. Care Med.* **41**, 546–553.

Subramanian V. S., Sabui S., Moradi H., Marchant J. S., Said H. M. (2018a) Inhibition of intestinal ascorbic acid uptake by lipopolysaccharide is mediated via transcriptional mechanisms. *Biochim. Biophys. Acta - Biomembr.* **1860**, 556–565.

Subramanian V. S., Sabui S., Subramenium G. A., Marchant J. S., Said H. M. (2018b) Tumor necrosis factor alpha reduces intestinal vitamin C uptake: A role for NF-κB-mediated signaling. *Am. J. Physiol. - Gastrointest. Liver Physiol.* **315**, G241–G248.

Subramanian V. S., Teafatiller T., Agrawal A., Kitazawa M., Marchant J. S. (2021) Effect of Lipopolysaccharide and TNFα on Neuronal Ascorbic Acid Uptake. *Mediators Inflamm.* **2021**, 4157132.

Toft K., Tontsch J., Abdelhamid S., Steiner L., Siegemund M., Hollinger A. (2019) *Serum*

biomarkers of delirium in the elderly: a narrative review. Ann Intensive Care.

Travica N., Ried K., Sali A., Scholey A., Hudson I., Pipingas A. (2017) Vitamin c status and cognitive function: A systematic review. *Nutrients* **9**, 1–21.

Trzepacz P. T., Leavitt M., Ciongoli K. (1992) An Animal Model for Delirium. *Psychosomatics* **33**, 404–415.

Tyml K., Li F., Wilson J. X. (2008) Septic impairment of capillary blood flow requires nicotinamide adenine dinucleotide phosphate oxidase but not nitric oxide synthase and is rapidly reversed by ascorbate through an endothelial nitric oxide synthase-dependent mechanism. *Crit. Care Med.* **36**, 2355–2362.

Unger M. S., Schernthaner P., Marschallinger J., Mrowetz H., Aigner L. (2018) Microglia prevent peripheral immune cell invasion and promote an anti-inflammatory environment in the brain of APP-PS1 transgenic mice. *J. Neuroinflammation* **15**, 274.

Villa P., Saccani A., Sica A., Ghezzi P. (2002) Glutathione protects mice from lethal sepsis by limiting inflammation and potentiating host defense. *J. Infect. Dis.* **185**, 1115–1120.

VS S., T T., A A., M K., JS M. (2021) Effect of Lipopolysaccharide and TNF α on Neuronal Ascorbic Acid Uptake. *Mediators Inflamm.* **2021**, 1–11.

Walker J., Dixit S., Saulsberry A., May J., Harrison F., Dis Author manuscript N. (2017) Reversal of high fat diet-induced obesity improves glucose tolerance, inflammatory response, β-amyloid accumulation and cognitive decline in the APP/PSEN1 mouse model of Alzheimer's disease HHS Public Access Author manuscript. *Neurobiol Dis* **100**, 87–98.

Ward M. S., Lamb J., May J. M., Harrison F. E. (2013) Behavioral and monoamine changes following severe vitamin C deficiency. *J. Neurochem.* **124**, 363–375.

Wilson J. X. (2005) *Regulation of vitamin C transport*. Annu Rev Nutr.

Wilson J. X. (2009) *Mechanism of action of vitamin C in sepsis: Ascorbate modulates redox signaling in endothelium*. NIH Public Access.

Wilson J. X. (2013) *Evaluation of Vitamin C for Adjuvant Sepsis Therapy*. Mary Ann Liebert, Inc.

Wilson J. X., Peters C. E., Sitar S. M., Daoust P., Gelb A. W. (2000) Glutamate stimulates ascorbate transport by astrocytes. *Brain Res.* **858**, 61–66.

Wilson J. X., Wu F. (2012) Vitamin C in sepsis. *Subcell. Biochem.* **56**, 67–83.

Wintergerst E. S., Maggini S., Hornig D. H. (2007) *Contribution of selected vitamins and trace*

elements to immune function. Ann Nutr Metab.

Wolters A. E., Slooter A. J. C., Kooi A. W. Van Der, Dijk D. Van (2013) *Cognitive impairment after intensive care unit admission: A systematic review*. Intensive Care Med.

Wu F., Wilson J. X., Tyml K. (2004) Ascorbate protects against impaired arteriolar constriction in sepsis by inhibiting inducible nitric oxide synthase expression. *Free Radic. Biol. Med.* **37**, 1282–1289.

Wu Y., Dissing-Olesen L., MacVicar B. A., Stevens B. (2015) *Microglia: Dynamic Mediators of Synapse Development and Plasticity*. Elsevier.

Yaffe K., Fiocco A. J., Lindquist K., Vittinghoff E., Simonsick E. M., Newman A. B., Satterfield S., et al. (2009) Predictors of maintaining cognitive function in older adults: The Health ABC Study. *Neurology* **72**, 2029–2035.

Yamazaki E., Horikawa M., Fukushima R. (2011) Vitamin C supplementation in patients receiving peripheral parenteral nutrition after gastrointestinal surgery. *Nutrition* **27**, 435–439.

Yende S., Austin S., Rhodes A., Finfer S., Opal S., Thompson T., Bozza F. A., Larosa S. P., Ranieri V. M., Angus D. C. (2016) Long-term quality of life among survivors of severe sepsis: Analyses of two international trials. *Crit. Care Med.* **44**, 1461–1467.

Yende S., D'Angelo G., Kellum J. A., Weissfeld L., Fine J., Welch R. D., Kong L., Carter M., Angus D. C. (2008) Inflammatory markers at hospital discharge predict subsequent mortality after pneumonia and sepsis. *Am. J. Respir. Crit. Care Med.* **177**, 1242–1247.

Yende S., Kellum J. A., Talisa V. B., Peck Palmer O. M., Chang C. C. H., Filbin M. R., Shapiro N. I., et al. (2019) Long-term Host Immune Response Trajectories among Hospitalized Patients with Sepsis. *JAMA Netw. Open* **2**, e198686–e198686.

Yin J., Valin K. L., Dixon M. L., Leavenworth J. W. (2017) The Role of Microglia and Macrophages in CNS Homeostasis, Autoimmunity, and Cancer. *J. Immunol. Res.* **2017**, 1–12.

Yoshida Y., Umeno A., Shichiri M. (2013) *Lipid peroxidation biomarkers for evaluating oxidative stress and assessing antioxidant capacity in vivo*. The Society for Free Radical Research Japan.

Young J. I., Züchner S., Wang G. (2015) Regulation of the Epigenome by Vitamin C. *Annu. Rev. Nutr.* **35**, 545–564.

Zaghloul N., Addorisio M. E., Silverman H. A., Patel H. L., Valdés-Ferrer S. I., Ayasolla K. R., Lehner K. R., et al. (2017) Forebrain Cholinergic Dysfunction and Systemic and Brain Inflammation in Murine Sepsis Survivors. *Front. Immunol.* **8**, 1673.

Zampieri F. G., Park M., Machado F. S., Azevedo L. C. P. (2011) *Sepsis-associated encephalopathy: Not just delirium*. Hospital das Clinicas da Faculdade de Medicina da Universidade de Sao Paulo.

Zarea A., Charbonnier C., Rovelet-Lecrux A., Nicolas G., Rousseau S., Borden A., Pariente J., et al. (2016) Seizures in dominantly inherited Alzheimer disease. *Neurology* **87**, 912–919.

Zhang N., Zhao W., Hu Z.-J., Ge S.-M., Huo Y., Liu L.-X., Gao B.-L. (2021) Protective effects and mechanisms of high-dose vitamin C on sepsis-associated cognitive impairment in rats. *Sci. Rep.* **11**, 14511.

Zhao J., Bi W., Xiao S., Lan X., Cheng X., Zhang J., Lu D., et al. (2019) Neuroinflammation induced by lipopolysaccharide causes cognitive impairment in mice. *Sci. Rep.* **9**, 5790.

Zhou G., Kamenos G., Pendem S., Wilson J. X., Wu F. (2012) Ascorbate protects against vascular leakage in cecal ligation and puncture-induced septic peritonitis. *Am. J. Physiol. - Regul. Integr. Comp. Physiol.* **302**.

APPENDIX

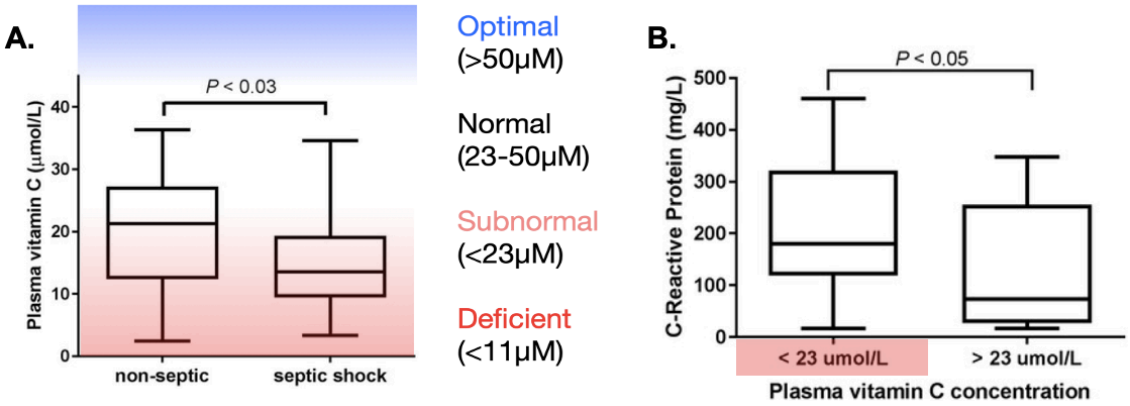

Supplemental Figure 1 – Adapted from Carr *et al.* 2017.
Lower plasma vitamin C is associated with (**A**) greater sepsis severity and (**B**) higher inflammatory response.

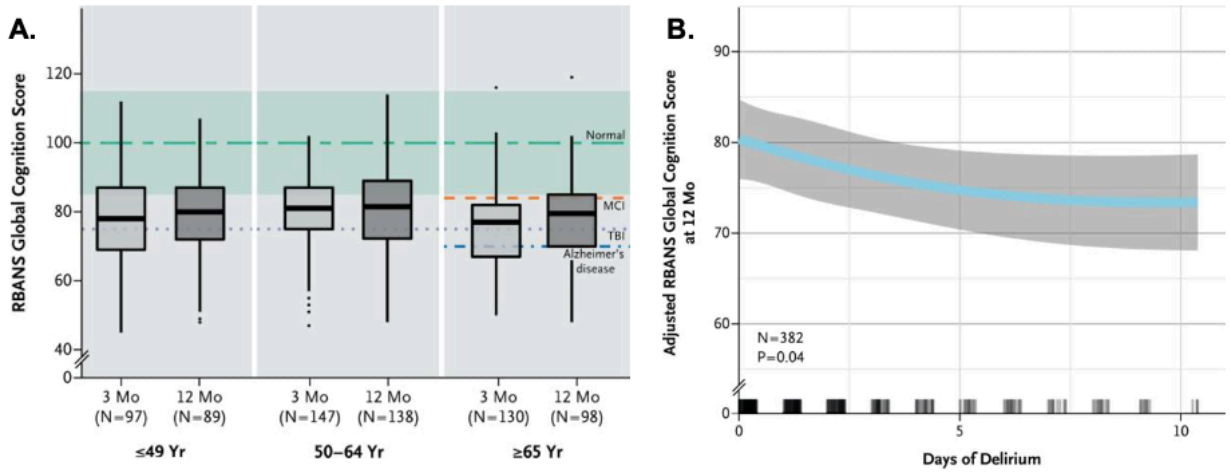

Supplemental Figure 2 – Pandharipande *et al.* 2013.
ICU delirium is associated cognitive deficits (**A**) regardless of age and (**B**) dependent on delirium duration.

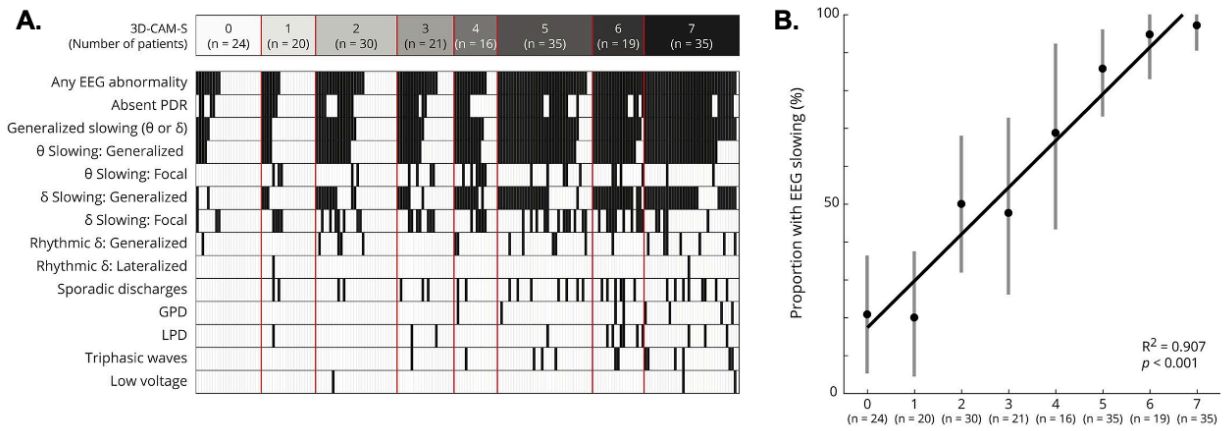

Supplemental Figure 3 – Kimchi et al. 2019.
Clinical EEG slowing correlates with delirium severity and predicts poor clinical outcomes.